Abstract

Birol Uner. Adhesion Mechanism between Polymer and Metal Interface. (Under the direction of Drs. M.K. Ramasubramanian, J.F.Kadla)

The creping process is used to develop bulk, stretch, absorbency and softness in tissue paper. Typically, an adhesive material, e.g. polyvinyl alcohol and polyamidoamine, is used to attach paper on to the drum surface. The severity of the creping process is dependent upon a number of factors, including the adhesion between the adhesive and the metal surface of the Yankee Dryer. Therefore, the objective of this project is to understand the interaction mechanism between the adhesive and metal surface specifically with respect to acid-base interactions, in order to have better control in the creping process.

Using well-characterized polymers and surfaces, the role of surface energy of the polymer, radius of gyration, and chemical composition on adhesion has been investigated. Through the use of microscopic and spectroscopic analyses of the surface chemistry at the polymer-metal interface, in conjunction with creping experiments, the role of the chemical constituents in the microstructural and the physiochemical development of adhesion, and the critical parameters for processing operations have been studied. Acid-base interactions between substrates and adhesives appear to affect surface wetting and the resulting adhesive bond strength.

Atomic force microscopy with chemically functionalized colloidal probes--mounted on the end of the force sensing cantilever--were used to study “acid-base” interactions between adhesives and metal/paper surfaces. The probes used in our experiments were silica spheres decorated with mixed, self-assembled monolayers of hydroxyl- and methyl-terminated thiols. Cast iron was used as the substrate. Force vs. distance curves, recorded in air and in water, showed that adhesive force depends strongly on the

chemical functionality of the tip and the degree of acetylation of the intervening poly(vinyl-alcohol), an adhesive used in paper creping. These results suggest that adhesion forces in the paper creping process likely can be controlled through tailoring “acid-base” interactions. It was observed that with an increase acetyl content of the poly(vinyl-alcohol) adhesion force decreased. There results were support by other empirical and theoretical force measurements.

Cast iron is a porous material. When adhesive is applied to this surface, it may penetrate into the pores. After evaporation of solvent, adhesive solidifies and may act as a mechanical anchor. We used optical microscopy and crystalline polymer to observe this relationship. The results indicated that some penetration occurred, but that it was sparse and not uniform. There results were supported by the comparison of the cast iron surface roughness and polymer radius of gyration. Therefore, it does not appear that mechanical interlocking plays a significant role in the adhesion of polymer to cast iron surface.

Adhesion Mechanism between Polymer and Metal Interface

By

Birol Üner

A dissertation submitted to the Graduate Faculty of North Carolina State University in partial fulfillment of the requirement for the Degree of Doctor of Philosophy in Wood and Paper Science

Department of Wood and Paper Science

Raleigh

2002

Approved by

Dr. Martin Hubbe	**Dr. Stefan Zauscher**
Dr. M.K. Ramasubramanian	**Dr. John F. Kadla**
Chair of Advisory Committee	**Co-chair of Advisory Committee**

Biography

Birol Uner was born in Aydin, Turkey, on April 13, 1968. He received his high school degree in Electricity from Mimar Sinan Technical High School. In August of 1991, the author received his B.Sc. degree in Forest Industrial Engineering from Karadeniz Technical University. After completing his undergraduate degree, he served mandatory duty in the Turkish military. Birol, then, went to Clemson University to complete a master's degree in Wood Chemistry. In the fall of 1997, the author began the PhD curriculum in the Department of Wood and Paper Science under the direction of Drs. M. K. Ramasubramanian and J. F. Kadla.

Acknowledgements

The author wishes to express his sincere appreciation to all those that have been a source of encouragement and support in the preparation of this study. His deepest appreciation goes to Drs. M.K. Ramasubramanian and J. F. Kadla.

Sincere gratitude is also extended to Dr. M. Hubbe, Dr. S. Zauscher and Dr. J. van Zanten for their invaluable assistance and guidance. The author would also like to thank Dr. B. Koc, Dr. O. Ozen and Dr. F. Isik for their help in sample preparation and statistical analysis. The author is especially thankful to Dr. S. Kubo, Dr. T. Kishimoto, Dr. T. Yokoyama, and Dr. T.Ikeda for their valuable discussion, N. Garoff, M. Ptak and D. Kieweg for sharing their time and expertise in AFM techniques.

The author expresses his deepest gratitude to his wife, Sue, for her patience, sacrifice and assistance in completing this study. Special appreciation goes to the author's family for their constant support and encouragement throughout this study.

The author would also like to acknowledge the financial support of Suleyman Demirel University for the completion of his degree.

Table of Contents

Lists of Tables

List of Figures

Chapter 1 - Overview and Background

1.1 Motivation and Objectives

Tissue constitutes approximately 20% of all paper produced in the United States. These paper products are offered in the form of facial tissue, toilet paper, and absorbent towels. In order to obtain softness, bulkiness and absorbency, these products are mechanically processed in a manner that is called “creping”. The creping process reduces the compaction of the paper web by breaking some of the fiber-to-fiber bonds (1). The severity of the creping process is dependent upon a number of factors, including the adhesion between the adhesive and the metal surface of the Yankee Dryer (2,3,4).

The creping process is implemented on the cast iron surface of the Yankee dryer. In the presence of water and oxygen, the cast iron surface can oxidize and form an oxide layer on the surface (5,6). When adhesive is applied to this surface, the oxide layer can form a bridge between the adhesive and the metal surface. Thus, the adhesion properties of the coating chemistry will determine how much mechanical force is required to scrape the paper off of the Yankee dryer surface. Too much adhesion can cause tearing and picking of the paper, whereas too little adhesion prevents creping and leads to poor product appearance and operational difficulties (7,8).

A papermaker has several good reasons for maintaining good control of adhesion while carrying out the creping process. Paper is produced as a continuous web. Good control means less down time on the paper machine because of breaking and/or loss of tension on the sheet in winding. Uniform attachment of the paper sheet to the Yankee dryer surface provides more efficient heat transfer and even and fast drying of the paper sheet. The result will be more uniform product quality and it is likely that production speed

would be increased. In addition to improving product quality, controlling the adhesion on the Yankee Dryer surface may reduce operational costs.

Several methods are commonly used to control adhesion on the Yankee dryer surface. These include chemical debonding agents, release agents, and multicomponent adhesive systems. Typical chemical debonding agents include quaternary ammonium salts such as cocotrimethylammonium chloride, and oleyltrimethylammonium chloride (9-14). These chemicals interrupt interfiber bonding and produce a creped paper with enhanced softness and bulk. Similarly, release agents, generally hydrocarbons or oil-based chemicals, interfere with the polymer network, blocking crosslinking sites and weakening the overall network (1,10). Multicomponent adhesives require two or more adhesives such as polyacrylic-polyacrylamide copolymers, ethylene vinylacetates, polychloroprenes, etc (15). In this system, the first creping adhesive is applied to the Yankee dryer surface, and the second creping adhesive is applied to the web surface. When the paper web is creped from the surface, the blade tends to shear the layer of the first creping adhesive rather than the second creping adhesive. Controlling the ratio between these two adhesives controls the adhesion and release of the paper from the surface of the Yankee dryer. However, controlling the ratio of these adhesives can be difficult due to variations in drying as adhesive layers build up on the dryer surface. These multicomponent systems, which enable better control of adhesion, are more complex, requiring higher operating costs and more careful control of the operating conditions.

Although the mechanism of adhesion has been thoroughly studied, there is no universal theory or model to accommodate all substrate-adhesive systems (16-22). The most commonly accepted theory is the adsorption theory. According to adsorption theory, adhesion is the result of intermolecular forces arising from intimate molecular contact (23,24). The most significant forces are van der Waals forces, covalent bonding forces, and hydrogen bonding forces, *etc*. The corresponding bond strength will vary

according to the magnitude of the respective bond energy. To our knowledge, there is little published about the adhesion mechanism in the creping process. A more fundamental understanding of the adhesion mechanism can lead to better control over the creping process.

In this research, the creping process is being studied on a laboratory designed creping machine with the cast iron dryer surface. We use a cast iron substrate, which is presumably covered with iron oxide, as is our assumption for the Yankee dryer surface in the creping process. Metal oxides have surface sites, which are either acidic or basic, or both. When the adhesive is applied, it has direct contact with the oxide layer. These sites can control the interaction between adherents and adhesives. Therefore, we hypothesize that the adhesion mechanism in the creping process is mainly controlled by acid-base interactions.

The overall goal of this study is to understand the adhesion mechanism in the creping process. More specifically, this study will analyze the role of acid-base interactions in creping. A better understanding of the mechanism will help to improve the creping process so that higher productivity and better production quality can be achieved and at the same time possibly lead to the development of new adhesive polymers.

1.2 Background

1.2.1 Creping Process

Paper is made by depositing dilute slurry of fibers on a moving screen of the paper machine. This part of the paper machine is called the forming section. The pulp slurry is dewatered in the forming section. Further, dewatering is carried out by pressing the pulp mat between felts, followed by a drying section. For the production of tissue and towel grade papers, it is common to use a large rotating hot cylinder, called a Yankee dryer, in the drying section.

The Yankee dryer is a steam heated pressure vessel. The Yankee dryer's function is (25):

1. To supply energy for drying,
2. To transport the sheet during drying process,
3. To provide a base for the creping process (Figure 1.1).

The drying capacity of a typical tissue machine is mainly affected by the size of the Yankee dryer. Its diameter usually ranges from 2.4 to 7.0 meters. The Yankee dryer runs at speeds of 1500 cm/min to as high as 2150 m/min (7,26).

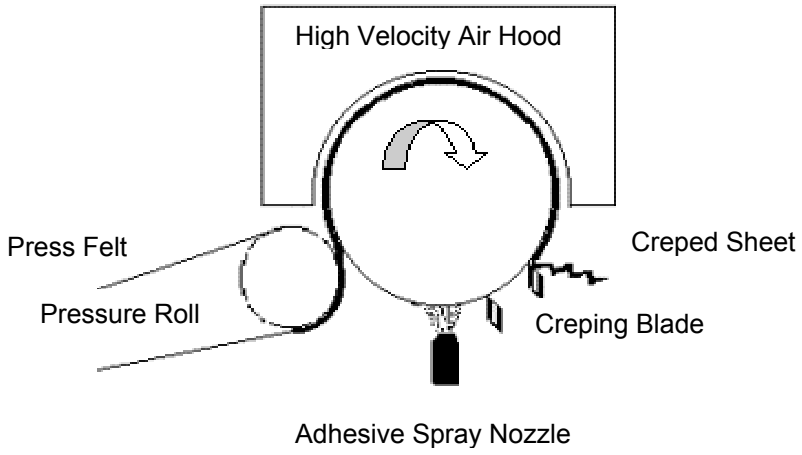

Figure 1.1 *Yankee Dryer and creping (26).*

In a typical creping process, the sheet is carried on the press felt at a moisture content of 60% and transferred to the Yankee dryer surface with the help of an adhesive. A sprayer is employed to apply the polymeric adhesive onto the drum surface prior to the pressure roller so that the paper web can adhere onto the drum surface. The attached paper is then scraped off the surface with a creping blade, known as a doctor blade. When the paper is scraped off the surface, a cut occurs in the adhesive bond between the paper and the drum surface. During this process, some of the fiber-to-fiber bonds in

the sheet are destroyed and the creped paper is wrinkled and folded. The creped paper has higher bulk and improved softness and absorbency.

The adhesion between the sheet and the underlying surface is important to understand since it affects the creping efficiency and paper properties. Figure 1.2 shows the effect of different adhesion properties on the creping of paper. If the adhesive strength between metal and paper surface is too small, the paper will not stick the drum surface very well and the creping process cannot be carried out due to weak adhesion. If the adhesion is too strong, the paper will stick tenaciously to the drum surface. When the paper hits the doctor blade, the creping doctor will tear the paper, and part of the paper will remain on dryer surface. Thus, the adhesive used in creping is very important and adhesion provided by the adhesive plays a significant role in the production of well-creped paper.

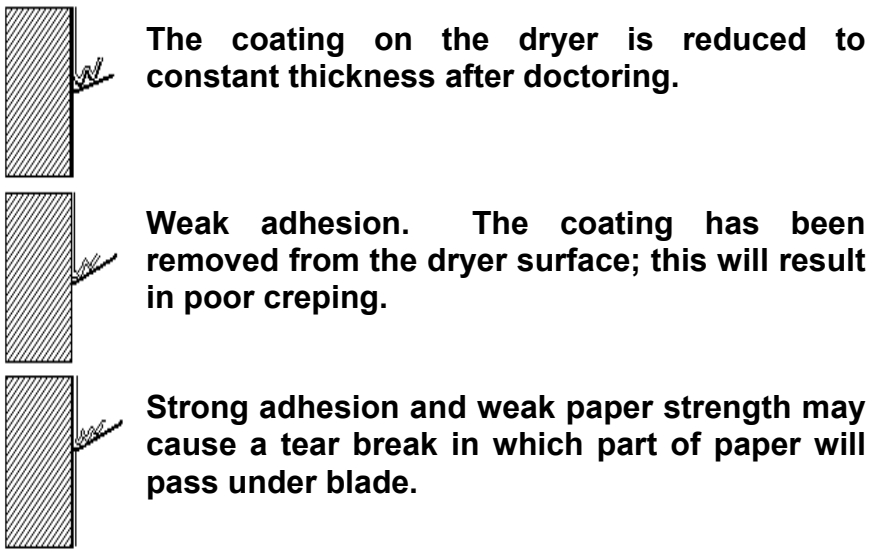

Figure 1.2 *The effect of adhesion level on the creping process (25).*

The surface properties of the Yankee Dryer and the chemistry of the adhesive polymers can play a significant role in the adhesive strength via the

type of interaction. Due to the water and oxygen that come into contact with the Yankee dryer through the wet paper web, adhesive solution and oxygen in the air, oxidation of the iron on the Yankee dryer surface can occur. Thus, in this corrosive environment, a layer of iron oxide will cover the polished Yankee dryer surface. When an adhesive solution is sprayed on this surface, the oxide layer will form a bridge between the metal surface and the adhesive layer (Figure 1.3). Metal oxides have surface sites, which are either acidic or basic, or both. These sites can control the interaction between adherents and adhesives. Polymers can have functional groups that can be electron donors (bases) or electron acceptors (acids). These functional groups provide a site where acid-base interactions can take place. For example, a hydroxyl group attached to polyvinyl alcohol can interact with the iron oxide surface and form a hydrogen bond. Hydrogen bonds are typically categorized as acid-base interactions (27).

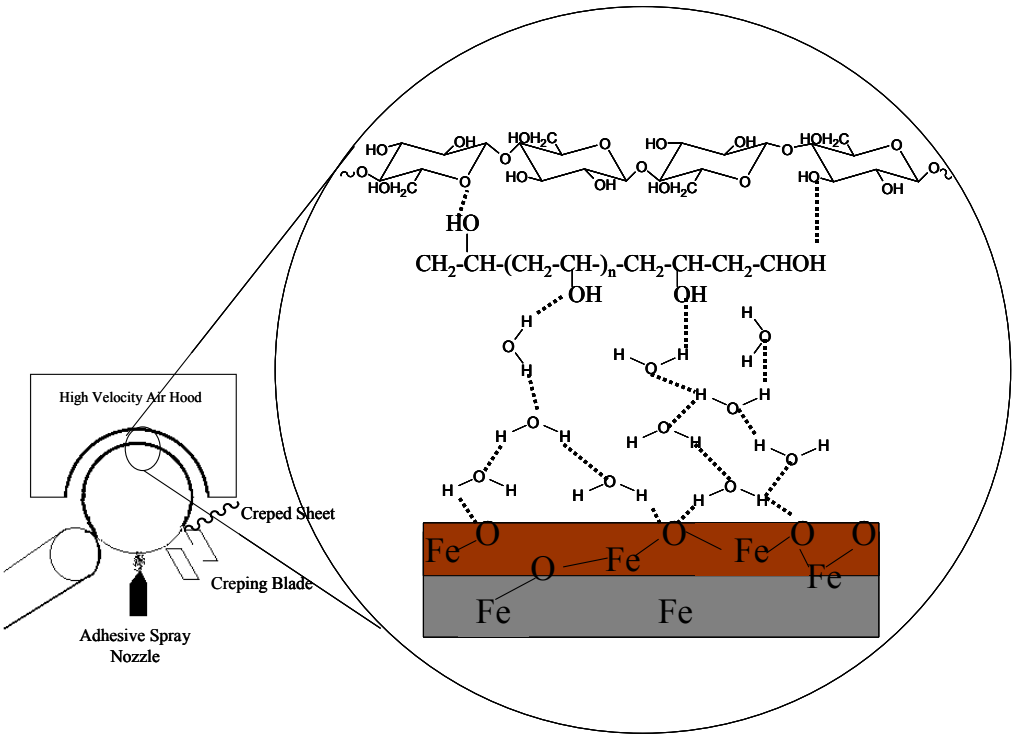

Figure 1.3 *Yankee dryer surface in creping process.*

1.2.2 Adhesion and Adhesives

An adhesive is a substance that has the ability to hold materials together by surface attachment so that they resist separation (24,28,29). Any materials that are bound to each other by an adhesive form a system that includes adhesion and cohesion (29). Adhesion is established between two surfaces due to intermolecular forces whereas cohesion is the bonding of molecules together in the bulk. The intermolecular forces result from van der Waals forces, electrostatic forces, hydrogen bonds, and/or other chemical bonds such as ionic, covalent or metallic interfacial bonds (24,27).

Adhesion between two materials may involve physical or chemical bonding. Thus, the mechanism of adhesion can be different for various materials. There are several different adhesion theories that may apply to the creping system.

In processes like creping, in which porous materials such as paper and cast iron are used, mechanical interlocking theory may apply. When an adhesive is applied to the substrate, it spreads over the surface. The low viscosity of an adhesive will allow it to wet the surface of the substrate easily and will allow it to penetrate into the pores of the surface. The adhesive can then act as a mechanical anchor holding the materials together (19,24).

Two other common theories of adhesion are the diffusion and electronic theories (16,19,23,24). The diffusion theory of adhesion is based on the adhesion of two macromolecules in intimate contact via the interdiffusion of the molecules. According to this theory, polymers must be compatible in one another and mobile at a certain temperature (t_g= glass transition temperature)(19,29). If two materials are compatible, these two materials diffuse in each other at the interface (Figure 1.4)(30). The diffusion theory may not be applied to polymers whose solubility parameters are not similar, if one polymer is highly crosslinked, crystallized, or if the temperature

of the system is below the t_g. Therefore, this theory does not appear to be compatible with the creping system.

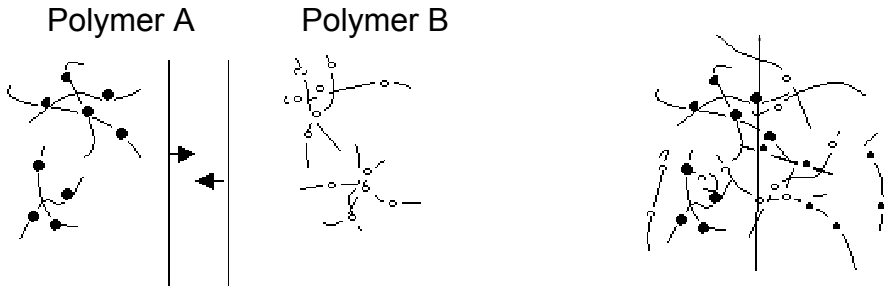

Figure 1.4 *Diffusion of polymer at the interface (18,30).*

The electronic theory of adhesion indicates that if two metals are placed into contact, electrons will be transferred from one metal to the other and it will form an electrical double layer, which gives a force of attraction (16). Polymers are usually insulators, and would therefore disrupt the transfer of electrons from one material to another (30). Thus, this theory of adhesion may not be appropriate for the creping process.

In adhesion science, the most commonly accepted theory is the adsorption or wetting theory. According to adsorption theory, adhesion is the result of intermolecular forces arising from intimate molecular contact (23). In order to form intimate contact, an adhesive must spread freely and wet the surfaces. Complete wetting occurs when the molecular attraction between a liquid and a solid surface is greater than that between similar liquid molecules (31,32). Whether or not a given liquid will wet a solid surface depends on the surface tension of both substances. The ability of a liquid to wet a solid surface is predicted by the value of the spreading coefficient, *S,* which is obtained from the surface tensions of the solid and liquid and can be expressed as:

$$S = \gamma_{sv} - \gamma_{sl} - \gamma_{lv} \qquad [1.1]$$

where γ_{sv} is the surface tension of the solid, γ_{sl} is the interfacial surface tension between solid and liquid, and γ_{lv} is the surface tension of the liquid. A large positive number implies complete wetting of the solid surface.

Surface tension is a direct measurement of intermolecular forces (33). If the intermolecular forces are due to dispersion forces, as in the case of saturated hydrocarbons, the surface tension measures only the contribution of dispersion forces (33). If the liquid includes more than one kind of intermolecular interaction, such as hydrogen bonding and dispersion forces, then the surface tension is the sum of the intermolecular forces as shown in equation [1.2]:

$$\gamma = \gamma^d + \gamma^h \qquad [1.2]$$

where the first term (γ^d) arises from London dispersion or van der Waals interactions and the second term (γ^h) arises from hydrogen bonding.

Work of adhesion can be predicted based on the surface tension of the adhesive and material being adhered. When an adhesive is applied to a solid substrate and it has no interaction with the solid (i.e. – Work of Adhesion = 0) then the interfacial surface tension (γ_{12}) between the solid and the adhesive is the sum of the surface tension of the adhesive (γ_1) and the surface tension of the solid (γ_2). However, van der Waals forces are always present in between any two given materials and these interactions decrease the interfacial surface tension. This decrease represents the interfacial attraction, termed as the work of adhesion, and is shown in equation [1.3]:

$$W_{ad} = \gamma_1 + \gamma_2 - \gamma_{12} \qquad [1.3]$$

where W_{ad} is the work of adhesion between two surfaces, γ_1 is the surface tension of sample 1, γ_2 is the surface tension of sample 2, and γ_{12} is the interfacial surface tension between sample 1 and 2. Work of adhesion can be used to predict the interfacial forces between two different materials.

1.2.2.1 van der Waals Forces

Van der Waals forces are long-range forces arising from the interactions between induced dipole moments in neighboring molecules. They can be effective over separation distances greater than 10 nm (34). The force on a sphere near a solid surface in a liquid medium is (35):

$$F_{vdW} \approx +\frac{A_H}{6}\frac{a}{h^2} \qquad [1.4]$$

where A_H is the Hamaker constant, a is the radius of the sphere and h is the distance between the surfaces. The value of A_H depends on the solid material, as well as the liquid medium. For like materials, the value of A_H is greater than zero and the force is always attractive. Van der Waals forces are usually weaker than polar forces such as hydrogen bonding.

Van der Waals forces can be classified in three groups, dipole-dipole attraction, dipole-induced dipole attraction, and London dispersion forces (36). Dipole-dipole attraction results from the electrostatic attraction of the positive end of one polar molecule for the negative end of another. This polarity results from the preferential location of electrons relative to atoms in the molecule (Figure 1.5). For example, CF_3CH_3 with electronegative fluorine (F) atoms on the one end of the molecule will induce partial charge separation such that the CF_3 side becomes more negative, while the CH_3 side is more positive. Thus, the negative end of one molecule attracts the positive end of another molecule.

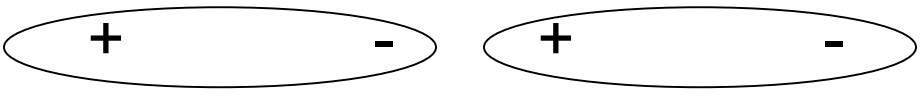

Figure 1.5 *Dipole-Dipole interactions.*

Dipole-induced-dipole, on the other hand, is due to electron clouds surrounding the molecule. Electrons move in a molecular orbital and this

molecular orbital interact with other charges, changing the probability distribution of the electron in its orbital. The electrons in the spherical, symmetrical molecule see the dipole as two charges. The electrons are attracted to the positive end of the dipole and repelled by the negative end; this creates dipoles. We then have a dipole interacting with a dipole that was created by the first dipole (Figure 1.6).

Finally, dispersion forces are due to induced dipole-induced-dipole interactions. At any given point in time, electrons can be on one side of the molecule, which can develop a temporary dipole moment. A second molecule can be distorted by the appearance of the dipole in the first molecule, where its nuclei are attracted to the negative end of the first molecule (Figure 1.6).

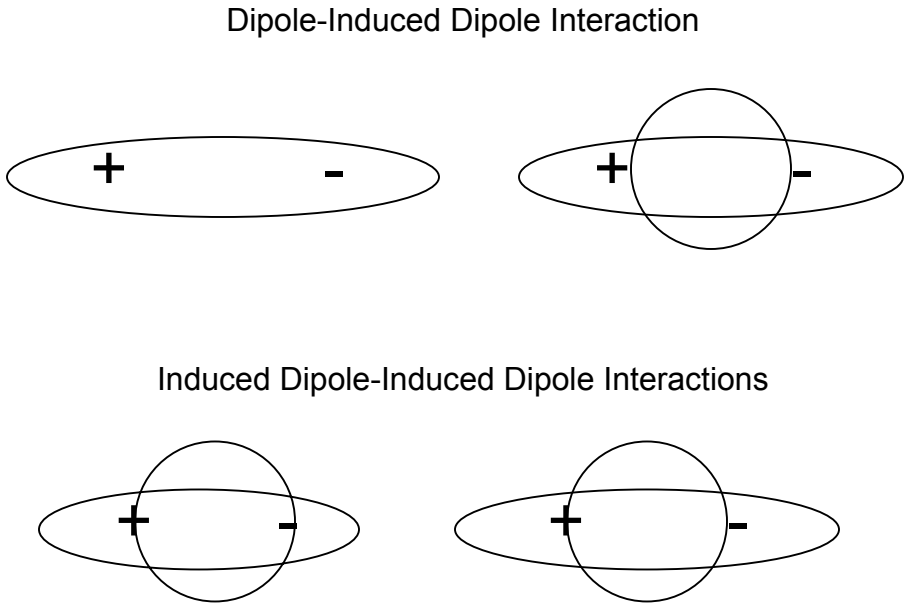

Figure 1.6 *The attractive forces between two molecules (37).*

1.2.2.2 Acid-Base Interactions

According to adsorption theory, adhesion is the result of intermolecular forces arising from intimate interfacial molecular contact (24). The

corresponding bond strength will vary according to the magnitude of the respective bond energy. It has been proposed by Fowkes and coworkers that the acid-base interactions between an adhesive and a substrate may represent the major type of adhesion bonds that operate across the interface (38-44).

An acid-base reaction involves the transfer of an electron pair from the base to the acid. Acids in the Bronsted sense are defined as substances that give off protons, and bases accept protons. In the Lewis sense, acids are electron pair acceptors and bases are electron pair donors. Electron donating groups on an atom can increase the Lewis basicity of that atom, while electron-withdrawing groups can increase the Lewis acidity.

In acid-base systems, the transfer of electrons is governed by basicity or polarizability (45). Polarizability means the ability to allow deformation of the electron cloud in an electric field. Since things that are easily deformed are soft, this leads to the two classes of acids being called hard and soft. Deformation occurs in the presence of other atoms or groups to which bonding is occurring. The hard Lewis acids are relatively small, have a high oxidation state (electron poor), high electronegativity (high ability to attract electrons), and have low polarizability (do not easily deform in an electric field) (46). The soft Lewis acids are relatively large, have a low oxidation state (electron rich), low electronegativity, and have high polarizability (easily deforms in an electric field). Similarly, hard Lewis bases have high electronegativity, low polarizability, and are difficult to oxidize and soft Lewis bases have low electronegativity, high polarizability, and are easily oxidized. Thus, the softness of a base can be associated with ease of oxidation, i.e. empty low-lying orbitals. Hard acids and bases are most effective in electrostatic bonding; soft acids and bases are most effective in forming covalent bonds.

The Yankee dryer is made of cast iron, and it is in contact with the wet paper web, adhesive solution and oxygen from the air. These components

are providing a perfect condition for the corrosion of the iron surface. Thus, the polished cast iron surface will oxidize, and a layer of iron oxide will cover the surface (5,6,47,48). Metal oxides have surface sites that may be acidic, basic, or both (46). These sites will control the interaction between adherents and adhesives. As Lewis acids, metal oxides (Fe_2O_3, Cr_2O_3, SiO_2) are more polar (or harder) than metals. For example, Cu_2O is a stronger acid than Cu metal.

In terms of polymers, Schultz *et al*. have shown that grafting small quantities of acrylic groups on polyethylene can enhance the adhesion to aluminum, and the acrylic groups appear to orient themselves at the polymer/metal oxide interface (49). As a result, chemical linkages are formed between the oxide and the oriented carboxylic groups. Likewise, Fowkes *et al.* showed that the absorption of a polymer on an iron oxide is controlled by the acidic and basic sites of the metal surface (50).

In creping, after the application of the adhesive and paper web to the dryer surface the oxide layer can become a bridge between the metal surface and the adhesive (3,6). These bonds between the adhesive and the oxide layer of the cylinder surface can form in much the same way as the bonds form in the paper. In paper, when wet fibers are brought together on the paper machine, bonding is promoted by the polar attraction of the water molecules for each other and for the hydroxyl groups on the cellulose chain. During drying, the water is evaporated, and the hydroxyl groups on fibers form hydrogen bonds. As more water is removed on a Yankee dryer, hydrogen bonds can form between the adhesive and the oxide layer of the dryer surface. Since hydrogen bonding is considered to be a subset of acid-base interaction, it follows that the acid-base interactions control the adhesion and the resulting creping force.

Hydrogen bonding is due to the attraction between a hydrogen atom and strongly electronegative atoms such as fluorine, oxygen, nitrogen or chlorine (Figure 1.7). The covalent bonds of N-H, O-H, and F-H become

extremely polar. Therefore, if an atom of adjacent molecule is the negative end of a dipole, a strong attraction to the hydrogen atom can occur (37). Hydrogen bonds are stronger than van der Waals forces and 5 to 10% as strong as covalent bonds. The intermolecular hydrogen bond distance is only 0.176 nm (34). It is larger than covalent bond (0.1nm) but smaller than summing of two van der Waals radii (0.26 nm).

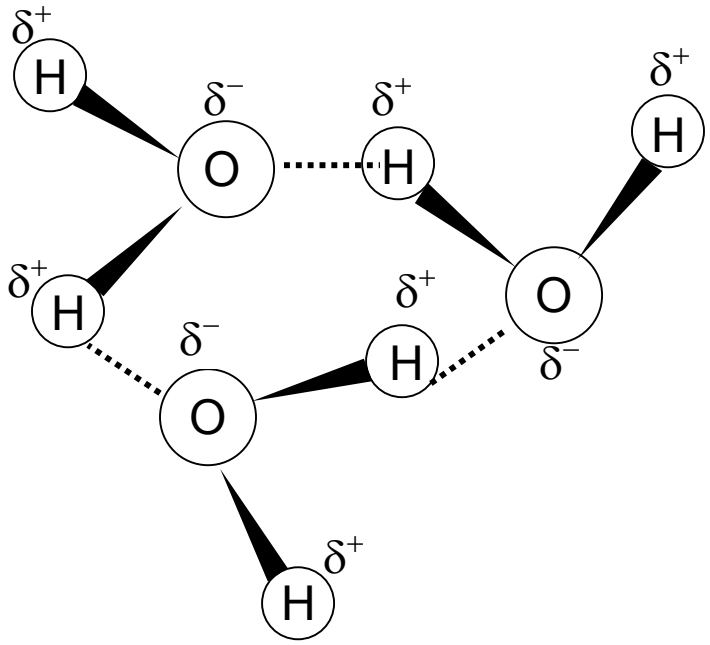

Figure 1.7 *Hydrogen bonding in water molecules.*

Various bond types and the corresponding energies are summarized in Table 1.1. These bonds energies are indicative of adhesive bond strengths. Depending on the polymer and surface chemicals, some of these bonds can form during adhesion. If the adhesion mechanism is known, then the adhesive strength can be controlled by changing the chemical structure of the polymer and the surface chemistry.

Table 1.1 *Bond types and typical bond energies (24)*

Type	Bond Energy (kj/mol)
Ionic	600-1100
Covalent	60-700
Lewis Acid-Base Interactions	Up to 80
Bronsted Acid-Base Interaction	Up to 1000
Hydrogen Bonds involving fluorine	Up to 40
Hydrogen Bonds excluding fluorine	10-25
Dipole Dipole Interactions	4-20
Dipole-Induced dipole	Less than 2
Dispersion Forces	0.08-40

Lewis acid-base interactions have been extensively studied by Drago *et al*. (51-57) using calorimetry, infrared spectra, and NMR spectroscopy. They have shown that acid-base interactions can be related to the heat of reaction (ΔH_{AB}) by:

$$-\Delta H_{AB} = E_A.E_B + C_A.C_B \qquad [1.5]$$

where *E* represents the electrostatic contributions of the acid and base to adduct stability and the *C* parameters represent the covalent contributions. The *C/E* ratio represents the softness or polarizability of the acid or base. Later, this equation was utilized by Fowkes *et al.* to determine the work of adhesion (50, 58). E and C constants were determined by wavenumber shifts in the infrared spectra (50). These values were used in equation [1.5] to determine the heat of interaction. The work of adhesion due to acid-base interaction was estimated using equation [1.6].

$$W_{SL}^{ab} = f(n^{ab})(\Delta H^{ab}) \qquad [1.6]$$

where *f* is a factor (close to unity) for converting heat of interaction to a free energy of interaction, *n* is the interfacial concentration of acid-base pairs, and ΔH^{ab} is the heat of acid-base interaction (27).

1.2.3 Force Measurements

Many tests have been developed to measure adhesive bond strength. Summaries of the general methodology are given in the literature (31). Most of the measurements are usually carried out on a testing machine measuring tensile strength (e.g. Instron®). These methods are not capable of detecting adhesion in a molecular level.

Adhesion is an interfacial phenomena and in order to understand it, one needs to study fracture mechanics, the rheological aspects etc. However, in this thesis we will focus on the chemistry of adhesion to control the creping process. Therefore, in order to detect surface forces, atomic force microscopy (AFM) will be used.

Recently, atomic force microscopy (AFM) has been used to study forces at the molecular level (59-65). The AFM measures attractive and repulsive forces between a cantilever probe tip and a sample surface. As the sample surface and probe tip are brought close to each other and pulled away, the amount of force felt by the cantilever is recorded. The cantilever used in the force measurement has a very sharp tip at the end. AFM measures local property. The measured force is very much dependent on the surface chemistry of the AFM tip and the surface being probed. Interatomic forces between the probe tip and the sample surface causes the deflection of the cantilever as the surface topography or the chemical property changes (16). A laser light reflected from back of the cantilever measures the deflection and it is registered in the computer. AFM can achieve a resolution of 10pm and unlike other instruments, it can image sample surfaces and measure forces in air and liquids.

Cantilever deflection is measured by the piezo, which moves up and down with the sample during a run. The deflection of the cantilever is converted to a force measurement, which is displayed on the monitor. The cantilever starts the cycle at a specified distance from the sample (A). The sample starts to move up with the piezo and cantilever starts to feel forces from the sample. At the point where the forces overcome the cantilever spring constant, the cantilever makes contact with the sample surface (B). The sample and cantilever then move together (C). The piezo returns and the cantilever continues to move with the sample due to adhesion forces (D). The cantilever separates from the sample surface at point E. This point represents the adhesion forces measured between the sample and the cantilever. In order to obtain a force value, the deflection of the cantilever is converted via Hooke's Law, with the known spring constant of the cantilever (force= spring constant $\times$ deflection). A typical deflection-displacement curve can be seen in Figure 1.8.

Based on the functional groups of the polymer on the cantilever tip, different interaction forces between the surfaces can be measured, such as hydrogen bonding and van der Waals forces. One of the objectives of this study is to investigate these interactions by measuring the adhesion forces quantitatively. Adhesion measurements can also be taken by attaching a glass sphere on a cantilever tip (62,66,67). This technique has been termed colloidal probe microscopy (CPM). The glass spheres are attached to the end of the cantilever using micromanipulator and ultraviolet light cured epoxy resin (62).

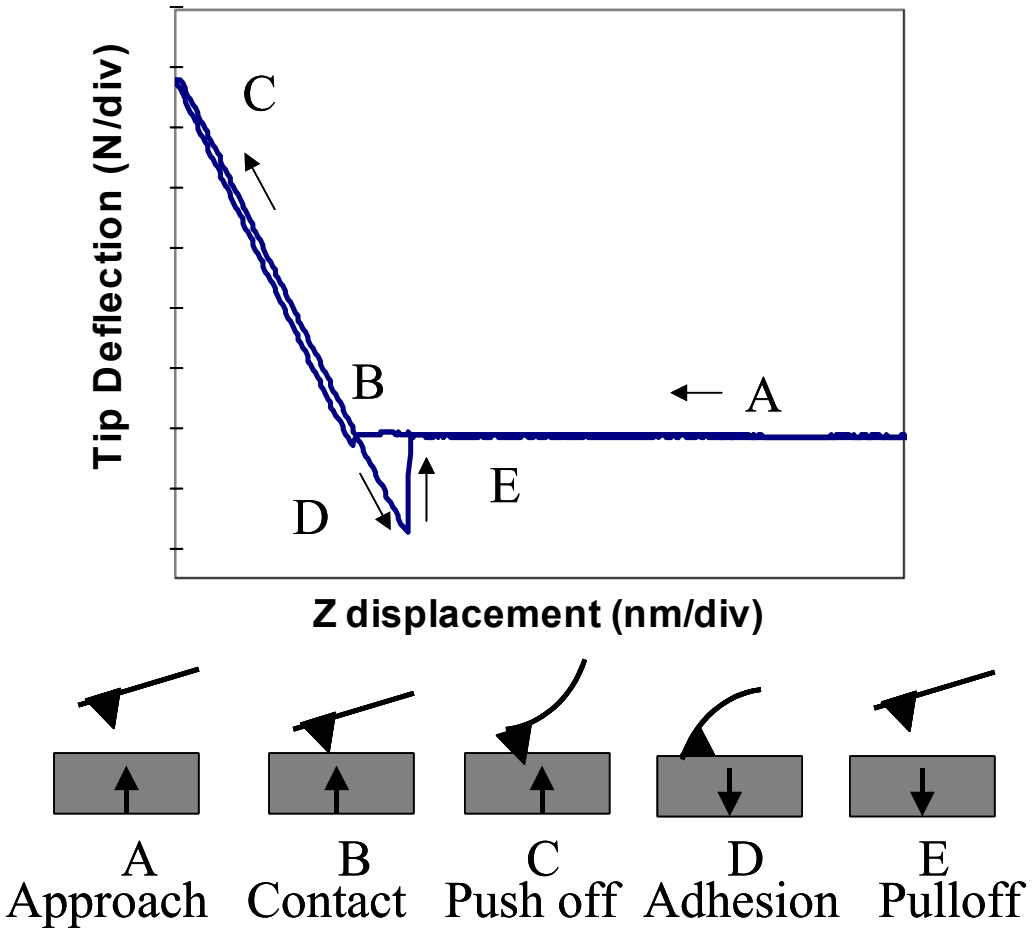

Figure 1.8 *Cantilever-sample interaction during adhesion force measurement*

1.2.3.1 The Johnson-Kendall-Roberts Theory

Johnson-Kendall-Roberts (JKR) theory can be used to estimate adhesion forces between the cantilever tip and sample surface in a medium. The JKR theory neglects long-range forces and considers only short-range forces on the contact region (68). This system assumes that interaction takes place between a flat surface and the large radii of curvature on the tips. The

force varies proportionally with the contact radius as indicated in equation [1.7]:

$$F_{ad} = \frac{3}{2}\pi R W_{ad} \qquad [1.7]$$

where F_{ad} is adhesion forces, R is the radius of curvature on the tip and W_{ad} is the work of adhesion. The thermodynamic work of adhesion is obtained using the interfacial surface tension of the sample and medium, the interfacial surface tension of the tip and medium and the interfacial surface tension of the tip and sample as shown in equation [1.8] (60).

$$W_{ad} = \gamma_{SM} + \gamma_{TM} + \gamma_{TS} \qquad [1.8]$$

1.3 Dissertation Organization

Each of these chapters is self-contained and can be read independently.

Chapter 2 describes the study of creping on a laboratory creping machine developed at North Carolina State University. The creping process, strength properties of the creped paper, and crepe structure for different adhesives are examined.

In Chapter 3, chemical force microscopy is discussed. Chemical force microscopy is a convenient tool for the study of adhesive forces and adhesion mechanism in the creping process. Chemical force microscopy provides a more controlled adhesive experiment where most unknowns can be eliminated. Colloidal probe microscopy is introduced. Normal force interactions between a cast iron surface and polymer in aqueous solution are presented in Chapter 2 and 3.

In Chapter 4, FT-infrared spectroscopy methods are utilized for the determination of chemical interaction. FT-infrared spectroscopy provides more information about the bonding of adhesive to the metal surface. It also gives information about the chemical properties of the adhesive polymer.

The major conclusion of this thesis and recommendations for future work are presented in Chapters 5 and 6.

1.4 References

1. Allen, A.J., Lock, G.; “Creping Release Agents”, US Patent 5,660,687, Aug 26, 1997.
2. Chan, L.L.; “Creping Aid and Creping Process”, 1983 Papermakers Conference Proceedings, Tappi Press, 197-199.
3. Oliver, J.F.; “Dry-creping of Tissue Paper-A Review of Basic Factors”, Tappi J., **63**(12), 91,1980.
4. Fuxelius,F.K.; “Adhesion of Paper Web to Glazing Cylinders Druing Dry Creping”, Svensk Papperstidgn. **70**(5), 164-168, 1967.
5. Almar-Naess, A.; “Method for corrosion protection” US Patent 3350288, 1967.
6. Nordman, L., Uggla, R.; “Adhesion between fiber webs and Metal Surfaces During Drying” in Fibre-Water Interactions in Papermaking, Vol:1, Trans. Symposium, Tech.Div. the BP&BIF, Oxford, UK, 459, 1977.
7. Krelid, I.; “Drying of Tissue” in Papermaking Part 2, Drying, 147, 2000.
8. Vinson, K., Weisman, P.T., Phan, D.V.; “Strong and Soft Creped Tissue Paper and Process for Making The Same by Use of Biodegredable Crepe Facilitating” US Patent 5487813, 1996.
9. Oriaran,T.P, Awofeso, A.O, Kershaw, T.H, Luu, P.V., Neculescu, C.M., Huss, M.E.; “Soft Strong Towel and Tissue Paper” US. Patent 5399241, Mar 21, 1995.
10. Vinson, K.D.,Deason, H.T., Hersko, B.S.; “Creping adhesive for creping tissue paper” US Patent 6,207,734, Mar 27, 2001.
11. Conte, J.S., Bender, G.W.; “Softening and Debonding Agents” in Chemical Processing Aids in Papermaking A Practical Guide Tappi Press Atlanta, Edited By K. J. Hipolit, 1992.

12. Poffenberger, C., Deac, Y., Zeman, W.; “Novel Hydrophilic Softeners for Tissue and Towel Applications” in 2000 Tappi Papermakers Conference and Trade Fair Proceedings, 85, 2000.
13. Mann, R.L., Leah, P.J.; Fluff Pulp and Debonding Agents”, Paper Southern Africa, **7**(6), 41, 1987.
14. Liu, J., Hsieh, J.; “Application of Debonding Agents in Tissue Manufacturing”, in 2000 Tappi Papermakers Conference and Trade Fair Proceedings, 71, 2000.
15. Lazorisak, N.W., Christiansen, F.A., Harriz, J.M.; “Creping process using two-position adhesive application” US Patent 4064213, 1977.
16. Derjaguin, B.V., Toporov, Y.P., “Role of the Molecular and The Electrostatic Forces in the Adhesion of Polymers” in International Symp. On Physicochemical Aspects of Polymer Surfaces, Vol:2, Edited By K.L.Mittal, Plenum Press, NY, 605, 1981.
17. Fowkes, F.M.; “Acid Base Interactions in Polymer Adhesion” in International Symp. on Physicochemical Aspects of Polymer Surfaces, Vol:2, Edited By K.L.Mittal, Plenum Press, NY, 583, 1981.
18. Fourche, G.; “An Overview of the Basic Aspects of Polymer Adhesion. Part 1: Fundamentals”, Polymer Engineering and Science, **35**(12), 957, 1985.
19. Pocius, A.V.; Adhesion and Adhesives Technology an Introduction, Hanser Publisher, Cincinnati, 118, 1997.
20. Burkstrand, J.M.; “Chemical Interactions at Polymer Metal Interfaces and Correlation with Adhesion”, J.Vac.Sci.Technol., **20**(3), 440, 1982.
21. Burkstrand, J.M.; “Metal-Polymer Interfaces: Adhesion and X-ray Photoemission Studies “, J.Appl. Phys., **52**(7), 4795, 1981.
22. Mittal, K.L.; “Adhesion Aspects of Metallization of Organic Polymer Surfaces”, J.Vac.Sci.Technol., **13**(1), 19, 1976.
23. van Ooij, W.J.; “Interfacial Interactions between Polymers and Other Materials and Their Effects on Bond Durability” in Physicochemical

Aspects of Polymer Surfaces, Edited By K.L Mittal, Plenum press, 1035, 1981.

24. Kinloch, A.J.; Adhesion and Adhesives Science and Technology, Chapman Hall, 18, 1987.
25. Krelid, I.; "Drying of Tissue" in Papermaking Part 2, Drying, 147, 2000.
26. Desai, M.; MSc. Thesis, NCSU, Raleigh, NC, 1999.
27. Fowkes, F.M.; "Acid-Base Interactions" in Encycl. Polymer Science and Eng.,Wiley-Interscience, NY, supplement, 1, 1989.
28. Good, R.J.; "Definition of adhesion", J. Adhesion, **8,**1, 1976.
29. Skeist, I.; Handbook of Adhesives, 2nd Edition, Van Nostrand Reinhold Company, NY, 1977.
30. Comyn J.; Adhesion Science RSC Paperbacks, 3, 1997.
31. Wu, S.; Polymer Interface and Adhesion, Marcel Dekker Inc. NY, 1982.
32. Gans, D.M.; "Measurement of equilibrium spreading coefficients of liquids on solids and liquids", J. Paint Technol. **41**(536), 515, 1969.
33. Fowkes, F.M.; "Molecular Forces at Interfaces" in Surfaces and Coatings Related to Paper and Wood Edited by R.H.Marchessault, C.Skaar, Syracuse University Press, 99, 1967.
34. Israelachvili, J.N.; Intermolecular and Surface Forces, 2nd Edition, Academic Press, San Diego CA, 1992.
35. Zauscher, S.; PhD Thesis, University of Wisconsin, Madison, WI, 1998.
36. Holtzclaw, H.F., Robinson, W.R., Odom, J.D.; General Chemistry with Qualitative Analysis, D.C. Heath Company, Lexington, MA, 297, 1991.
37. Kotz, J.C.; Purcell, K.F.; Chemistry and Chemical Reactivity, Second Edition, Saunders College Publishing, Philadelphia, 1991.
38. Allara, D.L., Fowkes, F.M., Noolandi, J., Rubloff, G.W., Tirrel, MV; "Bonding and Adhesion of Polymer Interfaces " Materials Sci. Eng., **83**, 213, 1986.

39. Fowkes, F.M.; “Quantitative Characterization of the Acid-Base Properties of Solvents, Polymers and Inorganic Surfaces” J. Adhesion Sci. Technol., **4**(8), 669, 1990.
40. Fowkes, F.M., Mostafa, M.A.; “Acid-Base Interaction in Polymer Adsorption” Ind. Eng. Chem. Prod., Res. Dev. **17**(1), 3, 1978.
41. Joslin, S.T., Fowkes, F.M.; “Surface Acidity of Ferric Oxide Studied by Flow Microcalorimetry” Ind. Eng. Chem. Prod., Res. Dev. **24**, 369, 1985.
42. Fowkes, F.M., Tischler, D.O., Wolfe, J.A., Lannigan, L.A., Hallwell, M.J.; “Acid-Base Complexes of Polymers” J.Polymer Sci. Polymer Chem., **22**, 547, 1984.
43. Fowkes, F.M.; “Donor-Acceptor Interactions at Interfaces” J. Adhesion, **4**, 155,1972.
44. Fowkes, F.M.; “Role of Acid-Base Interfacial Bonding in Adhesion” J. Adhesion Sci. Tech., **1**(1), 7, 1987.
45. Ho, T.; “Hard and Soft Acids and Bases Principle in Organic Chemistry” Academic Press, New York, NY, 4, 1977.
46. Pearson, R.G.; Chemical Hardness, Wiley-VCH, Weinheim, Germany, 1, 1997.
47. Bolger, J.C.; “Acid-Base Interactions Between Oxide Surfaces and Polar Organic Compounds” in in International Symp. On Physicochemical Aspects of Polymer Surfaces, Vol:2, Edited By K.L.Mittal, Plenum Press, NY, 3, 1981.
48. L.H. Lee; “Molecular Bonding and Adhesion at Polymer-Metal Interface” J. Adhesion, **46**,15-38, 1994.
49. Schultz, J., Carre, A., Mazeau, C.; “Formation and Rupture of Grafted Polyethylene/Aluminum Interfaces” Int. J. Adhesion Adhesives, 163, 1984.

50. Fowkes, F.M., Huang, Y.C., Shah, B.A., Kulp, M.J., Lloyd, T.B; “Surface and Colloid Chemical Studies of Gamma Iron Oxides for Magnetic Memory Media” Colloids Surfaces, **29**, 243, 1988.
51. Epley, T.D., Drago, S. R.; “Calorimetric Studies on some Hydrogen Bonded Adducts” J.Am.Chem. Soc., **89**(23), 5770, 1967.
52. Drago, R.S., Epley, T.D.; “Enthalpies of Hydrogen Bonding and Changes in Delta NuOH for a Series of Adducts with Substituted Phenols” J.Am.Chem. Soc., **91**(11), 2883, 1969.
53. Drago, R. S., O’Bryan,N., Vogel, G.C.; “Frequency Shift-Enthalpy Correlation for a Given Donor with Various Hydrogen-Bonding Acids” J.Am.Chem. Soc., **92**(13), 3924, 1970.
54. Drago, R.S, Vogel, G.C.,Needham, T.E.; “4-Parameter Equation for Predicting Enthalpies of Adduct Formation” J.Am.Chem. Soc., **93**(23), 6014, 1971.
55. Drago, R.S., Parr, L.B., Chamberlain, C.S.; “Solvent Effects and Their Relationship to E and C Equation” J.Am.Chem.Soc. **99**(10), 3203,1977.
56. Drago, R., Vogel, G.C.; “Interpretation of Spectroscopic Changes upon Adduct Formation and Their Use to Determine E Parameter and C Parameter” J.Am.Chem. Soc., **114**, 9527, 1992.
57. Joesten, M.D., Drago, S. R.; “Validity of Frequency Shift-Enthalpy Correlations to Adducts of Phenol with Nitrogen and Oxygen Donors” J.Am.Chem. Soc., **84**, 3817, 1962.
58. Riddle, F.L., Fowkes, F.M.; “Spectral Shifts in Acid-Base Chemistry. 1. Van der Waals Contributions to Acceptor Numbers” J.Am.Chem. Soc.,**112,** 3259, 1990.
59. Binnig, G., Quate, C.F., Gerber, Ch.; “Atomic Force Microscope” Physical Rev. Letters, **56** (9), 930, 1986.
60. Noy, A., Vezenov, D., Lieber, C.M.; “Chemical Force Microscopy” Annu. Rev. Mater. Sci., **27,** 381, 1997.

61. Florin, E.-L., Moy, V.T., Gaub, H.E.; “Adhesion Forces Between Individual Ligand-Receptor Pairs” Science, **264,** 415, 15 April, 1994
62. Zauscher, S., Klingenberg, D.J.; “Normal Forces Between Cellulose Surfaces Measured with Colloidal Probe Microscopy” J. Colloid Interface Sci., **229,** 497, 2000.
63. Vezenov, D., Noy, A., Rozsnyai, L.F., Lieber, C.M.; “Force Titrations and Ionization State Sensitive Imaging of Functional Groups in Aqueous Solutions by Chemical Force Microscopy” J.Am.Chem. Soc., **119,** 2006, 1997.
64. Lee, G., Chrisey, L.A., Colton, R.J.; “Direct Measurement of the Forces Between Complementary Strands of DNA” Science, **266**, 771, 4 Nov. 1994.
65. Sinniah, S.K., Steel, A.B., Miller, C.J., Reutt-Robey. J.E; “Solvent Exclusion and Chemical Contrast in Scanning Force Microscopy” J.Am. Chem. Soc. **118,** 8925, 1996.
66. Ducker, W.A., T.J.Senden, Pashley, R.M., “Direct Measurement of Colloidal Forces Using an Atomic Force Microscope” Nature, **353**(2), 239, 1991.
67. Ducker, W.A., T.J.Senden, Pashley, R.M; “Measurement of Forces in Liquids Using a Force Microscope” Langmuir, **8,** 1831, 1992.
68. Johnson, K.L., Kendall, K., Roberts, A.D.; “Surface energy and the contact of elastic solids”, Proc. Royal Soc. London A **324**, 301, 1971.

Chapter 2 - Micro and Meso Force Measurement in Creping Process and Their Interrelationship

2.1 Introduction

Tissue constitutes approximately 20% of all paper produced in the United States. These paper products are offered in the form of facial tissue, toilet paper, and absorbent towels. In order to obtain softness, bulkiness and absorbency, these products are mechanically processed in a manner that is called “creping”.

The creping process reduces the compaction of the paper web by breaking some of the fiber-to-fiber bonds (1). Creped tissue paper has the unique feature of a wrinkled structure. The wrinkled structure is achieved by scraping a paper web off of a cast iron surface which has been attached by an adhesive. The properties of the wrinkled structure contribute to the stretchiness and the softness of the final product.

The severity of the creping process is dependent upon a number of factors, including the adhesion between the adhesive and the metal surface of the Yankee Dryer (2,3,4). Too much adhesion can cause tearing and picking of the paper, whereas too little adhesion prevents creping and leads to poor product appearance and operational difficulties (5,6). Good control of the creping process is essential in producing soft tissue products with the consistent quality.

Although numerous theories have been developed to explain the mechanism of adhesion (2-7), presently there is no universal theory or model to accommodate all adherent and adhesive interphase phenomena. Of the various theories, the adsorption or wetting theory is the most widely accepted (2, 3, 5, 6, 8). According to the adsorption theory, the adhesive must form intimate contact with the substrate surface. After intimate contact, adhesion is the result of interatomic and intermolecular forces (3). These forces range

in magnitude from weak van der Waals forces to strong covalent bonds. In order to control adhesion in the creping process, it is therefore essential to understand the interaction mechanism between the adhesive and the metal surface.

Of all possible types of interactions, hydrogen bonding may be a controlling factor in the interaction of the adhesive and Yankee Dryer surface in the creping process. Typically, adhesive materials, *e.g.* polyvinyl alcohol and polyamidoamine, are used to attach a paper web to the cast iron Yankee Dryer surface. In the presence of water and oxygen, the cast iron can oxidize and form an oxide layer on the surface. When adhesive is applied to the dryer surface, it can form hydrogen bonds and the oxide layer becomes a bridge between the adhesive and the metal surface.

In order to analyze the strength of the interaction of the adhesive and the cast iron surface, three different strength measurements were utilized, including atomic force microscopy, lap shear strength and creping force. The adhesion force measurement in the AFM was used to analyze the strength of the microscopic interactions (4,5). The lap shear test was used to analyze the strength of the overall adhesive system.

In this chapter, we also explore the influence of adhesive strength on creping process. The creping study was conducted using a creping machine developed at NCSU to analyze the properties of the creped paper, creping structure, and other characteristics of the process.

2.2 Experimental Materials and Methods

All chemicals were used as received without further purification. Filtered (0.02μm filter) water (MilliQ, resistivity 18.2 MΩ cm, Millipore, Bedford MA) was used for all aqueous solutions. Isopropyl alcohol and heptane (ACS grade) were obtained from Fisher Chemical Company. Commercial polyvinyl alcohol (PVA) with various molecular weights and acetate contents was obtained from Air Products and Chemicals Inc (see Table 2.1). The PVA solutions were prepared by dispersing the polymer in water and dissolved by raising the temperature to 85^{o}C with continuous stirring for 1 hour to facilitate dissolution.

Table 2.1 *Polymer Acetylation and Molecular Weights*

Polymer Sample	Degree of Acetylation (%)	Molecular Weight
A325	2	80,000
A350	2	107,100
A425	5	80,000
A523	12	79,100
A540	12	110,000

Adhesive strength measurements were conducted on an Instron 4411 machine according to ASTM D 1002-99 Lap shear test. Accordingly, a 10w/v% polymer solution was applied to the one end of an iron plate, and the second plate was placed so that it overlapped the adhesive coated plate with an overlapping area of 10*35mm^2. The lap shear measurements were taken

in a controlled environment of 23^{o}C and 50% relative humidity. Five samples were measured and the average was reported as the shear strength.

Creping force was measured on a creping instrument in the Wood and Paper Science Department at NCSU. The creping process was conducted at 180^{o}F. The creping angle was set to 85^{o}. The applied blade force to drum surface was adjusted to 85N. The 2w/v% aqueous adhesive solution was applied twice to drum surface using a rolling brush. Tissue paper samples were prepared at a basis weight of 30g/m^2 and in 50.8mm by 152.4mm strips. In order to carry out the creping process, tissue samples were attached to the drum surface with the help of PVA. The adhesive was allowed to dry for one minute. The creping force measurements were then carried out at 144m/min. After every four creped tissue papers, the drum surface was cleaned with MAAS fine metal polishing crème (MAAS International Inc.) followed by isopropyl alcohol and deionized water. After conducting the creping experiment, the creping frequency was recorded and the tensile strength of the creped tissue paper was determined.

The maximum load to failure and Young's modulus were obtained from the tensile test of creped tissue paper. Before performing the tensile test, all creped tissue samples were conditioned at 50% relative humidity and 23^{o}C for 24hrs. These samples were prestretched to 10cm length. An Instron machine was used with line contact grips to hold the sample. The gauge length was set to 5cm and a crosshead speed of 10cm/min. The software was set up to collect load versus strain data.

Intrinsic viscosity of the polymers was measured using a Cannon-Ubbelohde dilution viscometer. Ten milliliters of polymer solution (concentration ranging between 0.008 and 0.01g/ml) was charged to the viscometer. The viscometer was then inserted into a holder in a 25$\pm$1^{o}C water bath. In order to reach equilibrium temperature, it was allowed to sit for 20 minutes. The run time of the solution in the capillary was recorded for each polymer. After each run, the viscometer was cleaned with chromic acid

and water to remove adsorbed polymer from the viscometer glass surface and dried used acetone.

The radius of gyration for each PVA sample was determined by multiangle laser light scattering (MALLS) (DAWN EOS Wyatt Technology Corp., Santa Barbara, CA). Aqueous polymer solutions (concentration range between 0.008 and 0.01g/ml) were analyzed using a UV light wave length of 632nm and a machine temperature of 25^{o}C.

Surface tension of the aqueous polymer solutions was measured using a Fisher Surface Tensiomat employing du Nouy principles at 25 ^{o}C. In du Nouy principles, a platinum-iridium ring of known dimensions is suspended from a counter-balanced lever arm. The arm is held horizontal by a stainless steel torsion wire. Increasing the torsion on the wire raises the arm and the ring. The ring carries a thin film of the liquid from which it is immersed. The force necessary to pull the test ring free from the surface is measured, and recorded as the surface tension.

To simulate a Yankee Dryer surface, metal plates were prepared from cast iron. In order to fit the AFM fixture, the plates were cut to a size of $10\times10mm^2$. The plate surface was polished with silicon carbide papers having a grit size ranging from 240 to 4000. Each metal plate was then polished with micropolish alumina powder 1C (Buehler Alpha, Union Carbide Product) to a mirror-like finish.

Colloidal probes were prepared by attaching a spherical glass bead, approximately 10μm in size (Polysciences Inc., Warrington, PA), to a standard 100μm long wide-legged triangular, Si_3N_4 cantilever (Model NP) using a one-component, solvent-free, epoxy adhesive (NOA 81, Norland Products, New Brunswick, NJ) (Figure 2.1). The epoxy adhesive was crosslinked with UV light (λ=320 nm) overnight. The glass beads were then coated with polyvinyl alcohol and its acetate derivatives by carefully dipping them into a polymer solution and placing them on a glass slide. After dipping,

the glass beads were placed in a 60^{o}C oven for 1 hour and then placed on the bench top for 24 hours (Figure 2.2).

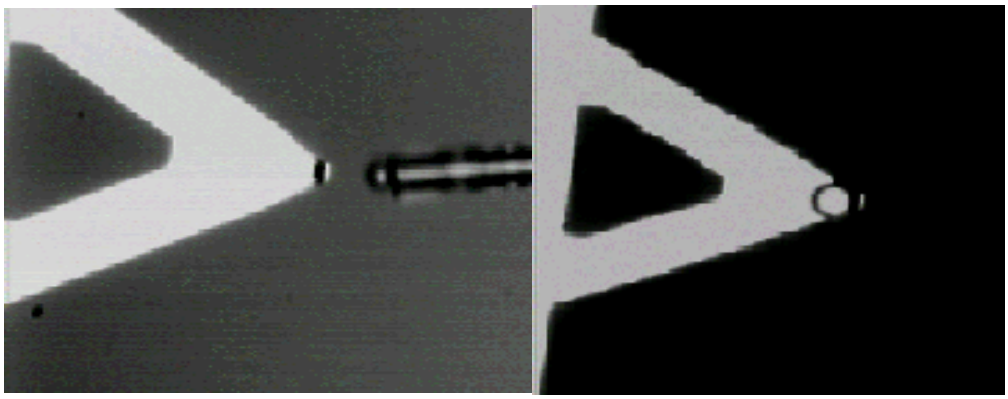

Figure 2.1 *Colloidal probe tip were prepared by application of UV curable adhesive on cantilever short wide leg (100μm) and spherical glass beads (D$\cong$ 10μm) were attached on top.*

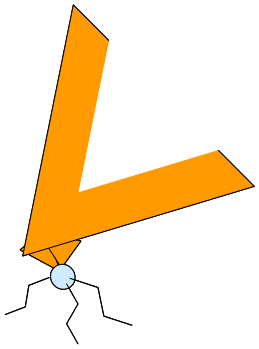

Figure 2.2 *Colloidal probe tips were utilized in order to measure adhesive bond strength. The glass bead on the probe tip was coated with the polymer of interest in and the measurement was performed in contact mode AFM in a liquid cell.*

Multimode AFM, equipped with a Nanoscope IIIa controller (Digital Instruments), was used to measure adhesion forces. The molecular adhesion

force measurement was carried out in contact mode AFM under water using a liquid cell on a cast iron surface. The sample surface was displaced up and down beneath the probe sphere attached to the cantilever. Thirty-five cycles were performed for each sample. Force measurements were carried out by recording the deflection of the probe tip. The deflection of the cantilever was detected by the position sensitive detector (PSD). The force detected by the AFM probe was calculated by multiplying the deflection of the cantilever with the cantilever spring constant. The cantilever spring constants were obtained using the thermal fluctuation method (9).

In order to evaluate the rate dependence of the adhesion failure, the AFM scan rate was varied between 0.49 Hz and 3.1 Hz at increments of 0.5Hz. This was done to determine whether adhesion failure occurred between the polymer on the probe tip and sample surface or viscoelastic properties of the adhesive.

As a control experiment, a glass surface was used to measure forces using one of polyvinyl alcohol coated probe tips (A350). A microscope glass slide was chosen as the sample because of its smooth surface. The objective of this experiment was to distinguish where the separation between the probe tip and sample surface occurs.

The adhesion strength obtained from the force-displacement curve was compared to a calculated JKR force value. In order to calculate the JKR force, the work of adhesion was determined. The following equation gives the relationship of the work of adhesion based on the interfacial surface tensions between the tip and sample, the sample and solvent and the tip and solvent.

$$W_{12} = \gamma_{12} + \gamma_{23} - \gamma_{13} \quad [2.1]$$

where W_{12} is the work of adhesion, γ_{12}, γ_{13}, and γ_{23} are the interfacial surface tensions between the tip and sample, the tip and medium, the sample and medium. Then, adhesion forces can be obtained by using Johnson-Kendall-

Roberts (JKR) theory (10). The JKR theory of adhesion describes the adhesion between a spherical tip 1 and a flat surface 2 in a medium 3:

$$Fa = (\frac{3}{2})\pi R W_{12} \qquad [2.2]$$

where R is the local radius of curvature and W_{12} is the work of adhesion between tip and sample surface.

2.3 Results and Discussion

Depending on the adhesive strength between the paper web and the cast iron surface, the creping force and frequency can be affected. In order to determine the adhesive strength effects on the creped tissue paper, various polyvinyl alcohol samples were utilized. All tissue samples showed different creping frequency and wavelength (Figure 2.3). The creping frequencies for the polymers are 25 for A350, 22 for A425, 13 for A523, and 21 for A540.

Polymer A350 gave the tissue a fine crepe; a creping frequency of 25 was obtained. Fine microfolds and small wavelengths indicate a high adhesive strength and creping force (11,12). Increased creping frequency and fine microfolds also imply more damage to the fiber. Creped tissue paper using adhesive A523 demonstrated a large wavelength and a coarse crepe structure. Coarse creping means large wavelength and smaller creping frequency. The creping frequency of 13 was obtained (A523). This value was much smaller than the frequency of A350. Large microfolds or a coarse crepe structure is an indication of low adhesive strength and creping force (11,12).

After determining the creping frequency, the question arises why each polymer has different crepe frequency and structure. In order to answer this question, each polymer was characterized by its intrinsic viscosity, radius of gyration, second virial coefficient, surface tension and adhesive strength on micro and meso levels.

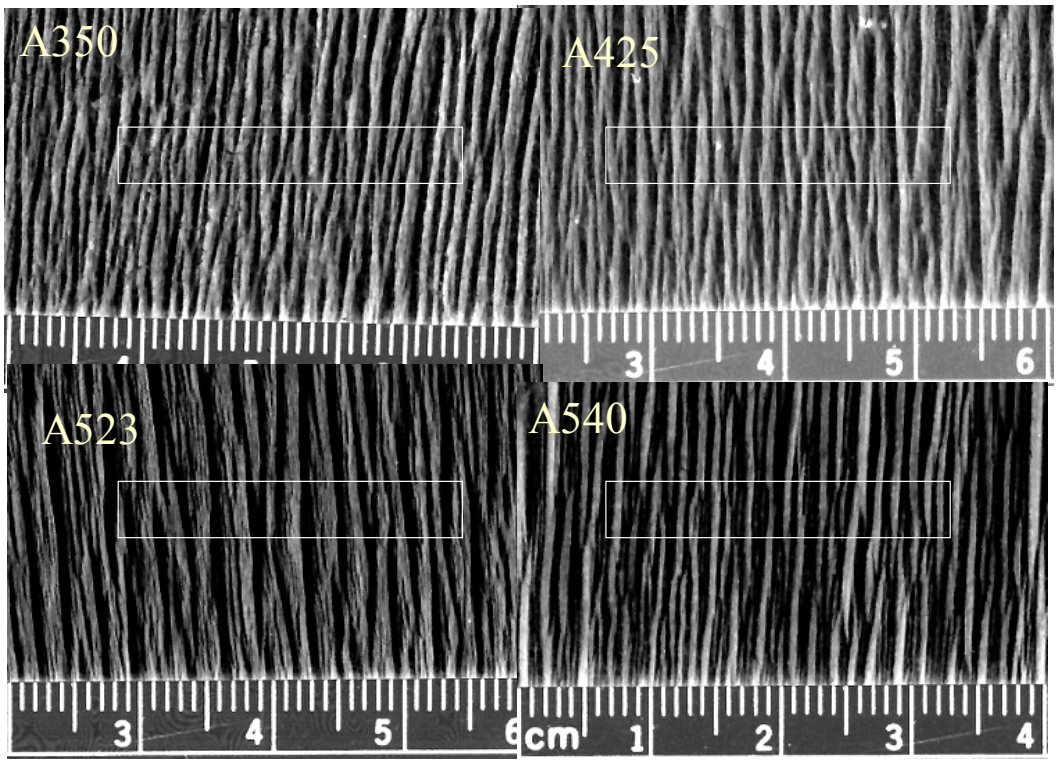

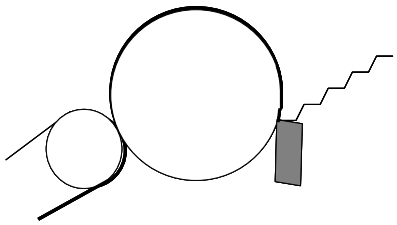

High adhesive bond strength cause fine small microfolds

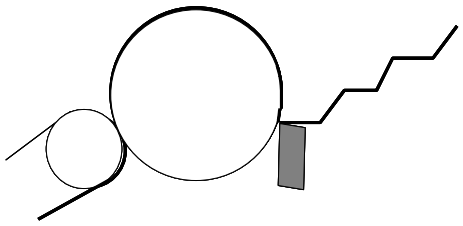

Low adhesive bond strength cause coarse big microfolds

Figure 2.3 *Tissue paper samples after creping process.*

2.3.1 Polymer Characterization

The way a liquid flows is one of the most obvious properties that reflects the size and shape of a dissolved solute in dilute solutions. Intrinsic viscosity is the easiest way to measure a polymer's molecular size and shape.

The relationship between the flow time of a polymer solution (t) and that of the pure solvent (t_o) is defined as the relative viscosity (13):

$$\eta_r = \frac{t}{t_o} \approx \frac{\eta}{\eta_o} \qquad [2.3]$$

From the relative viscosity, the specific viscosity of a polymer sample can readily be calculated:

$$\eta_{sp} = \eta_r - 1 = (t - t_o)/t_o \qquad [2.4]$$

The ratio of the specific viscosity (η_{sp}) to the concentration of the polymer solution gives the reduced viscosity. When the reduced viscosity (η_{sp}/c) is plotted against concentration (c), and extrapolated to $c=0$ concentration, the intrinsic viscosity of the sample can be obtained from the following equation:

$$(\eta_{sp}/c) = [\eta] + k'[\eta]^2 c \qquad [2.5]$$

where $[\eta]$ refers to intrinsic viscosity and k' indicates a shape dependent factor also called the Huggins constant. The Huggins constant (k') typically ranges between 0.3 and 1 for random coiling vinyl polymers (14). A higher value of k' indicates formation of aggregates and spherical polymers in solution. If the polymer is forming aggregates and behaves like spherical particles in solution, then it will flow easily in the viscometer. Thus, the intrinsic viscosity of the aggregates will be low.

Intrinsic viscosity can be further related to the molecular structure by:

$$[\eta] = \phi' R_g^3 M^{-1} \qquad [2.6]$$

where R_g is the radius of gyration and M is the molecular weight of the polymer. The parameter ϕ is a universal constant and equal to $2.1*10^{26}$ $kmol^{-1}$(32).

It can be seen in Figure 2.4 and Table 2.2 that the intrinsic viscosity of the polymers decreases with increasing acetyl content. Polyvinyl alcohol can readily associate with and extend in water due to the affinity of the hydroxyl groups to water. Compared to the hydroxyl groups in PVA, the acetyl groups are relatively hydrophobic affecting the polymer solubility and the shape of the polymer in solution (16). When a partially hydrolyzed polyvinyl acetate copolymer is put in water, it may collapse and cluster the acetate groups towards the center of the molecules, leaving the hydroxyl groups to the outside due to their affinity for water molecules (Figure 2.5). Clustering of acetate groups could lead to the formation of aggregates. Therefore, the intrinsic viscosity and radius of gyration would be low for a polyvinyl alcohol with high acetyl content.

The properties of the polyvinyl alcohol used in this experiment can be seen in Table 2.2. The high affinity of the hydroxyl groups to water appears to have an effect on the polymer properties. It can be seen from Table 2.2 that A350, which has a low acetyl content and a relatively high molecular weight, has a high intrinsic viscosity, a low Huggins constant (k') and a large radius of gyration. This polymer appears to be extending well in aqueous solution. When it is applied to a high-energy surface, it would be expected to establish a high contact area and have a relatively strong adhesive strength. In contrast, the intrinsic viscosity and radius of gyration for A540 was the lowest. This may indicate that the polymer A540 collapses in water to form aggregates due to its high acetyl content (Figure 2.5). In this case, when it is applied to a high-energy surface, a low contact area would result and a correspondingly weak adhesion strength could be obtained.

Table 2.2 *Polyvinyl alcohol properties.*

Polymer Sample	Degree of Acetylation (%)	Molecular Weight[17]	Intrinsic Viscosity (dl/g)	Huggins Constant (k')	Radius of Gyration (nm)
A325	2	80000	79.63.	0.56	99.5±8.2
A350	2	107100	115.29	0.36	111.7±13.3
A425	5	80000	72.95	0.75	79.1±13.6
A523	12	79100	71.82	0.80	71.3±16.0
A540	12	110000	56.28	0.71	46.7±8.3

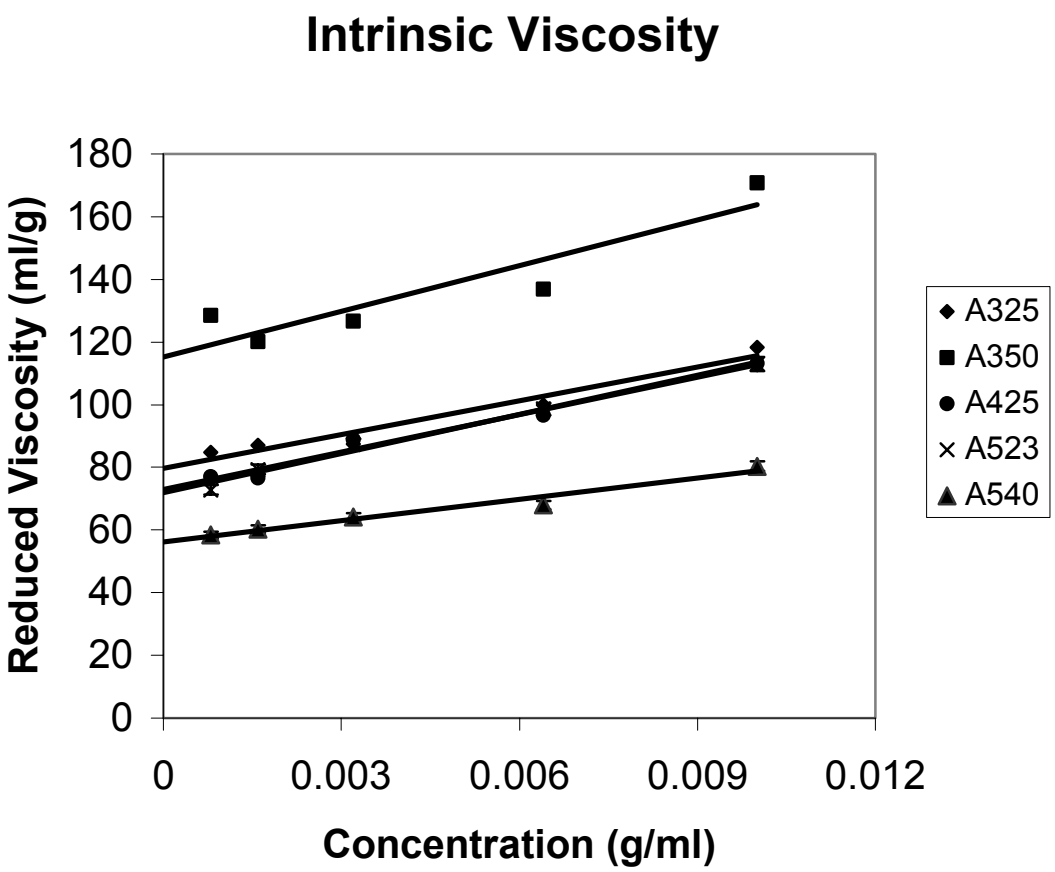

***Figure 2.4**. Intrinsic viscosity of polyvinyl alcohol in water at 25°C.*

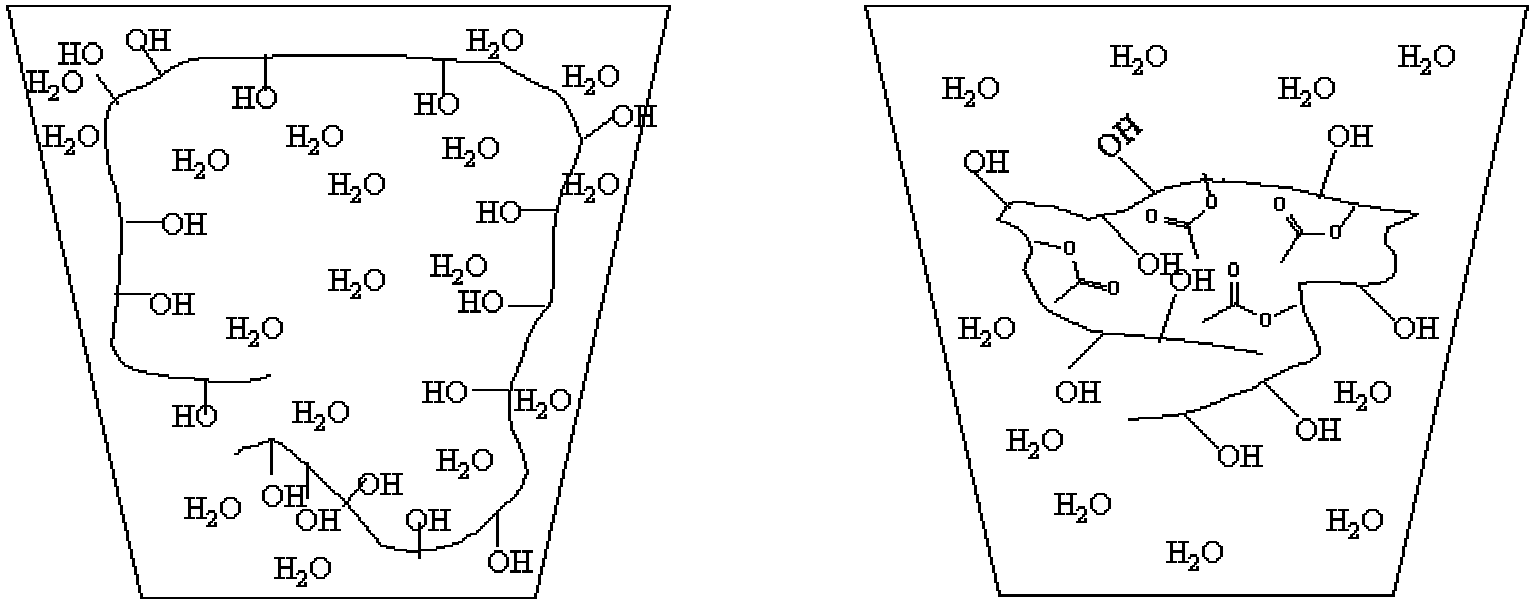

Figure 2.5 *Polyvinyl alcohol (A) and polyvinyl alcohol acetate copolymer (B) in water.*

Polymer-solvent interactions can be elucidated from the second virial coefficient. The second virial coefficient measures the solvent-polymer compatibility (18). In a good solvent, the second virial coefficient becomes a relatively large number and in a poor solvent, it becomes small. Comparing each polymer, we may be able to make some conclusions for polymer solvent interactions using the second virial coefficient. Table 2.3 shows the second virial coefficient for the various polyvinyl alcohol samples in water as obtained from light scattering measurement.

Table 2.3 *The second virial coefficient of polyvinyl alcohol.*

Polymer Sample	Second Virial Coefficient (A_2)(mol mL/g)
A325	0.15±0.02
A350	0.28±0.10
A425	0.18±0.04
A523	0.23±0.05
A540	0.15±0.07

Since a high value of the second virial coefficient indicates a better solvent for the polymer, water is a better solvent for A350 than the other polymers. This indicates that A350 has a higher affinity and extents better in water than the other polymers. A540 has the lowest affinity for water and the polymer may be forming aggregates by clustering acetate groups. A polymer that has a greater affinity for water can spread and extend to produce a larger radius of gyration. Then, when it is applied to a surface, it could have a larger contact area by spreading well on the surface, which could lead to a higher adhesive strength. Therefore, it would be expected that A350 with its high

radius of gyration should have a higher surface tension and adhesion strength than A540.

In order to adhere two materials, the atoms and molecules in two surfaces must come close together (19). Surface tension is a force that operates on the surface, which can control or limit the interaction of the two surfaces (18). Surface tension is responsible for the formation of liquid drops, the adsorption of liquids by porous substances and the ability of liquids to wet solid surfaces (20). The surface tension of the material can be changed by modifying its structure. In the case of a polymer, changing the chemical structure could change the surface tension and consequently the wetting ability of the polymer solution (21,22). Small amounts of certain functional groups can improve or reduce adhesion of polymers to a given substrate (21).

Figure 2.6 shows the surface tension measurements of the various polyvinyl alcohols with different acetyl content and molecular weight. It appears that the acetyl content significantly affects the intramolecular and intermolecular interaction in the polymer. The acetyl groups of the polyvinyl alcohol (A540 and A523) may have a more block-like chain distribution and form hydrophobic regions. These regions may cause collapse of the polymer chain and lower the surface tension of the polymer. For A350, the acetyl content is only 2% and this polymer has more hydrophilic groups than that of A540. When A350 is in water, it extents and offers more intermolecular interaction and this may give rise to higher surface tension. Increasing the concentration of A350 in water slightly decreases the surface tension.

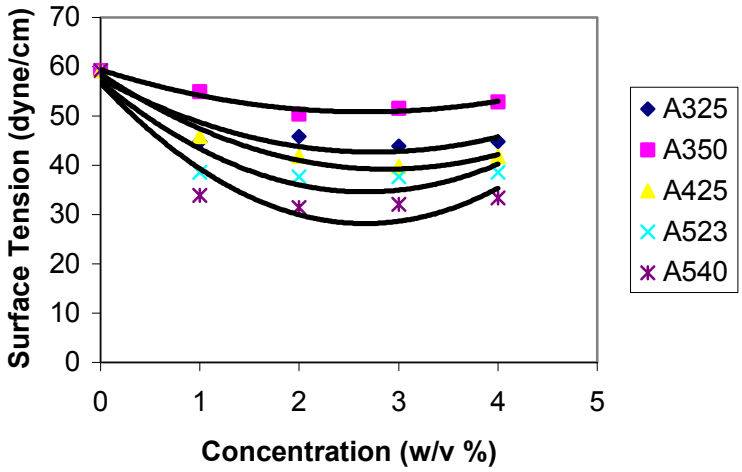

Figure 2.6 *Surface tension of aqueous solutions of polyvinyl alcohol with different acetyl content and MW.*

Surface tension is dependent upon intermolecular forces and measures the sum of the intermolecular forces, such as dispersion forces and hydrogen bonding (23). In saturated hydrocarbons, surface tension depends only on dispersion forces (γ^d). Thus, when the surface tension of a polymer solution is measured in heptane, the dispersion force contribution of the surface tension for the polymer solution can be determined. If the dispersion force component of the surface tension is subtracted from the surface tension of the polymer (γ), the acid-base contribution can be obtained. The surface tension due to dispersion forces (γ^d) and acid-base interactions (γ^{ab}) of the polyvinyl alcohols were obtained using heptane (Table 2.4).

Table 2.4 *Surface tension and its components of the polymer solutions at 25°C.*

Polymer Sample	Surface Tension (γ) (dyne/cm)	Dispersion Component (γ^d) (dyne/cm)	Acid-base component (γ^{ab}) (dyne/cm)
A325	45.9	21.4	24.5
A350	50.4	26.5	23.9
A425	41.8	17.6	24.2
A523	37.6	16.5	21.1
A540	31.4	21.5	9.9

As the polyvinyl alcohol hydroxyl groups are substituted with acetyl groups, the surface tension and the acid-base component of the surface tension appear to decrease. This may again be due to the hydrophobic character of the acetyl group. When they collapse, the aggregated polymers may reduce the number of available interaction sites and the contact area with the surface. Reduced contact area can be represented by an increase in contact angle (i.e. bad wetting) and may reduce the adhesive strength (Figure 2.7). It may also indicate that when the polymer is applied to a high-energy surface, the highly hydroxylated polyvinyl alcohol could give a higher adhesive strength.

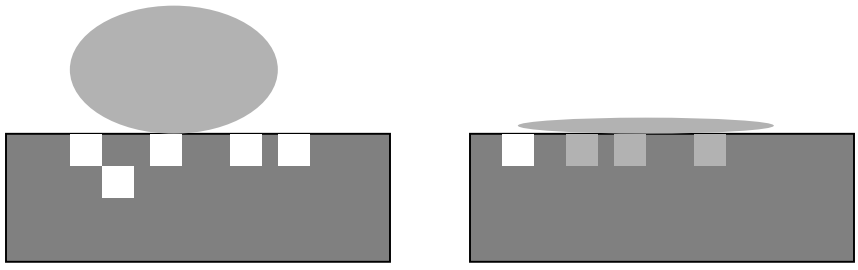

Bad Wetting Good Wetting

Figure 2.7 *Wetting ability of the adhesive solution on cast iron surface.*

The relationship between the surface tension and the work of adhesion has been designated as (24):

$$W_A = \gamma_L + \gamma_S - \gamma_{SL} \qquad [2.7]$$

where γ_L is the surface tension of the liquid, γ_S is the surface tension of the solid and γ_{LS} is the interfacial surface tension between the liquid and the solid.

Work of adhesion can also be represented as the sum of the work of adhesion due to dispersion forces (W_{SL}^{d}) and the work of adhesion due to acid base interactions (W_{SL}^{ab}) (25), assuming that only these two types of interaction exist in the system.

$$W_a = W_{SL}^{d} + W_{SL}^{ab} = 2(\gamma_s^{d}\ \gamma_l^{d})^{1/2} + W_{SL}^{ab} \qquad [2.8]$$

The dispersive component of the work of adhesion (W_{SL}^{d}) can be estimated from the geometric mean of the dispersive components of the surface tension of the solid and liquid (23). Therefore, the work of adhesion due to acid base interaction can be calculated by the subtraction of W_{SL}^{d} from W_a.

$$W_{SL}^{ab} = W_a - W_{SL}^{d} \qquad [2.9]$$

It has been reported that the surface tension due to dispersion forces for Ferric oxide is 107 dyne/cm (26). Using this value, the work of adhesion due to dispersion forces for the various PVA samples was determined (Table 2.5).

Table 2.5 *Work of adhesion between polyvinyl alcohol and iron oxide surface (W_a= Total Work of adhesion, W_{SL}^{d}= Work of adhesion due to dispersion forces, W_{SL}^{AB}= Work of adhesion due to acid-base interactions)*

Polymer Sample	W_a (dyne/cm)	W_{SL}^{d} (dyne/cm)	W_{SL}^{AB} (dyne/cm)
A325	150	94	56
A350	156	106	50
A425	140	87	53
A523	131	84	47
A540	119	96	23

The work of adhesion values and acid-base work of adhesion component appear to have the expected increase with respect go increasing hydroxyl content. Unexpectedly, the dispersion force contribution of the work of adhesion changes in all polymer samples. However, when all of the polymer samples are compared, these changes may not be significant. For example, A540 has a higher work of adhesion due to dispersion forces than that of A425 (Table 2.5). However, when the work of adhesion for the same polymers are compared, total work of adhesion for A425 is higher than A540. This could be due to the acid-base component of the work of adhesion. The acid-base contribution of the surface tension is low in A540. Therefore, acid-base interactions could be a controlling factor for adhesive strength and total work of adhesion.

Surface tension in saturated hydrocarbons is only due to dispersion forces (23). Thus, polypropylene, which is a saturated hydrocarbon polymer, interacts with high-energy surfaces due to dispersion forces. However, when carboxylic acid groups are introduced into polypropylene, modification introduces polar groups on the polymer chain. As a result, surface tension becomes the sum of dispersion and polar forces. Increased interaction forces between surfaces can therefore improve the adhesive strength. For example, in the literature, adhesive strength of polypropylene was improved when it is modified with carboxylic acid groups (21,27-29). Adhesion was enhanced by a factor of 2 to 10. Our results also agree with this experiment, insofar as the increasing acid-base component of the polymer increased the surface tension.

2.3.2 Adhesive Force Measurements

Adhesive bond strength can be measured on a macroscopic level with creping and lap shear tests (30). On a molecular level, it can be measured with colloidal probe microscopy (CPM) (9,15,31,33). In order to compare the

adhesive strength of various polyvinyl alcohol samples, ASTM D 1002-99 lap shear test was utilized.

High adhesive strength was obtained from the polymer (A350) having high hydroxyl content (Table 2.6). Increasing acetyl content in the same molecular weight polymer decreased the adhesive strength. These results were expected based on the properties of each adhesive polymer. When the more acetylated polymer is applied to surface, the polymer may collapse and reduce the contact area with the cast iron surface and increase the contact angle (Figure 2.7). This constraint in the polymer chain may result in a decrease in the adhesive strength.

2.3.2.1 Creping Force Measurement

An adhesive strength test was performed on a laboratory creping device. Higher creping force was obtained from the highly hydroxylated polymer (Table 2.6). The higher creping force indicates that the more hydroxylated polymer has a stronger adhesive interaction with the cast iron surface. These results are in good agreement with the lap shear test results.

Table 2.6 *Creping force was measured on the laboratory creping device for each polyvinyl alcohol sample.*

Polymer Sample	Lap Shear Strength (kN)	Creping Force (N)
A325	18.52±1.02	53.4
A350	19.61±1.1	55.1
A425	16.66±1.2	41.3
A523	14.38±1.7	40.9
A540	10.74±1.9	24.8

High adhesive strength improves the softness of the tissue paper, while also having an adverse effect on Young's modulus and tensile strength (11). Typical load curves for uncreped and creped tissue sample can be seen in Figure 2.8. During the creping process, many of the fiber-to-fiber bonds are broken, and this mechanical treatment reduces the strength of the paper. Figure 2.8 clearly demonstrates these properties of the tissue product.

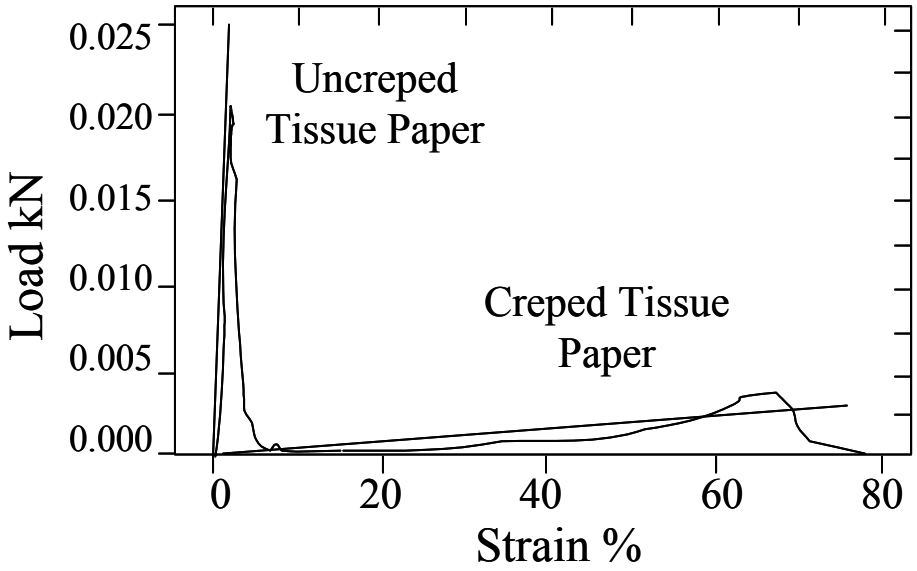

Figure 2.8 *Typical load versus strain curve for creped and uncreped tissue paper.*

In order to compare the effect of the different adhesive strengths on paper properties, Young's modulus was plotted versus creping force (Figure 2.9). An inverse relationship was found between the Young's modulus and the creping force; the creping force decreased while Young's modulus increased.

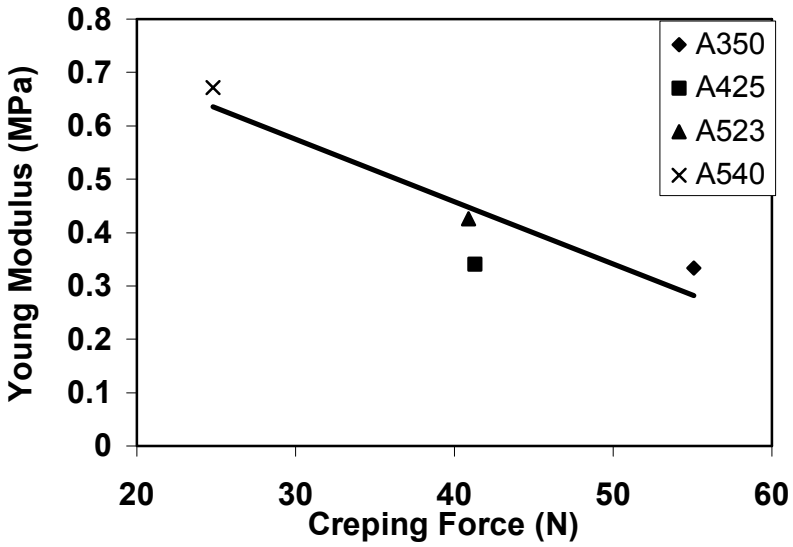

Figure 2.9 *Adhesive strength affects creping force.*

2.3.2.2 Colloidal Probe Microscopy in Creping Process

The adhesive bond strength of polyvinyl alcohol on a cast iron surface was measured with colloidal probe microscopy (CPM). Colloidal probe microscopy can provide nanometer-scale quantitative, chemically dependent information on the interaction between the colloidal probe and the sample surface. Before measuring the adhesion force between the polyvinyl alcohol and the cast iron surface, the effect of scan rate on the adhesion force was evaluated. Polyvinyl alcohol A523 was used (Figure 2.10). Figure 2.10 shows that the relationship between the adhesive strength and the scan rate. In general, the adhesive strength remained constant through changing scan rate. Thus, for the given experimental conditions and for the range of scanning rates tested, there is no dependence of the force results on scanning rate.

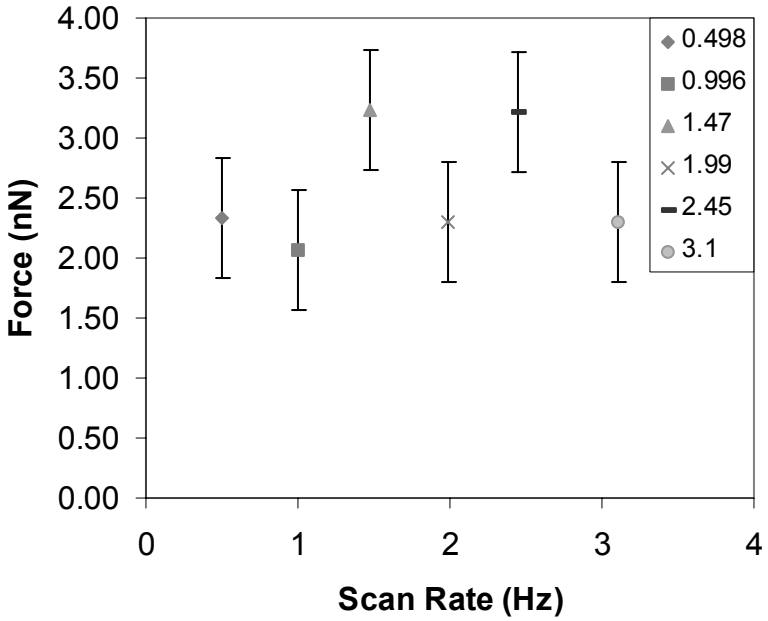

Figure 2.10 *The rate dependence of the adhesive failure on the cast iron surface.*

As a control experiment, a microscope glass slide was used as a substrate to measure adhesion forces with the cantilever. Glass is made of silicon oxide, which may have the ability to form hydrogen bonds with polyvinyl alcohol. A force-displacement curve of the interaction of a glass slide surface and a PVA coated bead can be seen in Figure 2.11. The cantilever starts to feel long-range forces around 0.3μm. These forces overcome the cantilever spring constants and the cantilever contacts with the surface around 0.35μm. The deep well at 0.33μm shows the adhesion amount between the surface and the colloidal probe. The adhesive force measured on glass surface with polyvinyl alcohol (A350) sample under water was 68±4.4nN. If the value obtained from metal-polymer interaction is equal to or less than this value, we may be able to say the separation is taking place between the polymer and metal. This would indicate that forces we observe in AFM would accurately reflect the interactions between the polymer

and metal surface. Also, it is proposed by Boland *et al.* that AFM is able to detect hydrogen bonding (34). The curves in the literature were similar to the figure below (Figure 2.11) and the authors observed that the second smaller peak represented the hydrogen bonding interaction. See Appendix A for the AFM results observed on the model system.

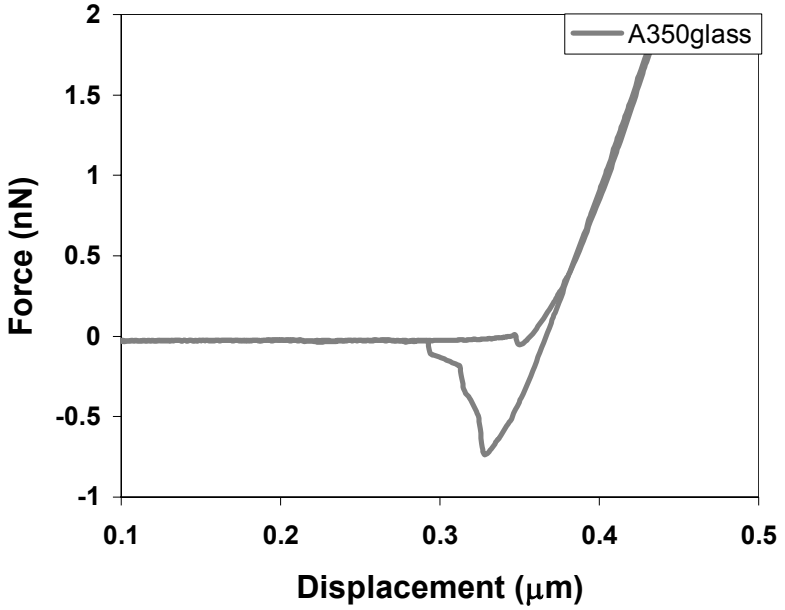

Figure 2.11 *Force-displacement curve on microscope glass slide in liquid cell.*

Typical force-separation curves for the various polyvinyl alcohol samples on a cast iron surface can be seen in Figure 2.12. The force-separation curve appears to demonstrate polymer bridging. This could be due to dangling polymer chains on the colloidal probe or polymer entanglement in the crevices and pores of the cast iron surface. In a good solvent, the polymer attached by one end of the chain to a colloidal probe surface could extend to form a brush-like structure (35,36). As a result,

multiple chain ends could start to break when the sample surface is pulled back.

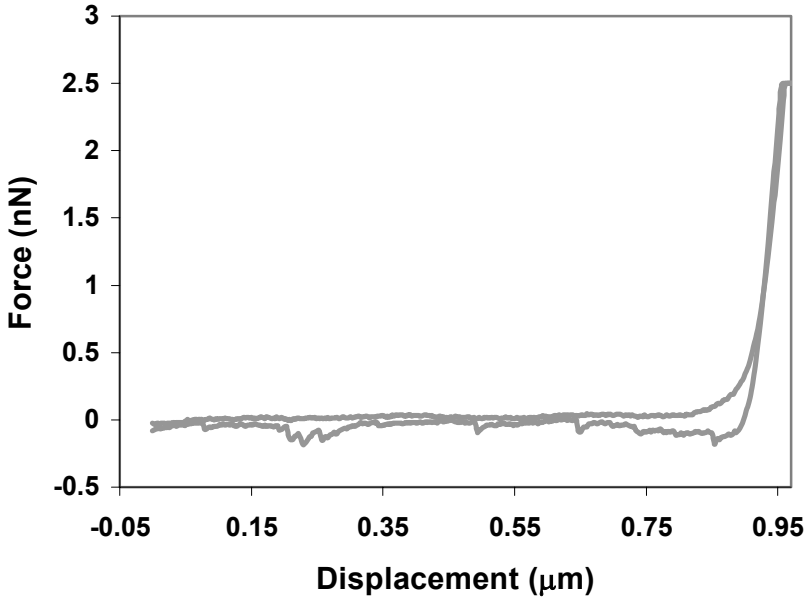

Figure 2.12 *Typical force-separation curve for polyvinyl alcohol on a cast iron surface in a liquid cell.*

All tip-sample interactions were characterized by measuring their adhesion forces. To quantify the differences in the adhesion measurements between different polymer samples, these data were plotted as histograms and the mean value of the adhesive interaction and standard error were determined (Figure 2.13).

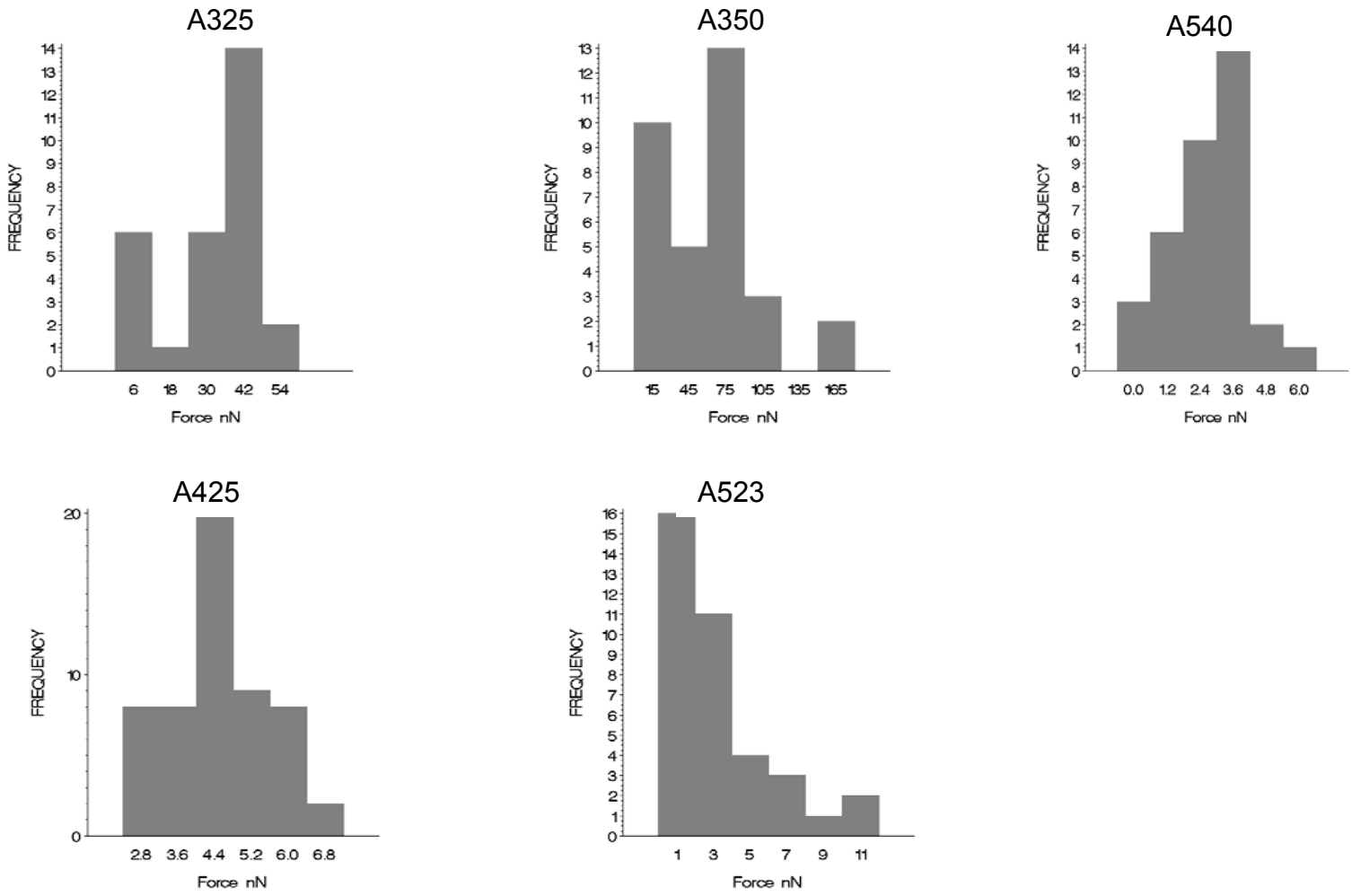

Figure 2.13 *A histogram of adhesion force was observed in repetitive measurements using various polyvinyl alcohol samples coated colloidal probe on cast iron surface in liquid cell. Normalized force data and tip radii can be found in Appendix B.*

The observed adhesive strengths were in agreement with the previous results from lap shear tests and the creping force experiment. The agreement can be seen in Table 2.7 and Figure 2.14 for each adhesive strength mean value. There is a significant difference between the highly acetylated polymer and highly hydrolyzed polymer. Polymers A350 and A325 were significantly different from the other three polymers (Figure 2.14). Adhesion forces were 64nN for A350 and 34nN for A325. In contrast, A540 and A523 had very close adhesive strength and they were smaller than A350, A325 and A425. Adhesion forces were 4.4nN for A425, 3.5 for A523 and 2.4 for A540. This difference in the adhesive forces could be due to the acid-base interactions of the polymer. We have found that the acid-base contribution to the surface tension for A540 was the lowest.

Pull-off forces were also estimated from JKR theory (see Table 2.7) (10). In order to obtain the pull off force, work of adhesion must first be calculated. In the calculation of the work of adhesion, we assumed that the metal surface was totally covered with iron oxide and for the tip-sample, medium-sample and sample-tip interactions, iron oxide surface tension (1357mN/m) was used. Comparing this value with the surface tension of the polymer solution, the iron oxide surface tension is very high. Therefore, when it was used to estimate pull-off forces, we obtained large force values. Even though the calculated adhesion forces were much larger than the observed forces, the trend followed the same direction. The highest adhesion strength was obtained with A350, whereas the lowest adhesion was obtained with A540.

Table 2.7 *Analysis of adhesive forces for each polymer on the cast iron surface.*

Polymer	F_m (nN)	Variance (nN^2)	Std. Dev. (nN)	Std. Error	F_{JKR} (nN)
A325	33.9	238	15	3	3327
A350	64	199	44	8	3511
A425	4.4	1.2	1	0.2	3003
A523	3.5	8.1	3	0.5	3240
A540	2.4	1.8	1	0.2	2984

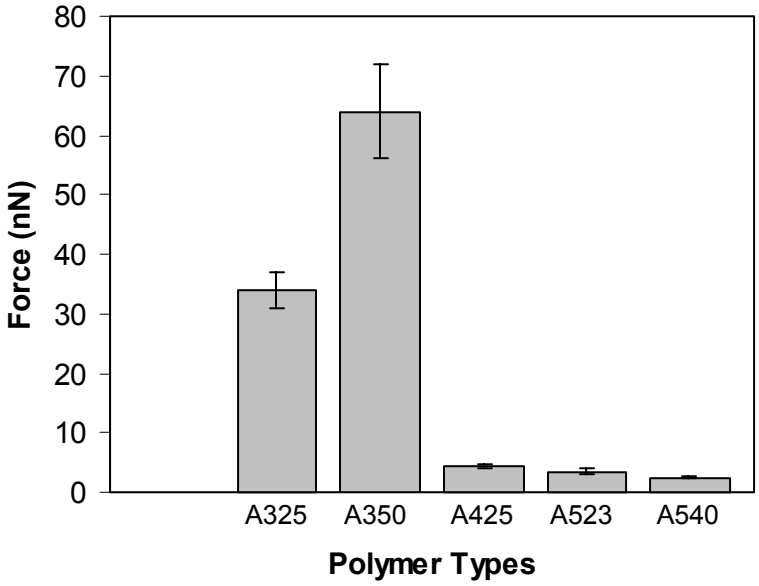

Figure 2.14 *Adhesive bond strength of each polymer represented with a 95 % confidence interval.*

2.4 Conclusions

Polyvinyl alcohol behaves differently in aqueous solution depending on its acetyl content. Low intrinsic viscosity was obtained for the polyvinyl alcohol with a higher hydrophobic acetyl content (A540). High radius of gyration and high surface tension were obtained from the polyvinyl alcohol that had high hydroxyl content (A325, A350). In contrast, a small radius of gyration and a small surface tension were obtained from the polyvinyl alcohol that had high acetyl content (A540).

The relatively hydrophobic acetyl groups seem to affect the intramolecular and intermolecular interactions. High acetyl content in polyvinyl alcohol would appear to cause collapse of the polymer chain. In the molecular collapse, the acetyl groups would remain in the center of the molecule. Collapsed and aggregated polymers flow easily through the viscometer. They may also reduce the contact area and intermolecular interaction. Thus, adhesive strength is low. Conversely, the hydrophilic hydroxyl groups appear to repel each other and extend in aqueous solution due to their affinity to the solvent. This improves the ability of the polymer to make contact for adhesion.

Surface tension is a direct measurement of intermolecular forces. It measures the sum of each intermolecular force contribution, such as dispersion forces and hydrogen bonding (23). Polyvinyl alcohol with high acetyl content yields a solution having a low surface tension. Acid-base interactions of this solution appear to have the lowest contribution to surface tension. This could be due to the collapsed structure of the polymer.

It is believed that the properties of the hydroxylated polymer will improve its ability for contact with the metal surface. This would facilitate improve adhesion based on more intimate contact for intermolecular interaction to occur.

In order to measure adhesive strength, ASTM D1002-99 lap shear strength standard test on Instron machine and creping force measurement on creping machine were performed. Both adhesive strength tests confirmed that acetyl content in polyvinyl alcohol reduced the adhesion on cast iron surface.

Adhesive strength was also measured by using colloidal probe microscopy. The trend in adhesive force measurement was consistent with the previous experiment results with 95% confidence; the bond strength was high for the high hydroxyl-content polymer and significantly decreased with increasing acetyl content.

Adhesive strength also affects the creped paper properties. High adhesive strength gave a fine microfold structure with a high creping frequency and a smaller wavelength. By contrast, low adhesive strength gave a coarse creping structure and low creping frequency. Low Young's modulus and breaking strength were obtained from the tissue paper, having a fine creping structure, whereas high Young modulus and breaking strength were obtained from the tissue paper having coarse creping structure and low creping frequency.

2.5 References

1. Krelid, I.; “Drying of Tissue” in Papermaking Part 2, Drying, 147, 2000.
2. Pocius, A.V.; Adhesion and Adhesives Technology an Introduction, Hanser Publisher, Cincinnati, 118, 1997.
3. Kinloch, A.J.; Adhesion and Adhesives Science and Technology, Chapman Hall, 18, 1987.
4. van Ooij, W.J.; “Interfacial Interactions between Polymers and Other Materials and Their Effects on Bond Durability” in Physicochemical Aspects of Polymer Surfaces, Edited By K.L Mittal, Plenum press, 1035, 1981.
5. Fourche, G.; “An Overview of the Basic Aspects of Polymer Adhesion. Part 1: Fundamentals” Polymer Engineering and Science, **35**(12), 957, 1985.
6. Moskvitin, N.I.; Physicochemical Principles of Gluing and Adhesion Processes, 3, 1969.
7. Comyn, J.; Adhesion Science, RSC Paperbacks, 3, 1997.
8. Allen, K.W.; “Some Reflections on Contemporary Views of Theories of Adhesion” Int. J. Adhesion and Adhesives, **4,** 67, 1993.
9. Vezenov, D., Noy, A., Rozsnyai, L.F., Lieber, C.M.; “Force Titrations and Ionization State Sensitive Imaging of Functional Groups in Aqueous Solutions by Chemical Force Microscopy” J.Am.Chem. Soc., **119,** 2006, 1997.
10. Johnson, K.L., Kendall, K., Roberts, A.D.; “Surface Energy and Contact of Elastic Solids” Proc. R. Soc. London A, **324,** 301, 1971.
11. Sun, Z., NCSU, PhD dissertation, Raleigh, NC 1999.
12. Hollmark, H.; “Study of the process on an experimental paper machine”, STFI meddelande, Serie B Nr 144, 1972.
13. Cowie, J.M.G; Polymers: Chemistry and Physics of Modern Materials, Intertext Books, 1973.

14. Huggins, M.L.; J. Am. Chem. Soc., **64,** 2716, 1942.
15. Zauscher, S., Klingenberg, D.J.; "Normal Forces Between Cellulose Surfaces Measured with Colloidal Probe Microscopy" J. Colloid Interface Sci., **229,** 497, 2000.
16. Moore, W.R.A.D., O'Dowd, M.; "Factors Affecting Aqueous Solubility of Polyvinyl Alcohol and Partially Hydrolyzed Polyvinyl Acetate" in Properties and Applications of Polyvinyl Alcohol Edited By C.A. Finch, SCI Monograph No: 30, Society of Chemical Industry, London, 77, 1968.
17. Nguyen, D.T.; "Determination of Equilibrium Surface Energy of Adsorbed PVA layers in Water at 25^{o}C" Colloids Surf. A. Physicochem. Eng. Aspects **116**, 145, 1996.
18. Rodriguez, F.; Principles of Polymer Systems; McGraw Hill, NY, 1970.
19. Good, R.J.; "Definition of Adhesion" J. Adhesion, **8,** 1,1976.
20. Hiemenz, P.H., Rajagopalan, R.; Principles of Colloid and Surface Chemistry, 3rd Edition, Marcel Dekker Inc., NY, 249, 1997.
21. Schultz, J., Carre, A., Mazeau, C.; "Formation and Rupture of Grafted Polyethylene/Aluminum Interfaces" Int. J. Adhes. Adhesives, 163, 1985.
22. Petke, F.D.; "Structure Property Performance Relationships in Synthetic Polymeric Adhesives" in Adhesion Science and Technology, Edited by L.-H. Lee, Plenum Press, New York,177, 1975.
23. Fowkes, F.M.; "Molecular Forces at Interfaces" in Surfaces and Coatings Related to Paper and Wood Edited by R.H.Marchessault, C.Skaar, Syracuse University Press, 99, 1967.
24. Israelachvili, J.N.; Intermolecular and Surface Forces, 2nd Edition, Academic Press, San Diego CA, 1992.
25. Allara, D.L.; Fowkes, F.M., Noolandi, J., Rubloff, G.W., Tirrell, M.V.; "Bonding and Adhesion Polymer Interfaces" Materials Sci. Eng., **86,** 213, 1986.

26. Fowkes, F.M.; “Attractive Forces at Interfaces” Industrial Eng. Chem., **56**(12), 40, 1964.
27. Jochen, F., Janke, A., Schmitt, F.J.; “Direct Force Measurements for the Characterization of Modified Polypropylene” Macromol. Chem. Phys., **202,** 194, 2001.
28. Hong, S.G., Ho, C.A.; “The Adhesion Properties of a Plasma Modified Thermoplastic Olefin Elasteromer” Macromolecular Materials and Engineering, **286**(10)**,** 583, 2001.
29. Hoore, M.C., Stevens, G.C.; “Adhesion Enhancement of Polymer Surfaces by Atmospheric Plasma Treatment” J. Physics D Applied Physics, **34**(18), 2754, 2001.
30. Ramasubramanian, M.K., Crews, W.R.; “Shear Strength of an Adhesively Bonded Paper-Metal Interface” J. Pulp Pap Science **24**(1), 31, 1998.
31. Noy, A., Vezenov, D., Lieber, C.M.; “Chemical Force Microscopy” Annu. Rev. Mater. Sci., **27,** 381, 1997.
32. Carreau, P.J., De Kee, D.C.R., Chabra, R.P.; Rheology of Polymeric Systems, Principles and Applications; Hanser/Gardner Publishers Inc., Cincinnati, 73, 1997.
33. Noy, A., Frisbie, C.D., Rozsnyai, L.F., Wrighton, M.S., Lieber, C.M.; “Chemical Force Microscopy – Exploiting Chemically Modified Tips to Quantify Adhesion Friction and Functional Group Distributions in Molecular Assemblies” J.Am.Chem. Soc., **117,** 7943, 1995.
34. Boland, T. and Ratner, B.D.; “Direct Measurement of Hydrogen Bonding in DNA Nucleotide Bases by Atomic Force Microscopy”, Proc. Natl. Acad. Sci. USA, Vol. 92, 5297, June 1995.
35. Milner, S.T., “Polymer Brushes” Science, **257,** 905, 1991.
36. Koutsos, V., van der Vegte, E.W., Grim, P.C.M., Hadziioannou, G.; “Isolated Polymers Chains via Mixed Self Assembled Monolayer

Morphology and Friction Studied by Scanning Force Microscopy" Macromolecules, **31**(1), 116, 1998.

Chapter 3 - Determination of Adhesion Forces between Adhesives and Metal Surfaces Using Atomic Force Microscopy

3.1 Introduction

Adhesion can be defined as the sum of intermolecular forces that act between two materials (1). The type and magnitude of the intermolecular forces that operate between the interfaces is important in many applications; it is particularly important in the creping process. The creping process is implemented on a Yankee dryer surface, which is made of cast iron. The paper is attached to the cast iron surface with the help of an adhesive. The severity of the creping process is dependent upon a number of factors, including the adhesion between the adhesive and the metal surface. Too much adhesion can cause tearing and picking of the paper, whereas too little adhesion prevents creping. Thus, the adhesion properties of the coating chemistry will determine what sort of paper properties will be produced and what operating conditions will be needed around the Yankee dryer. The creping process produces a soft and bulky paper by reducing fiber-to-fiber bonds in tissue paper (2). Ideally, the manufactured tissue product should have increased softness, bulk, stretch, and absorbency.

Adhesion can be the result of a number of intermolecular forces. Therefore, the key interactions controlling the adhesion should be broken down into fundamental types of chemical forces, including hydrogen bonding, van der Waals, or electrostatic forces in order to understand the adhesion mechanism better. This can be done by using Chemical Force Microscopy (CFM) (3).

The heart of AFM is a sharp tip that interacts with a sample surface at a distance of atomic dimensions (4,5). The interaction force between the tip and sample surface is affected not only by the morphology of the sample

surface but also by the tip and sample chemical composition. The medium in which the measurement is performed also affects the interaction forces (6,7,8). Adhesive forces are probed by measuring the deflection of the cantilever from the surface (6, 7, 8, 9, 10). To further understand the type of interaction, the probe tip and sample surface are typically modified with self-assembled monolayers of different functional groups such as carboxylic acid terminated thiols or methyl-terminated thiols to demonstrate the interactions between different tips and sample surfaces (3, 6,8,11).

Using the CPM, the influence of the chemical structure on the adhesion properties of the polymer to a cast iron surface was studied. We hypothesize that acid-base interaction in creping process controls adhesion on the cast iron surface and that mechanical interlocking plays a less important role. This hypothesis was examined by measuring the adhesion forces between a chemically modified tip of varying functionality and a modified model surface and compared to the results obtained on a cast iron surface.

3.2 Experimental Methods and Materials

3.2.1 Chemicals

All chemicals were used as received without further purification. Filtered (0.2 μm filter) MQ water (Milli-Q resistivity 18.2 MΩ cm, Millipore, Bedford, MA) was used for all aqueous solutions and for rinsing. Undecanethiol (95%), 11-mercaptoundecanol (95%), DMSO-d_6 and acetone-d_6 were obtained from Aldrich chemical company. Dimethyl sulfoxide (DMSO) (ACS grade), pyridine and acetic anhydride (certified, ACS grade) were obtained from Fisher Chemical Company. Polyvinyl alcohol was obtained from Eastman-Kodak Chemical Company with a molecular weight of 93400 and was 99-100% hydrolyzed. The cast iron plate was obtained from McMaster-Carr co. PA.

3.2.2 Polymer Synthesis and Characterization

Polyvinyl acetate samples were synthesized from 100% hydrolyzed polyvinyl alcohol. Therefore, the degree of polymerization for each polymer was kept constant at 2123 with the same number of carbons on the backbone. Acetylation of the polyvinyl alcohol was carried out in pyridine/acetic anhydride (2:1 v/v) solution with continuous stirring at 70^{o}C and different time intervals (see Table 3.1). Acetyl content of the polymers was quantified by ^{1}H-NMR spectra (GE 300 MHz). The resulting polyvinyl alcohol ^{1}H-NMR data are listed in Table 3.2.

Table 3.1 *Reaction conditions for polyvinyl alcohol acetylation.*

Polymer Type	% Acetylation	Reaction Time (min)	Temperature °C
PVA	-	-	-
PVAc25	25	10	70
PVAc42	42	20	70
PVAc85	85	25	70
PVAc	100	60	70

Table 3.2 *^{1}H-NMR Spectra data of polyvinyl alcohol*

Polymer	NMR Data*
PVA	^{1}H-NMR (DMSO) δ (ppm) 1.4 (d 2H), 3.85 (s 1H), 4.5 (t 1H)
PVAc25	^{1}H-NMR (DMSO) δ (ppm) 1.4 (d 2H), 1.7 (s 2H), 2 (s 3H), 3.8 (s 1H), 4.5 (t 1H), 5 (s 1H)
PVAc42	^{1}H-NMR (DMSO) δ (ppm) 1.4 (d 2H), 1.75 (s 2H), 2 (d 3H), 3.75 (s 1H), 4.5 (t 3H), 4.8 (s 1H)
PVAc85	^{1}H-NMR (DMSO) δ (ppm) 1.7 (s 2H), 1.95 (t 2H), 2.1 (s 3H), 4.8 (s 1H)
PVAc	^{1}H-NMR (Acetone) δ (ppm) 1.8 (d 2H), 2.3 (d 3H)

*See Appendix C for chemical shift and integration of polyvinyl alcohol samples.

The physical properties of the polymer are summarized in Table 3.3. Intrinsic viscosity of the polymers was measured using a Cannon-Ubbelohde dilution viscometer. In order to dissolve and compare all the polymers in the same condition, dimethyl sulfoxide (DMSO) was used as a solvent. See Chapter 2 for the general method for obtaining intrinsic viscosity of the polymers.

See Chapter 2 for the method obtaining surface tension of the polymers. Table 3.3 shows the properties of the tailored polymers tested in this chapter.

Table 3.3 *Polymer properties.*

Polymer Sample	Degree of Acetylation (%)	Molecular Weight	Intrinsic Viscosity (dl/g)	Huggins Constant k'	Radius of Gyration nm
PVA	0	93400	130.97	0.51	180
PVAc25	25	115689	112.16	0.3	184
PVAc42	42	124604	106.49	0.26	185
PVAc85	85	169181	55.91	0.63	165
PVAc	100	182554	49.12	0.82	162

3.2.3 Chemical Force Microscopy

In order to measure adhesion forces on a well-characterized surface, substrates were prepared from glass cover slides. These substrates were coated by thermal evaporation of an adhesive layer of chromium (Cr) (thickness of 2nm) followed by gold (Au) (500nm thickness). A monolayer of functional groups was formed immediately after evaporation of Au (Figure 3.1). Self-assembled monolayers of 11-mercaptoundecanol (OH) were prepared by immersion of the freshly Au coated substrate in 3mM ethanol solution for 12 hours.

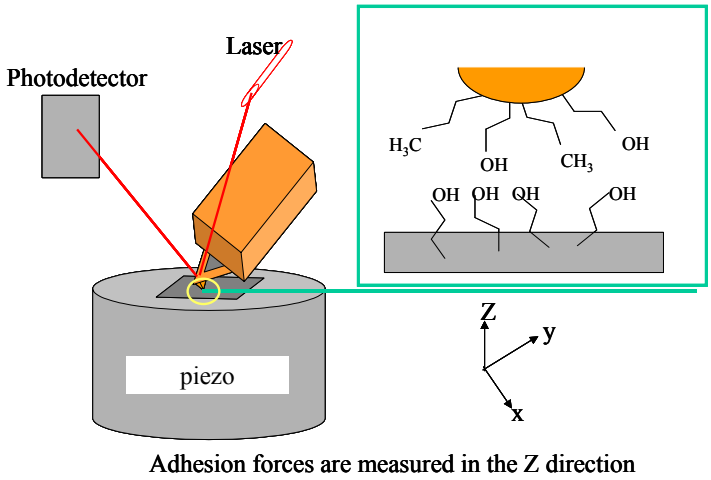

Figure 3.1 *Atomic force microscopy. Adhesion force measurements were carried out in the Z direction on chemically modified cantilever and sample surface.*

Metal plates were prepared from cast iron. See chapter 2 for the preparation procedure. In order to demonstrate adhesive-metal surface interaction, modified silicon nitride (Si_3N_4) cantilevers (Digital Instrument Santa Barbara, CA) were used. Cantilever modification was performed using the method that was used for the chemically modified substrates. The gold-coated cantilevers were immediately immersed in a 3mM ethanol solution of 11-mercaptoundecanol (OH terminated) and undecanethiol (CH_3 terminated). Prior to use, the cantilevers and chemically modified substrates were rinsed with excess ethanol followed by MQ water and immediately mounted in the atomic force microscope.

Cantilever calibration and force measurement procedures can be found in Chapter 2.

3.3 Results and Discussion

When adhesion forces are measured with AFM, the environment in which the surfaces interact plays an important role in determining the measured forces (12,13). If the force measurements are carried out in air, capillary forces arising from the water vapor between the surface and the AFM tip during contact lead to misleading force measurements (Figure 3.2). To eliminate the effect of capillary forces, all of the adhesion force measurements were performed in a liquid cell (Figure 3.3) (14).

3.3.1 Adhesion Force Measurement on a Model System

Adhesion force measurements were performed using a model system. This approach allows us to eliminate uncertainties such as contamination on the surface and the cantilever. It provides a chemically well-defined surface and probe tip to control the surface energy. For this model system, self-assembled monolayers of hydroxyl terminated 11-mercaptoundecanol were prepared on gold-coated glass cover slides. The probe tip was modified with hydroxyl and methyl terminated alkyl thiols. The adhesive force interactions between the functionalized tips and the sample surface were measured by recording force-displacement curves. When the probe tip contacts with a sample surface, an adhesion force develops between the tip and sample, and this force in the absence of capillary force arises from chemical interaction of the functional groups at the probe tip and sample surface.

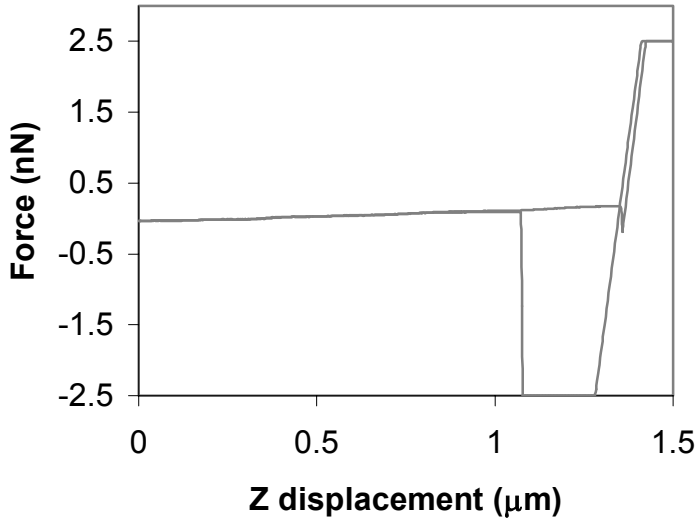

Figure 3.2 *Force versus displacement curves measured in ambient condition on self-assembled monolayer that terminates –OH group with -CH_3 terminated cantilever.*

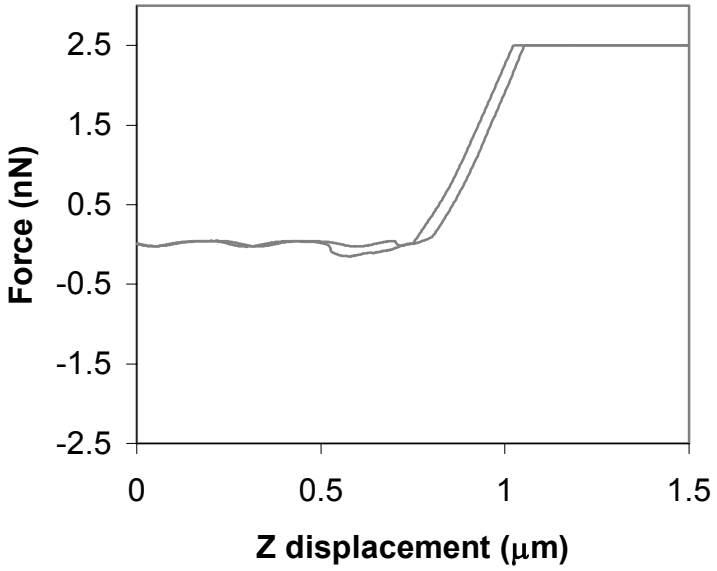

Figure 3.3 *Force versus displacement curves measured in ambient condition on self-assembled monolayer that terminates –OH group with -CH_3 terminated cantilever in water.. Deflection curves show the big difference on pull-off forces in air and water.*

Force versus cantilever displacement curves were recorded on OH terminated surfaces versus OH, OH-CH_3 mixture, and CH_3 terminated probe tips (Figure 3.4). All tip-sample interactions were characterized by measuring their adhesion forces. To quantify the differences in the adhesion measurements between the different functional groups, the force data were plotted as histograms and the mean value of the adhesive interaction and standard error were determined (Figure 3.5 and 3.6). The trend in adhesive force measurement was consistent with the expectation that the bond strength was stronger in the pure hydroxyl content tip and significantly decreases with the increasing methyl terminated alkyl thiol concentration on the tip. It is reasonable to expect that the hydroxyl group on the tip was forming hydrogen bonds with the hydroxyl-containing surface. Therefore, this indicates that hydrogen bonding could be contributing to adhesive bond strength. For the methyl-terminated tip, only van der Waals interaction appears to play a role in the interaction in the model system. Therefore, adhesion force could be low or eliminated under this condition.

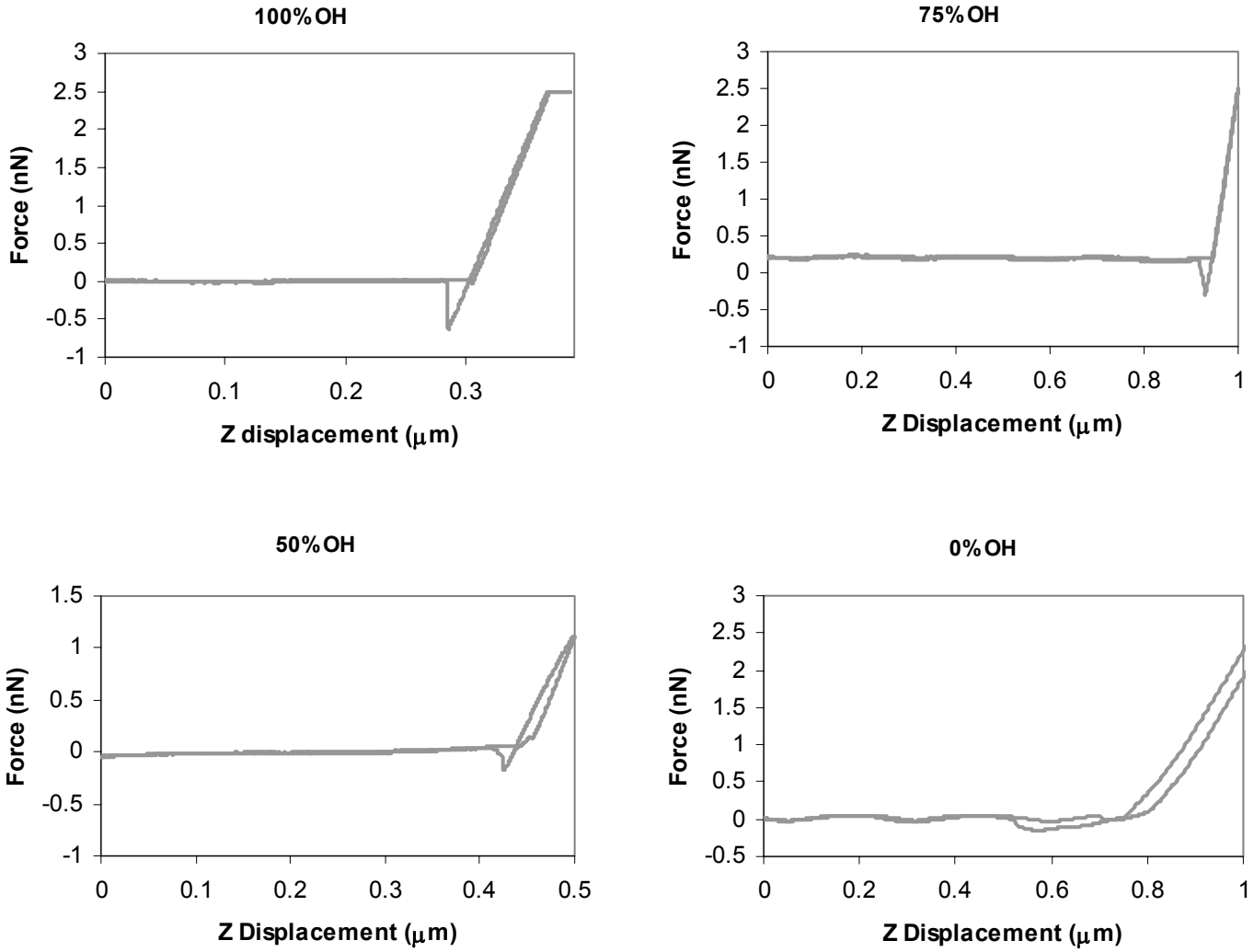

Figure 3.4 *Force-displacement curves between OH terminated surface and cantilever: 100% OH terminated cantilever; 50% OH + 50% CH_3; 75 % OH + 25 % CH_3; 100 % CH_3 terminated cantilever. Oscillation of the line is caused by the laser interference on the gold surface.*

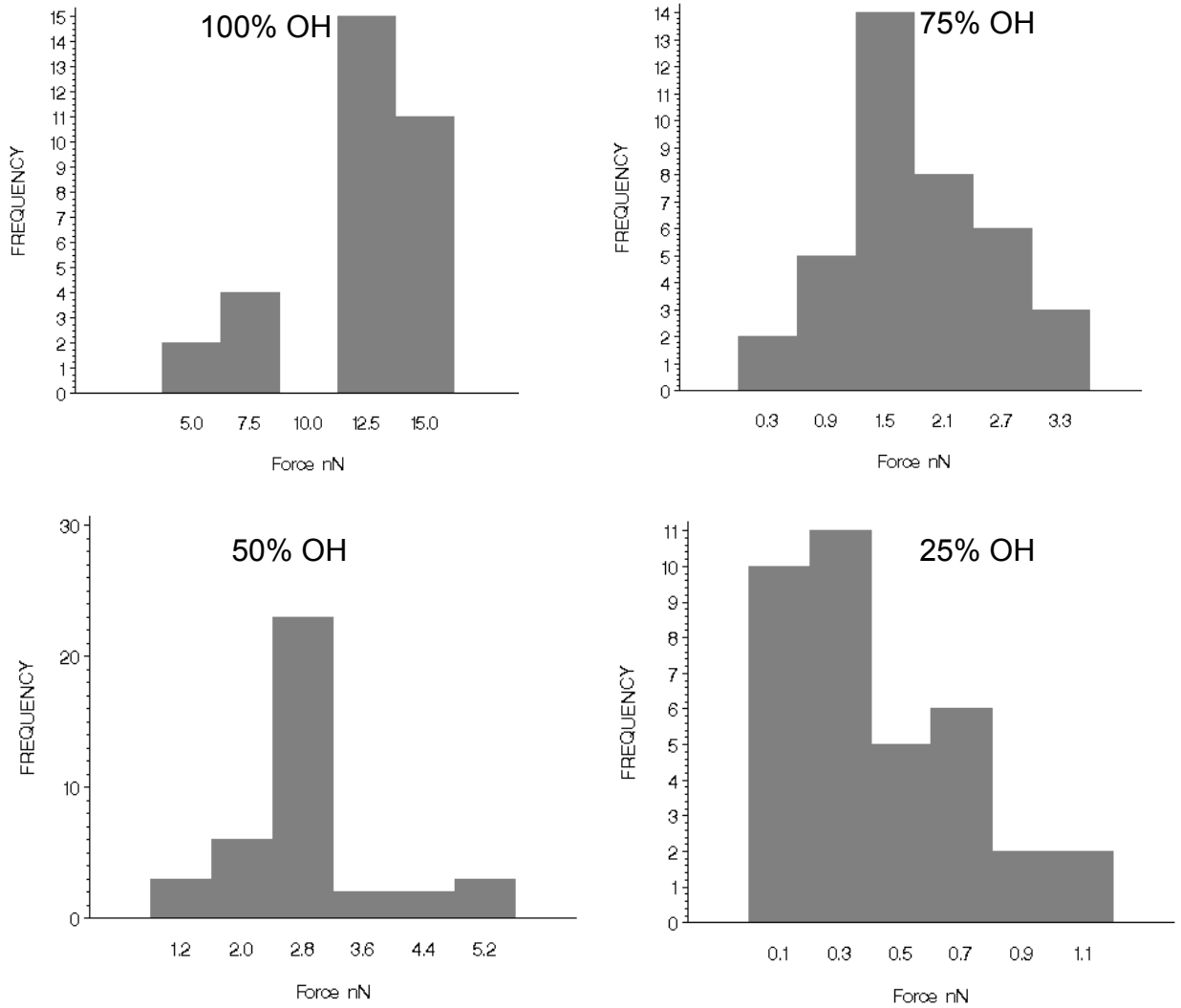

Figure 3.5 *Adhesive force was observed in repetitive measurements using functionalized tip on hydroxyl-terminated surface in water. Histograms are showing the number of repetitive adhesion forces.*

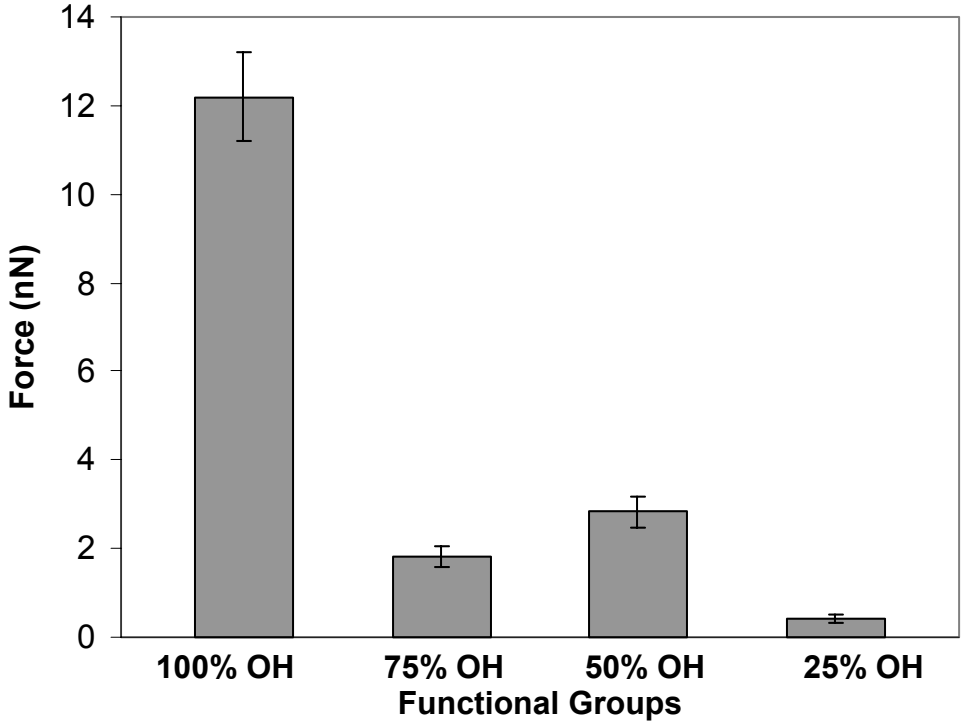

Figure 3.6 *Adhesion forces for each functionalized cantilever on hydroxyl containing surface. 100% OH cantilever; 75% OH=75% OH + 25% CH_3; 50% OH= 50% OH + 50% CH_3; 25% OH= 75% CH_3 + 25% OH. (See Appendix C for the normalized force data and tip radius).*

It was proposed by Williams *et al*. that the total adhesion forces between the tip and the sample is the sum of discrete bond forces (15). The total bond force has a mean value (μ) at $\mu=mF$ and variance (σ^2) where $\sigma^2=mF^{2,}$; F= individual bond strength and *m*=number of bonds. Thus, the ratio of the variance (σ^2) and mean of the total force (μ) gives the individual bond strength ($F=\sigma^2/\mu$). Using this equation, we have calculated the individual bond strength for each cantilever tip and listed the results in Table 3.4.

Table 3.4 *Individual bond strengths and bond energy measured with various SAM functionalized tips on a hydroxyl surface.*

Functional Groups	Mean (nN)	Variance (nN^2)	Std Error (nN)	Ind. Bond Strength (nN)	Bond Energy (kJ/mol)
100% OH	12.4	7.55	0.52	0.61	32.1
75% OH	1.82	0.57	0.12	0.31	16.7
50% OH	2.84	0.88	0.15	0.31	16.4
25% OH	0.44	0.08	0.05	0.18	10.6

The hydrogen bond energy may also be calculated using the individual bond strength. In order to calculate bond energy, equation [3.1] was introduced (10).

$$E = \int_{r_o}^{\infty} -NF(r_o / r)^3 \, dr \qquad [3.1]$$

In this equation, *N* represents Avogadro' s number, *F* the individual bond strength, and r_o the hydrogen bond length in water, respectively. Hydrogen bond energy typically ranges between 10 and 40 kJ/mol (3). The calculated bond energy for each cantilever tip can be found in Table 3.4. These values are in the range of hydrogen bond energy.

3.3.2 Adhesive Force Measurement on Metal Surface

The same chemically modified probe tips were used to determine adhesion forces between a cast iron surface and the various functionalized tips in water (Figure 3.7). Histograms of the pull off forces show the mean pull-off forces change with the hydroxyl content of the chemically modified probe tip. Adhesion bond strengths and bond energies for cast iron surface are listed in Table 3.5.

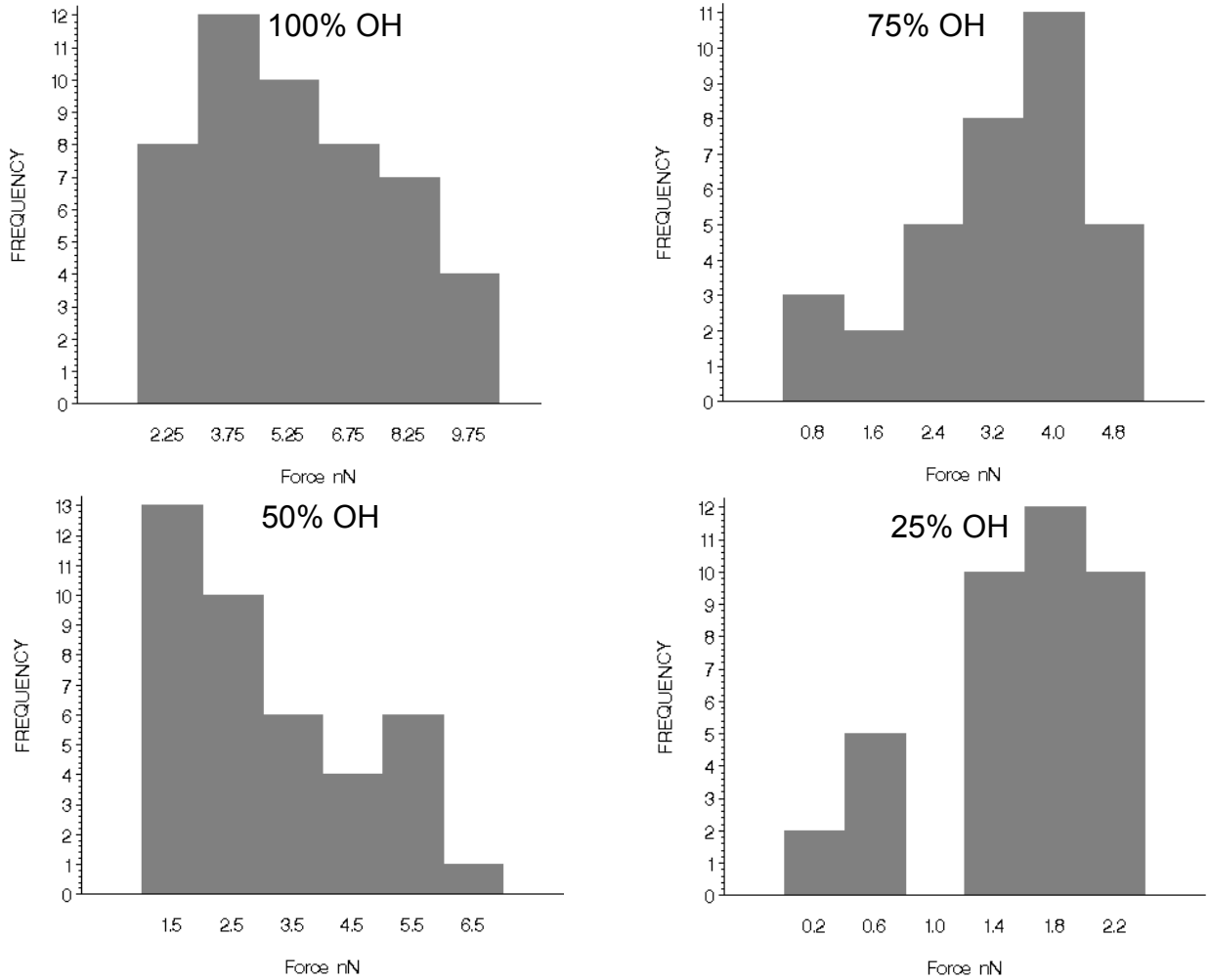

Figure 3.7 *Histograms of pull-off force distributions measured with 100% OH terminated tip; 25% CH_3 75% OH terminated tips; 50% CH_3 and 50% OH terminated tip; 75% CH_3 and 25% OH terminated tip on cast iron surface.*

Table 3.5 *Adhesion bond strength and bond energy measured on cast iron surface in water with various functionalized tips.*

Funct. Group	Mean (nN)	Variance (nN^2)	Ind. Bond. Strength nN	Adh.Bond Energy kJ/mol
100%OH	5.689	4.95	0.871	46.1
75% OH	3.32	1.34	0.401	21.2
50% OH	3.17	2.24	0.705	37.6
25% OH	1.56	0.34	0.218	11.5

The adhesive bond energies listed in Table 3.5 are within the range for hydrogen bonds. Increasing the hydrophobicity of the tip reduces the adhesive bond strength and the adhesive bond energy. This may be due to the number of available sites for bonding on the tip. The hydroxyl group content was reduced on the tip when it was mixed with methyl terminated alkyl thiol; this would be expected to reduce the bonding sites available for adhesion.

The modification of the cantilever tip provides a well-defined chemical structure on the tip to probe interactions with the surface. The use of mixed functional groups on the tip allows even more control over the adhesion properties with the surface. Similarly, it may also be possible to control adhesive bond strength in a polymer by tailoring its chemical structure.

In the next experiments, PVA with varying levels of acetyl content were applied to the cantilever tip. The cast iron plate was used as the substrate. Figure 3.8 shows the force-displacement curve for the interaction of the PVA-coated colloidal probe and the cast iron surface. The force-displacement curves demonstrate multiple rupture points and varying forces. Multiple polymer bridging may be occurring between the probe tip and the sample surface while the sample is moving with the piezoelectric transducer on the Z-

axis. When the sample is pulled back by the piezo movement, presumably, polymers adhering to the surface start to break, and the force displacement curve shows the multiple rupture points with varying force (5,16). Therefore, due to the probability of multiple attachments, the point where the adhesive force measurement was taken on the force-displacement curve may not represent the single bond strength. Other polymer chains may still be adhered to the metal surface and pulling down the CFM colloidal probe tip.

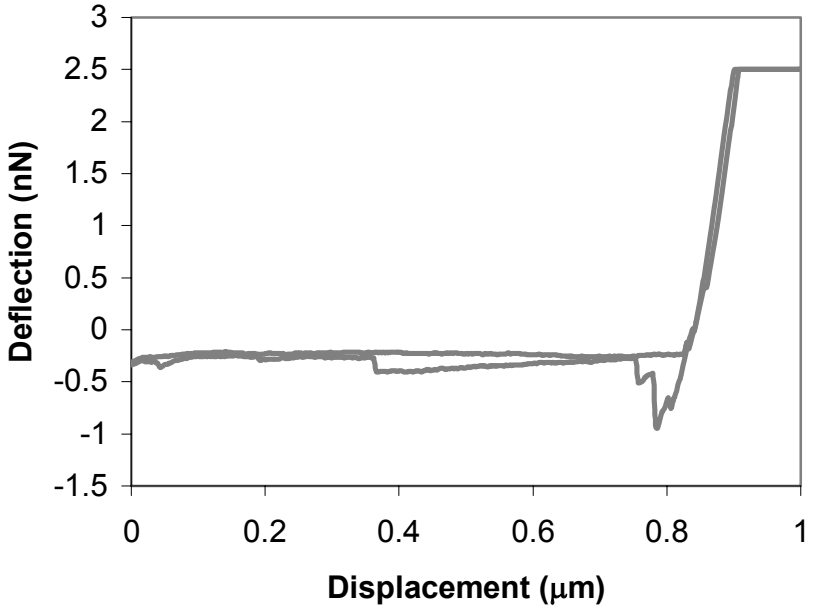

Figure 3.8 *Force-displacement curve for polyvinyl alcohol on a cast iron surface.*

In comparing the PVA and PVAc force-displacement curves, a difference between PVA and PVAc was noticed (Figure 3.9). The PVA curves as mentioned before appear to have multiple rupture points from the breaking of multiple polymer chains from the cast iron surface. The PVAc polymer does not show the same magnitude of rupture points as that of the PVA curve.

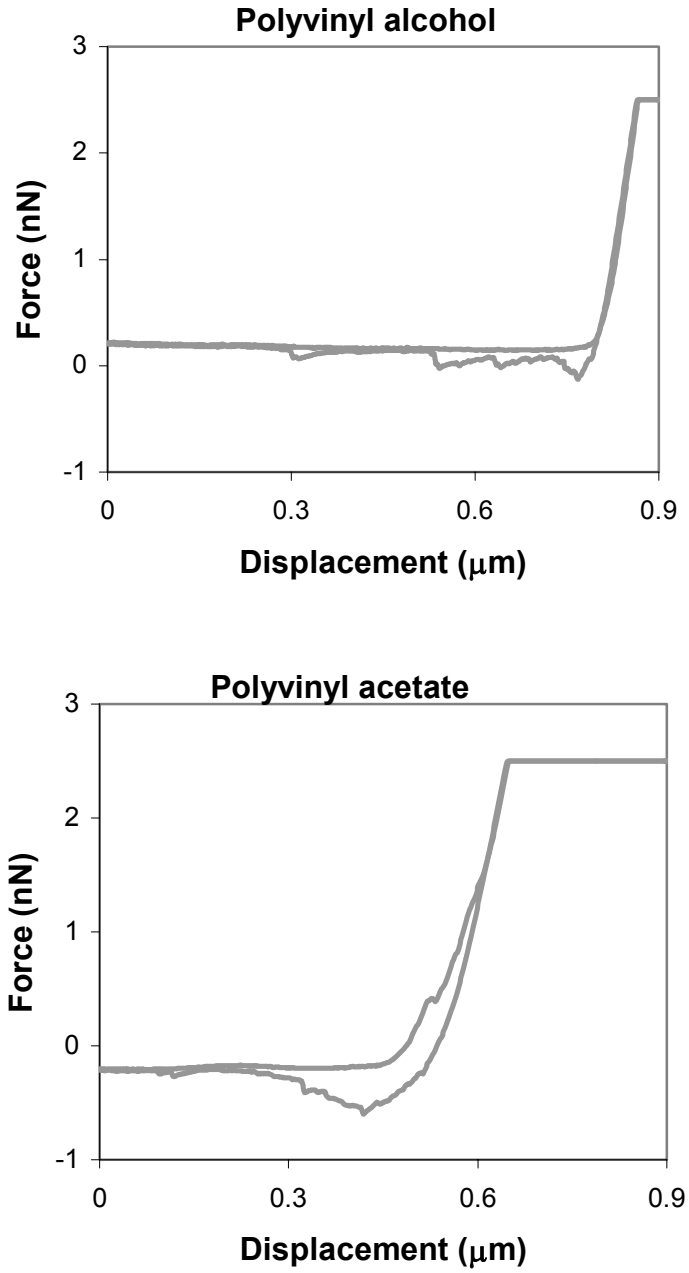

Figure 3.9 *Force-displacement curve of hydrophilic (Polyvinyl alcohol) and hydrophobic polymer (Polyvinyl acetate). Polyvinyl alcohol demonstrates multiple adhesive bonds with the surface whereas polyvinyl acetate does not show.*

As indicated in the previous section, the adhesive force measurements were carried out in water. The polymer attached to the colloidal probe has a

different chemical affinity for the solvent. When polymer is in a good solvent, it will stretch away from the probe surface, as for a hydrophilic polymer in water (17,18). If polymer is in a bad solvent, then it may collapse onto the surface, forming a uniform layer, as with a hydrophobic polymer in water. This may be the reason that force displacement curves show such unique and different properties.

Figure 3.10 shows the adhesive force histogram for the different levels of acetyl substituted PVA. To quantify the differences in the adhesion measurements the mean value of the adhesive interaction and standard error were determined (Figure 3.11). The trend in the results can indicate two possibilities. First, that with increasing hydroxyl content in the polymer, increased adhesive strength can be due to increased concentration of hydrogen bonds. The second possibility is that the multiple polymer bridging between the hydrophilic polymer (i.e. PVA) and the cast iron surface is increased with increasing hydroxyl content.

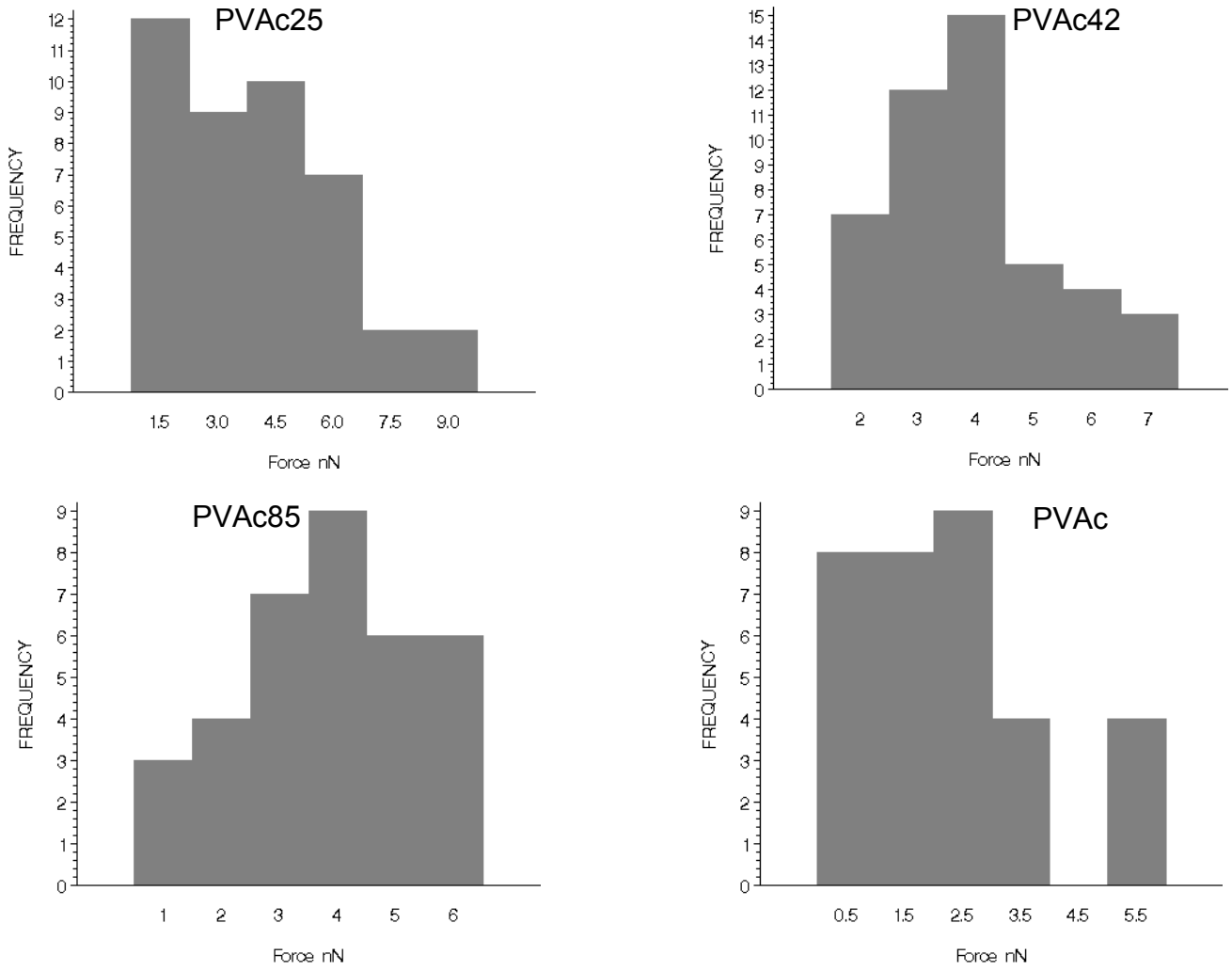

Figure 3.10 *Histogram of pull-off forces measured with a colloidal probe on a cast iron surface.*

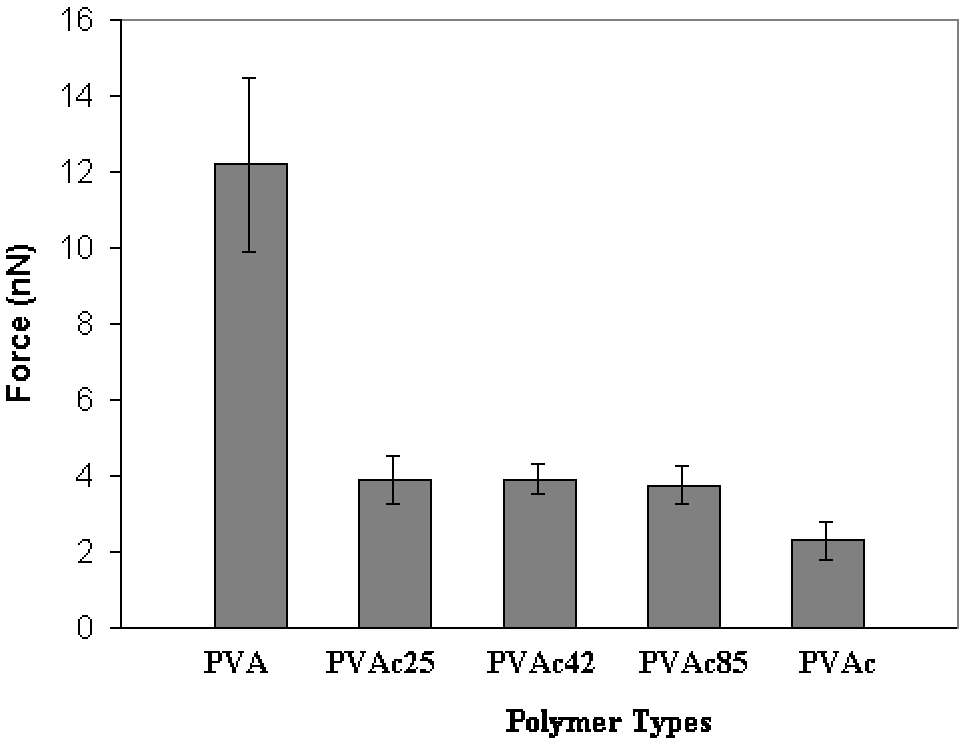

Figure 3.11 *Mean adhesion forces measured with colloidal probe microscopy on a cast iron surface in a liquid cell.*

Comparing the polymer study to the model system, the trend in the results was similar. Since multiple polymer bridging was not present in the model system, this would indicate that the trend in Figure 3.11 is more likely due to hydrogen bonding versus polymer bridging.

3.4 Conclusions

Atomic force microscopy was used to study the interactions between chemically modified surfaces to determine adhesion forces. We have modified AFM cantilevers and surfaces with thiol self-assembled monolayers in order to reduce unknowns in the system and to obtain well characterized surfaces.

The adhesion force between a hydroxyl-containing sample surface and a chemically functionalized tip was increased with increasing hydroxyl concentration on the probe tip. The same results were obtained with a funtionalized tip on a cast iron surface and with synthesized polymers on a cast iron surface. This would suggest that the acid-base interactions, i.e. hydrogen bonding, could be the dominant adhesion mechanism in these systems.

Individual bond force and adhesive bond energy were derived from the sets of contact force data based on a method by Williams *et al.* (10,15). Adhesive bond energies were in the range of 10 to 50 kJ/mol. These bond energies are within the limits of hydrogen bond energies. This also suggests that the adhesive forces measured with the functionalized tips were dominated by hydrogen bonding both in the case of the functionalized surface and in the case of the cast iron surface.

3.5 References

1. Kinloch, A.J.; Adhesion and Adhesives Science and Technology, Chapman Hall, 18, 1987.
2. Krelid, I.; "Drying of Tissue" in Papermaking Part 2, Drying, Tappi Press, Atlanta 147, 2000.
3. Vezenov, D.V., Noy, A., Rozsnyai, L.F., Lieber, C.M.; "" J. Am. Chem. Soc., **119**, 2006, 1997.
4. Eastman, T. Zhu, D.M.; "Adhesion Forces Between Surface Modified AFM Tips and the Mica Surface" Langmuir, **12**, 2859, 1996.
5. Cappella, B., Dietler, G.; "Force Distance Curves by Atomic Force Microscopy" Surface Science Reports, **34** 1, 1999.
6. Weisenhorn, A.L., Hansma, P.K., Albrecht, T.R., Quate, C.F.; "Forces in AFM in Air and Water" Appl. Phys. Lett. **54** (26), 2651, 26 June 1989.
7. Ducker, W.A., Senden, T.J.; "Measurement of Forces in Liquid Using a Force Microscope" Langmuir, **8,** 1831, 1992.
8. Noy, A., Vezenov, D.V., Lieber, C.M.; "Chemical Force Microscopy" Annu. Rev. Mater. Sci., **27**, 381, 1997.
9. Noy, A., Frisbie, C.D., Rozsnyai, L.F., Wrighton, M.S., Lieber, C.M., "Chemical Force Microscopy – Exploiting Chemically Modified Tips to Quantify Adhesion Friction and Functional Group Distributions in Molecular Assemblies" J. Am. Chem. Soc., **117**, 7943, 1995.
10. Han, T., Williams, J.M., Beebe Jr., T.P.; "Chemical Bonds Studied with Functionalized AFM Tips" Analytica Chim. Acta **307**, 365, 1995.
11. Sinniah, S.K., Steel, A.B., Miller, C.J., Reutt-Robey, J.E; "Solvent Exclusion and Chemical Contrast in Scanning Force Microscopy" J.Am.Chem.Soc.**118**, 8925, 1996.
12. Vezenov, D.V., Noy, A., Rozsnyai, L.F., Lieber, C.M.; "Force Titrations and Ionization State Sensitive Imaging of Functional

Groups in Aqueous Solutions by Chemical Force Microscopy" J. Am. Chem. Soc., **119**, 2006, 1997.

13. Weisenhorn, A.L., Hansma, P.K., Albrecht, T.R., Quate, C.F.; "Forces in AFM in Air and Water" Appl. Phys. Lett., **54**(26), 2651, 1989.
14. Sedin, D.L., Rowlen, K.L.; "Adhesion Forces Measured by AFM in Humid Air" Anal. Chem., **72**, 2183, 2000.
15. Williams, J.M., Han, T., Beebe Jr., T.P.; "Determination of Single Bond Forces From Contact Force Variances in AFM" Langmuir, **12**, 1291, 1996.
16. Lee, G.U. Chrisey, L.A., Colton, R.J; "Direct Measurements of the Forces Between Complementary Strands of DNA" Science, **266**, 771, 1994.
17. Koutsos, V., van der Vegte, E.W., Grim, P.C. Hadziioannou, G., "Isolated Polymer Chains via Mixed SAM Morphology and Friction Studied by Scanning Force Microscopy" Macromolecules, **31**, 116, 1998.
18. Milner, S.T.; "Polymer Brushes" Science, **251**, 905, 1991.

Chapter 4 - Interfacial Phenomena in the interphase between Adhesive and Metal Surface: Role of Acid-Base Interactions

4.1 Introduction

Understanding the adhesion mechanism for creping can lead to better control over the process. However, to our knowledge, there is little known about the adhesion mechanism for the creping process. The adhesion mechanism has been the objective of many studies, and yet, there is no universal theory or model to accommodate all substrate-adhesive systems (1-10). The most commonly accepted theory is the adsorption theory. According to adsorption theory, adhesion is the result of intermolecular forces arising from intimate molecular contact (11). These forces are van der Waals forces, covalent bonding, acid-base interactions, *etc*. Hydrogen bonding is considered to be a subset of acid-base interactions and is the focus of this thesis.

We hypothesize that the adhesion between metal and adhesive is mainly controlled by acid-base interactions with mechanical interlocking playing a less important role. To study the importance of mechanical interlocking, a progression of experiments was used. First, differential scanning calorimetry (DSC) was used to determine if selected polyvinyl alcohol (PVA) samples have a melting point, which would indicate the presence of crystalline structures in the polymer. Once it was determined that PVA had a crystalline structure, optical microscopy could be used to probe a cast iron surface for the presence of PVA under polarized light. Further, atomic force microscopy (AFM) and optical microscopy were applied to study the surface roughness of the cast iron surface. Crevices and pores can be seen from the optical microscopy and AFM, which provided information on the surface roughness of the cast iron.

Acid-base interactions require both acidic sites and basic sites. Polyvinyl alcohol can serve either as an acid (electron acceptor) or as a base (electron donor) whereas iron oxide (Yankee Dryer surface) can serve as a base (electron donor). To study the influence of these types of interactions on the adhesion of polymer to the metal surface, a gravimetric adsorption test can be used to determine the relationship between adsorption and hydroxyl content.

The magnitude of interaction between the solid surface and the polymer liquid can be characterized by the work of adhesion, W_A (6-8,12) and provide us information on adhesive strength. The relationship between surface tension and work of adhesion has been given as:

$$W_A = \gamma_L + \gamma_S - \gamma_{SL} \qquad [4.1]$$

where γ_L is the surface tension of the liquid, γ_S surface tension of the solid and γ_{LS} interfacial surface tension.

It is also suggested by Fowkes *et al*. that the work of adhesion can be predicted by the equation [4.2](13):

$$W_A^{ab} = -f\, n_{ab}\, \Delta H_{SL}^{ab} \qquad [4.2]$$

where *f* is a constant converting heat of interaction ΔH_{SL}^{ab} into free energies of interaction and n_{ab} is interfacial concentration of acid-base bonds (in mol/m^2).

Using FTIR spectroscopy, specifically a spectral shift technique, the work of adhesion can be obtained and could provide us information on adhesive strength (14). However, as FTIR measures the bulk properties versus the surface interactions that we are trying to measure. We are making some key assumptions in our interpretation of the FTIR spectra. First, we are assuming that the observed IR signals and other apparent shifts are due, at least in part, to surface interactions, and are not solely due to bulk polymer properties. Second, there may be other shifts in the bulk properties that may

not be due only to surface interactions. These bulk changes will be considered irrelevant and will not be analyzed in this paper. In addition, we use a cast iron substrate, which is presumably covered with iron oxide, as is our assumption for the Yankee dryer surface in the creping process.

4.2 Experimental Materials and Methods

All chemicals were used as received without further purification. Filtered (0.2 μm filter) MQ water (Milli-Q resistivity 18.2 MΩ cm, Millipore, Bedford, MA) was used for all aqueous solutions and for rinsing. The same industrial grade and laboratory tailored polymers that were used in earlier chapters were used for these experiments as well. Tables 4.1 and 4.2 below give the properties of these polymers.

Table 4.1 *Industrial grade polyvinyl alcohol properties.*

Polymer Sample	Degree of Acetylation (%)	Molecular Weight[15]	Intrinsic Viscosity (dl/g)	Huggins Constant k'	Radius of Gyration nm
A325	2	80000	79.63.	0.56	99.5±8.2
A350	2	107100	115.29	0.36	111.7±13.3
A425	5	80000	72.95	0.75	79.1±13.6
A523	12	79100	71.82	0.80	71.3±16
A540	12	110000	56.28	0.71	46.7±8.3

Table 4.2 *Polymer properties derived from PVA (99% hydrolyzed, DP 2123).*

Polymer Sample	Degree of Acetylation (%)	Molecular Weight	Intrinsic Viscosity (dl/g)	Huggins Constant k'	Radius of Gyration nm
PVA	0	93400	130.97	0.51	180
PVAc25	25	115689	112.16	0.3	184
PVAc42	42	124604	106.49	0.26	185
PVAc85	85	169181	55.91	0.63	165
PVAc	100	182554	49.12	0.82	162

Surface topography and roughness of the cast iron plate were determined by AFM imaging using silicon nitride tips with a spring constant of k=0.58N/m. The root mean square (RMS) value of the surface roughness was obtained from contact mode AFM. For a $5\times5\mu m^2$ scan size, the RMS roughness was between 4nm and 5nm.

Differential scanning calorimetry (DSC) was performed on the TA Instruments Thermal Analysis system. Four milligrams of each sample was placed in an aluminum hermetic pan. The sample was heated at a rate of 20^oC/min from -90^oC to $300\ ^oC$.

The results of the DSC for PVA and PVAc can be seen in the following figures (Figures 4.1 and 4.2). The presence of the melting temperature for PVA, 223.85^oC, indicates that the polymer has crystalline structures (Figure 4.1). Conversely, there is no melting point for PVAc, which suggests that there are no crystalline structures in this polymer. The DSC analysis indicates that PVA can be used for probing the cast iron surface for mechanical interlocking under polarized light.

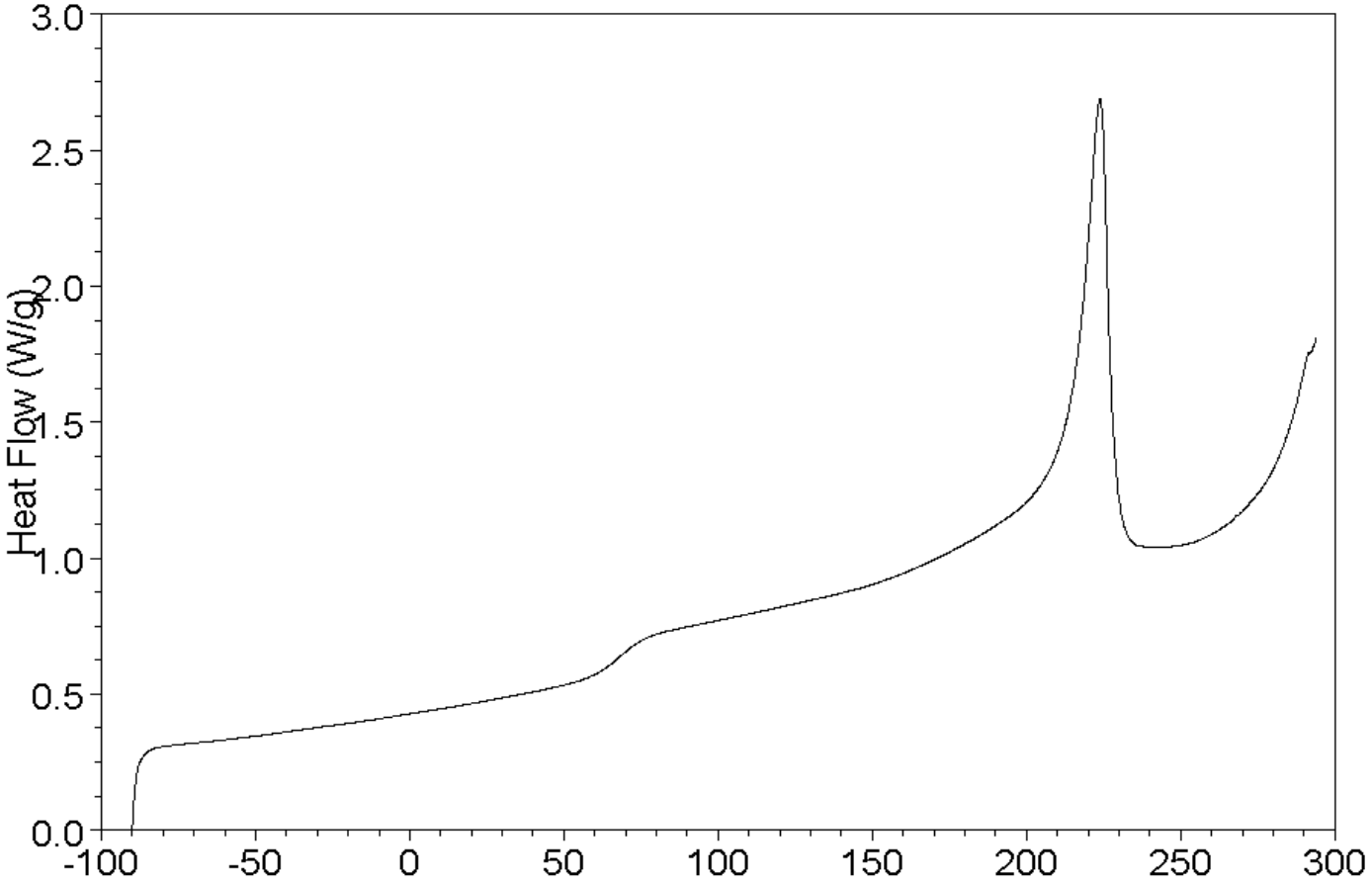

Figure 4.1 *DSC Thermogram of PVA, T_m=223.85^{o}C.*

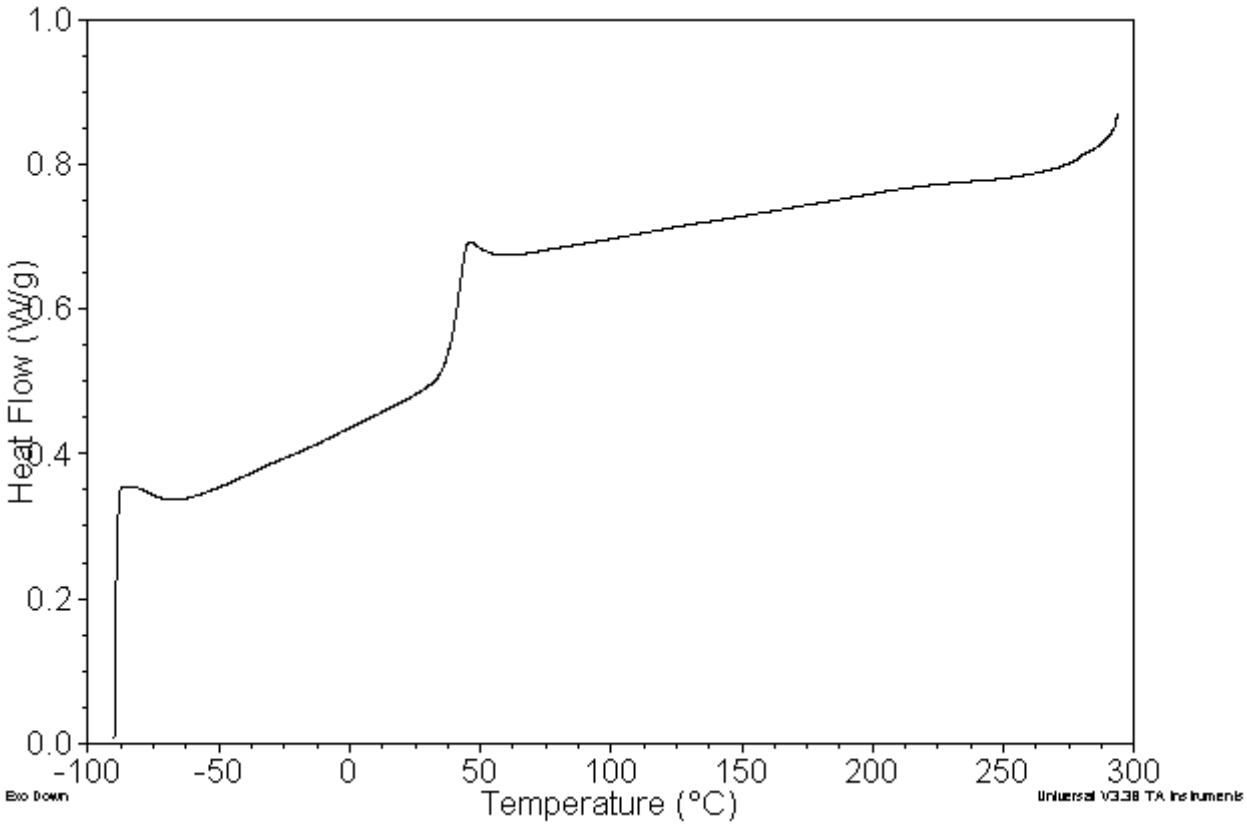

Figure 4.2 *DSC Thermogram of PVAc.*

An Olympus Reflectance Mode microscope was used to probe the cast iron surface for the presence of PVA under polarized light. The images were converted to PC files using a Sony digital camera.

FT-infrared (FTIR) spectra measurements were made with a Nicolet microscope IR (model Continuμm) at a resolution of 4cm^{-1}, using 32 scans, and an area of 50×50μm^2. Teflon plates were cleaned and leveled on a hot plate, then 1mL of polymer solution was applied to the center of each plate and allowed to spread. In order to determine the interaction between the cast iron and the polymer film, the cast iron plate was set in the middle of each film and dried overnight. FTIR measurements were taken on the film and at the polymer-metal interface (Figure 4.3).

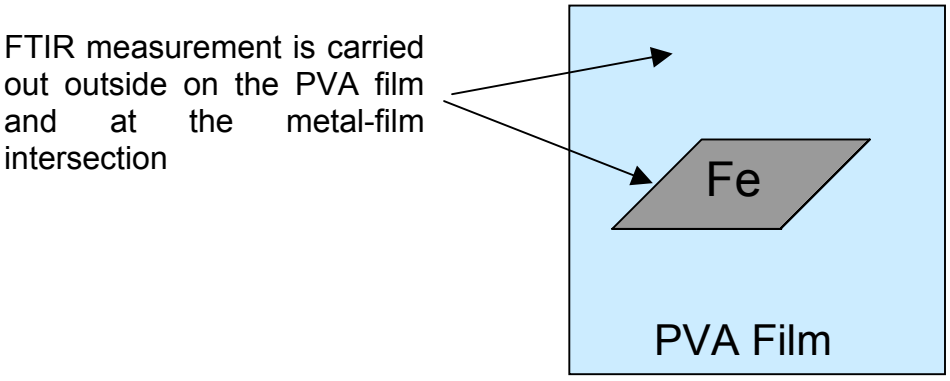

Figure 4.3 *Metal sample for FTIR measurement. The FTIR measurement was taken on the film and at the edge of the metal-film intersection.*

The methods for the lap shear strength (ASTM D1002-99) and surface tension tests can found in Chapter 2.

Adsorption tests were performed for the various polyvinyl alcohol and polyvinyl acetate samples in dimethyl sulfoxide (Fisher Chemical company, ACS grade). We choose DMSO as solvent for the adsorption experiments. Iron oxide (Fisher Chemical Company) particles with a size less than 300 mesh, approximately less than 48μm, were used in the adsorption test.

Determination of polymer adsorption was carried out by a gravimetric method (15). Adhesive solutions of different concentrations (0.002-0.16g/mL) were prepared and polymer adsorption was determined using 10mL of each polymer solution and 0.025g of iron oxide. The mixture was agitated with a wrist shaker for 60 minutes. The mixture was then centrifuged for 30 minutes for separation of the polymer solution from the iron oxide. The adsorbed amount was calculated from the difference in the polymer solution concentrations before and after adsorption. The concentration of the solutions were determined by drying 1mL of solution in an oven to acquire the dry weight of the polymer.

4.3 Results and Discussion

When an adhesive is sprayed on a heated surface, it will solidify shortly after evaporation of the solvent. The application of an adhesive involves wetting of the surface and flow of the adhesive into the spaces (valleys, crevices, and pores) on the substrates. As can be seen in Figure 4.4 (A), cast iron is a relatively porous material. When the adhesive is applied on this surface, it may penetrate these pores and asperities depending on its viscosity and surface energy. After penetrating into these openings, the adhesive solidifies and may act as a mechanical anchor. Once the adhesive is applied and scraped from the cast iron surface, the presence of penetrated polymer can be assessed. Figure 4.4 (C) and (D) show shiny spots under polarized light, indicating the presence of crystalline polymer in some of the crevices and pores after removal of the bulk of the adhesive.

Mechanical interlocking can take place if the adhesive penetrates this rough structure. Therefore, the adhesive must be able to conform to the roughness of the metal surface to provide close contact. However, the contribution of mechanical interlocking in adhesion strength may not be significant on smooth or highly polished surfaces. Using contact mode AFM, surface roughness measurements of a ground and polished surface showed that the deviation from nominal surface was only 5nm (Figure 4.5 and Figure 4.6). This value is much smaller than the radius of gyration of the various polymers used (Table 4.1 and Table 4.2). Therefore, the polymer may not be able to penetrate into these surface openings. If air is entrapped in these crevices or pores, the interaction between the adhesive and the surface will be further limited. In order to have good adhesion, intimate contact is required. After intimate contact is accomplished, intermolecular forces can play an important role in adhesion.

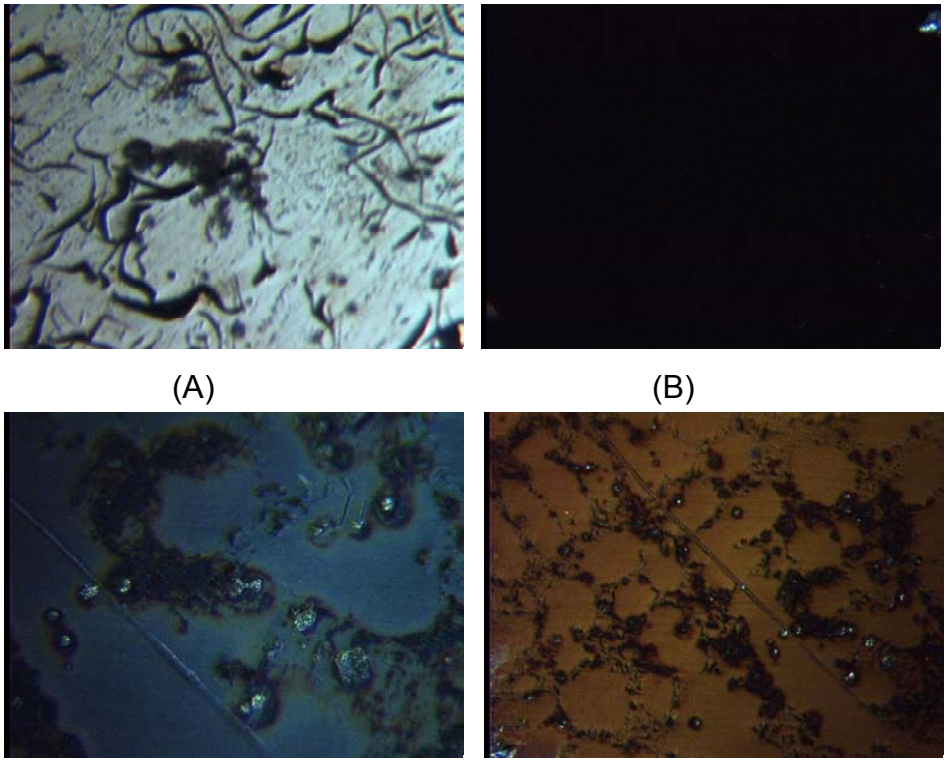

Figure 4.4 *Cast iron surface before application of adhesive (A). Cast iron surface under polarized light (B). Cast iron surface after application of adhesive and scraping off (C-D). Bright spots are crystalline polyvinyl alcohol that remains on the surface after creping.*

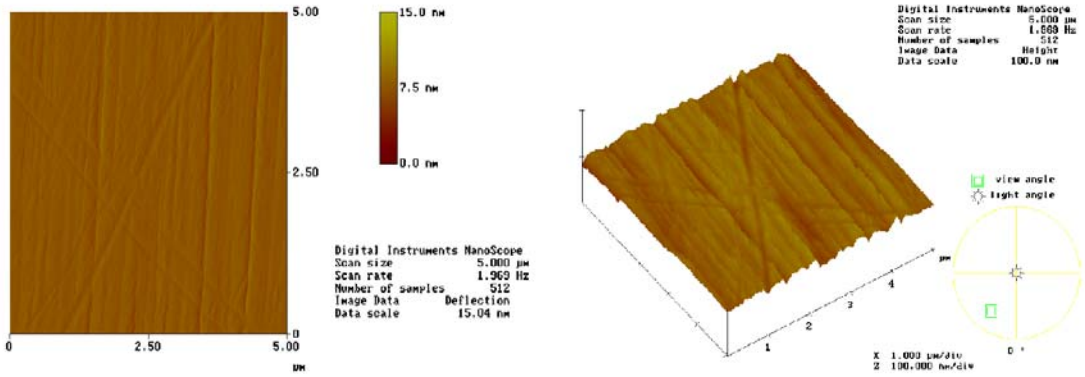

Figure 4.5 *AFM image of cast iron surface.*

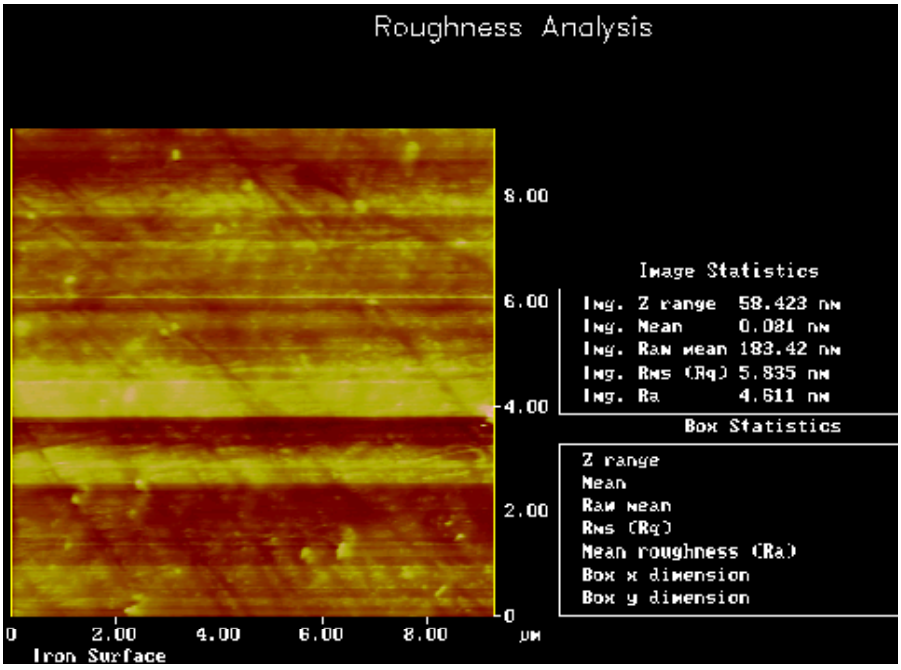

Figure 4.6 *Roughness Analysis of the cast iron surface. RMS value is 5.8 nm.*

Surface tension is a direct measurement method for intermolecular forces (16). If the surface tension of the solution is measured against a saturated hydrocarbon, the dispersion force (γ^d) contribution can be obtained (16). In order to make such a determination for polyvinyl alcohol and polyvinyl acetate, heptane was used as the saturated hydrocarbon. First, polyvinyl alcohol and polyvinyl acetate dilute solutions (2w/v%) were prepared in DMSO, and the surface tension (γ_L) of these solutions was measured. Then, the 2% polymer solutions were mixed with the heptane, and the dispersion force (γ^d) contribution was obtained. The results are listed in Table 4.3.

These results (Table 4.3) show that there is a decrease in surface tension of polyvinyl alcohol with an increase in the acetyl content. It is also noticed that the dispersion force contribution towards surface tension is slightly increased with decreased acetyl content. Similar trends were found for the surface tension of the industrial grade polymers tested in Chapter 2.

In order for a liquid to wet a solid surface, the surface tension of the solid surface *(γ_s)* must be greater than or equal to the sum of the interfacial surface tension between the solid and liquid *(γ_{sl})*, the surface tension of the liquid *(γ_l)* and the equilibrium-spreading pressure *(π_e)* as depicted in equation [4.3] (11):

$$\gamma_s \geq \gamma_{sl} + \gamma_l + \pi_e \qquad [4.3]$$

The equilibrium-spreading pressure π_e can be obtained from equation [4.4]:

$$\pi_e = 2(\gamma_s^d + \gamma_l^d)^{1/2} - 2\gamma_l \qquad [4.4]$$

where γ_s^d , γ_l^d , and γ_l represent the dispersion force contribution of the surface tension of the solid, the dispersion force contribution of the surface tension of the liquid, and the surface tension of the liquid, respectively. Combining equations [4.3] and [4.4], we can obtain the following equation:

$$\gamma_s \geq \gamma_{sl} + \gamma_l + 2(\gamma_s^d + \gamma_l^d)^{1/2} - 2\gamma_l \qquad [4.5]$$

For spreading to occur, the right hand side of the equation [4.5] must be equal to or smaller than the substrate surface tension.

Based on equation [4.5], we can see the trend of wettability versus acetyl content by comparing PVA, PVAc42, and PVAc. The iron oxide surface tension was found in the literature to be 1357 dyne/cm (11). If we replace the values from Table 4.3 for these polymers in equation [4.5], we will obtain 1336.9 dyne/cm, 1340.9 dyne/cm and 1343 dyne/cm, respectively, for the right hand side of the equation. These values are smaller than the surface tension of the iron oxide, and they are in increasing order from PVA to PVAc. With decreasing acetyl content in the polymers, a slight decrease in surface tension due to dispersion forces and overall smaller surface tension gives a higher equilibrium spreading pressure. Thus, the right hand side of the equation [4.5] becomes larger and decreases the wetting ability and contact area of the adhesive.

In the adsorption theory, an adhesive will adhere to a surface due to intermolecular forces. Thus, forces controlling the chemical interaction between the surface and the adhesive material would also control the adsorption of polymers onto substrate from dilute solution. If interaction between iron oxide and polyvinyl alcohol was due only to the acid-base interactions of hydrogen bonding, then the interaction of a more acetylated polymer with dry iron oxide should be lower in an organic solvent. Thus, the adsorption of polyvinyl alcohol on iron oxide was performed in dilute solution (Figure 4.7).

Table 4.3 *Surface tension and dispersion force contributions of the adhesive solution at 25°C.*

Sample Solutions	**Surface Tension (γ_L) (dyne/cm)**	**Surface Tension, dispersion (γ_L^d) (dyne/cm)**	**Surface Tension, acid-base int. (γ_L^{ab}) (dyne/cm)**
PVA	41.6±0.6	9.2±0.2	32.4
PVAc25	41.3±0.1	9.3±0.2	32
PVAc42	37.5±0.8	8.5±0.2	29
PVAc85	35.3±0.7	7.3±0.2	28
PVAc	35.1±0.8	7.3±0.2	27.8

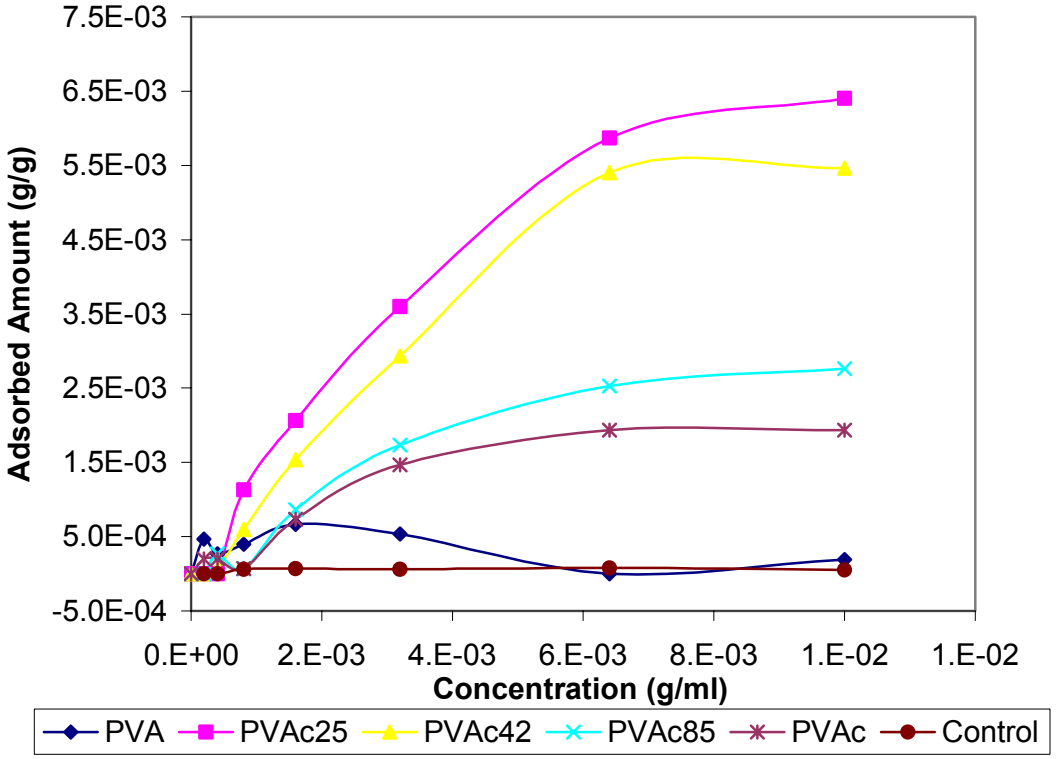

Figure 4.7 *Adsorption of PVA on Fe_2O_3 from DMSO solution. Increasing acetyl content decreased the adsorption on Fe_2O_3.*

The results of the adsorption test showed that the adsorption on the iron oxide surface was higher in the case of the polymer with the higher hydroxyl content than the polymer with the lower hydroxyl content. However, polyvinyl alcohol (99-100% hydrolyzed) showed the lowest adsorption on the metal surface. This could be due to the polymer solvent interaction. At low PVA concentrations, the adsorption of individual macromolecules is believed to dominate. However, formation of aggregates may be a competing process. With the increase of concentration, the formation and adsorption of aggregates may play a greater role (17).

In order to determine the chemical interaction between the metal and adhesive polymer, infrared spectroscopy was applied. The polymer samples listed in Table 4.1 and Table 4.2 were tested. The FTIR spectra of the polymer films can be seen in Figures 4.8 and 4.9.

In order to see the specific differences in the IR spectra and understand what they mean, specific ranges of wavenumbers will be analyzed. The tacticity of different polyvinyl alcohols can be identified from the FTIR spectra of the CH_2 groups in the polymer chain. Tacticity is the regularity of the configuration of the pseudoassymetric carbons. Syndiotactic and isotactic vinyl polymers have a higher probability of being crystalline than the atactic polymers. It was also proposed that isotactic polymer had lower degree of crystallizability than syndiotactic polymer.

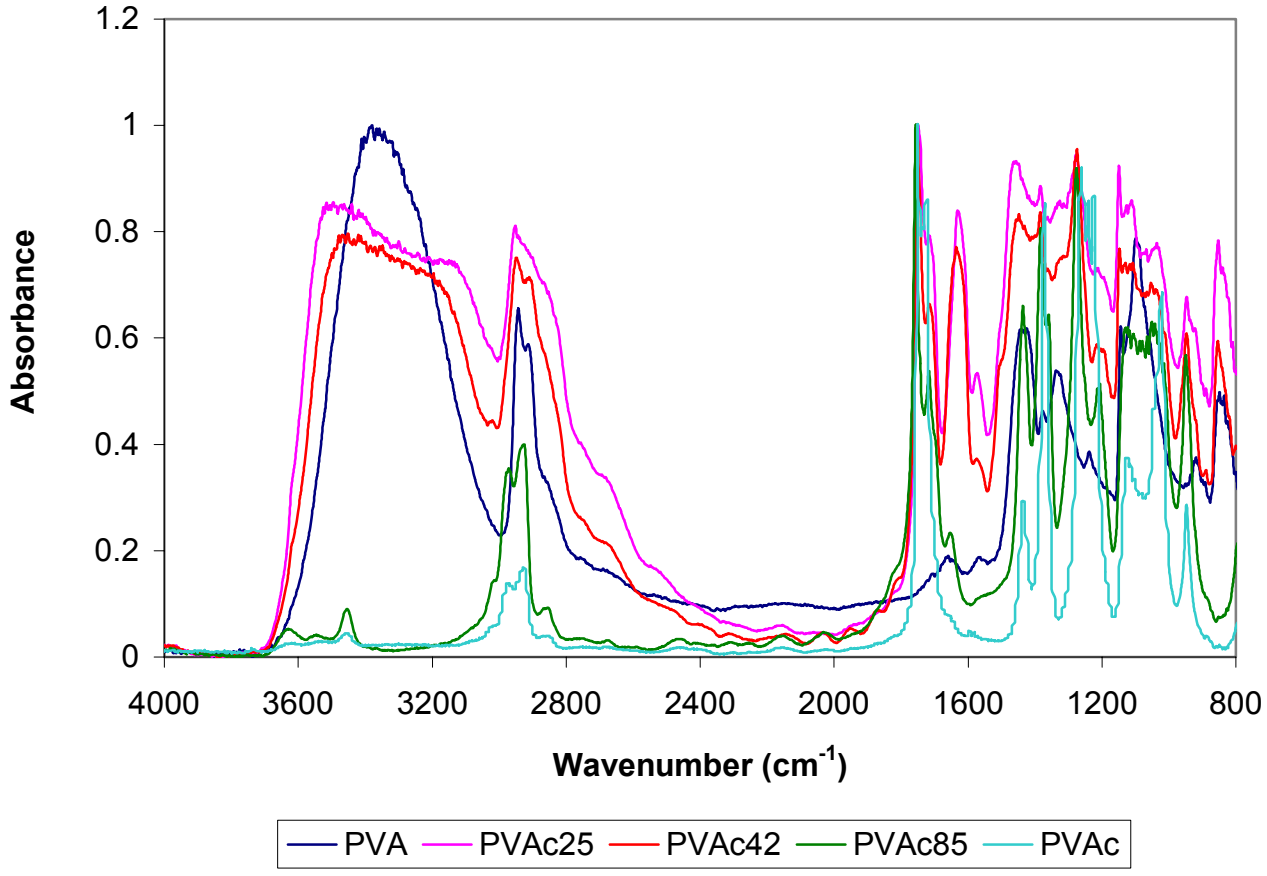

Figure 4.8 *FTIR Spectra of synthesized polymer films.*

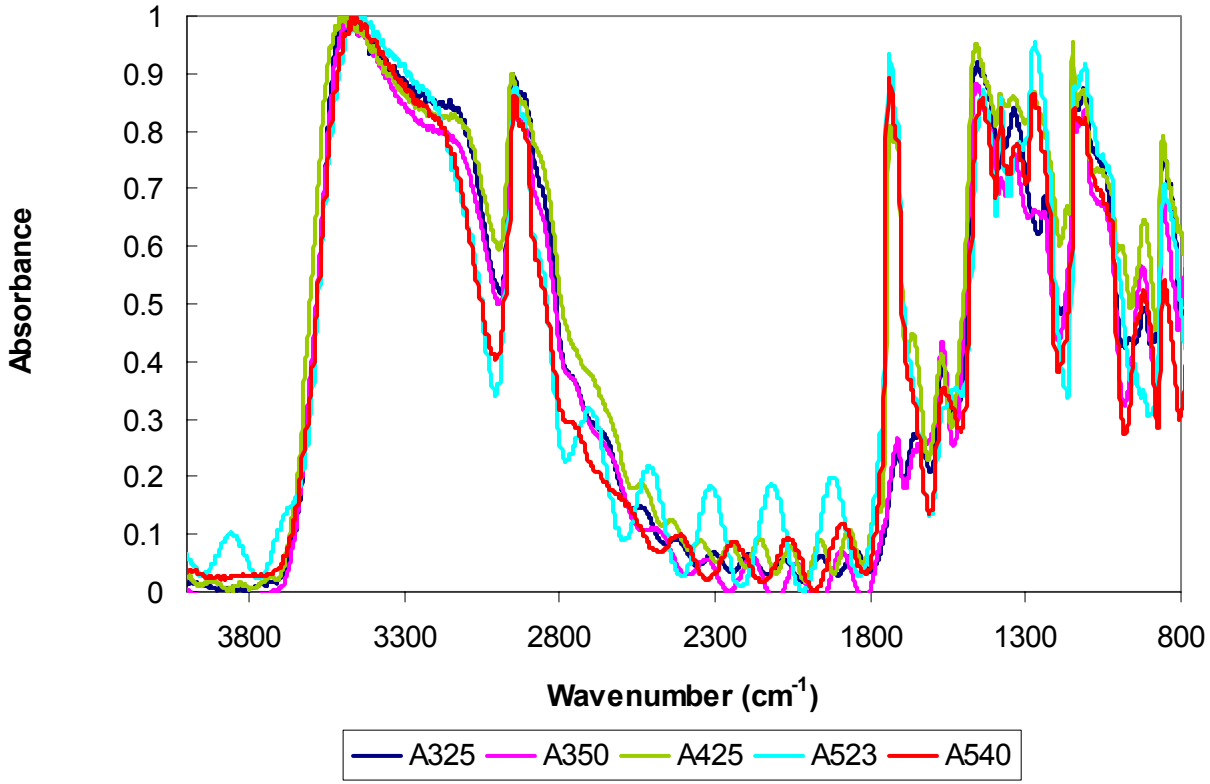

Figure 4.9 *FTIR Spectra of industrial polymer films.*

Figure 4.10 shows the transmittance peak for isotactic and syndiotactic polymers. It shows that the peak tip has a fork; one leg of the fork is longer than the other leg of the fork. The location of the longer leg alternates positions for syndiotactic and isotactic polymers. From this difference, tacticity in polyvinyl alcohol chain could be distinguished.

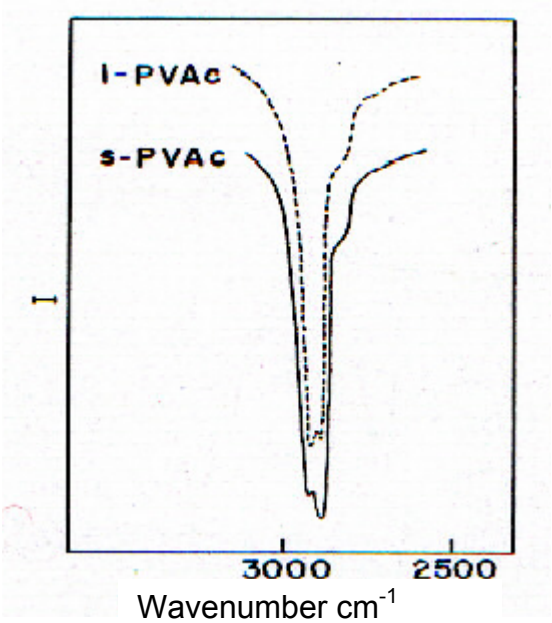

Figure 4.10 *Polyvinyl acetate shows different stereoregularity (18).*

FTIR spectra of the CH_2 group showed that polyvinyl alcohol with less than 80% acetyl group substitution had the isotactic configuration (Figure 4.11). However, increasing the acetyl group changes the stereoregularity of the polymer chains and causes a syndiotactic configuration. Therefore, this indicates that acetyl group concentration in PVA has an effect on the tacticity of the polymers.

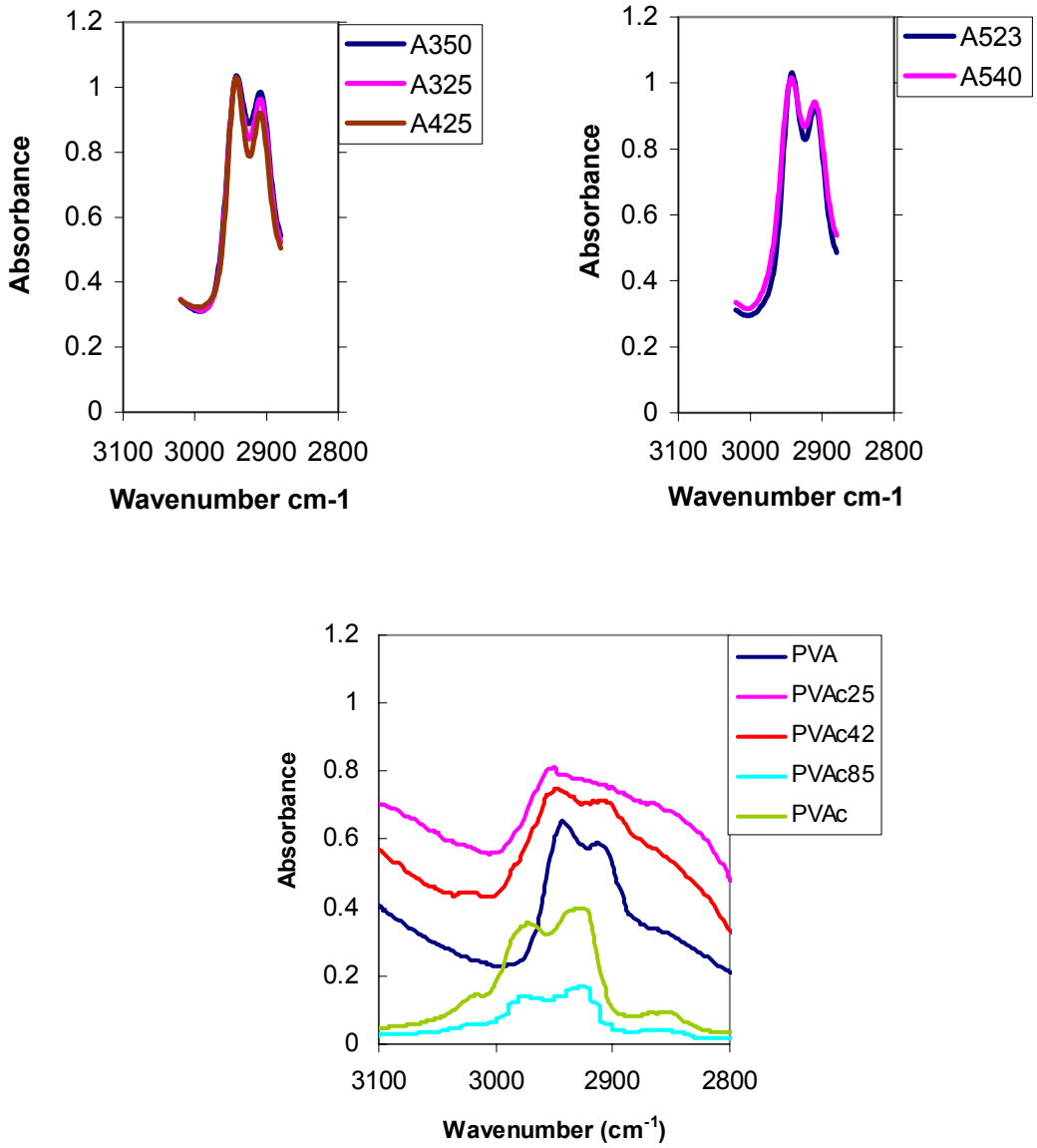

Figure 4.11 *FTIR spectra of CH_2 group in Polyvinyl alcohol. Polyvinyl alcohol with acetyl content more than 80% became syndiotactic.*

Syndiotactic polymers are known to have distinct peaks at 916cm^{-1} (Figure 4.12) (18,19). PVA, the starting material for PVAc25, PVAc42, PVAc85 and PVAc, has the same distinct peak at 916cm^{-1} (Figure 4.13). This peak is also present in polyvinyl alcohols A325, A350, and A425. In contrast, the peak was located at 942cm $^{-1}$ in PVAc25, PVAc42, PVAc85, A523 and A540. The intensity of these peaks was low in A325, A350, and A425, A523, and A540. Therefore, the relative amount of syndiotactic conformation on these polymer chains could be low. The frequency difference between 916cm^{-1} and 942cm^{-1} could be due to intramolecular hydrogen bonding. Thus, the PVAc polymer has a mostly isotactic conformation, but it may also contain small amounts of syndiotactic structure.

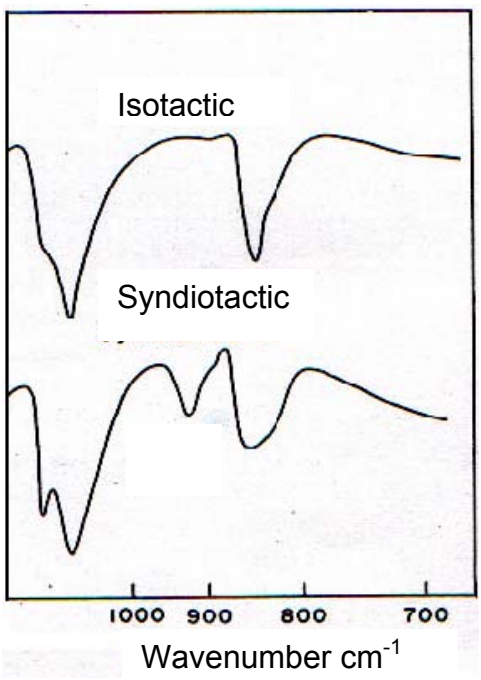

Figure 4.12 *FTIR spectra of isotactic and syndiotactic polyvinyl alcohol (18).*

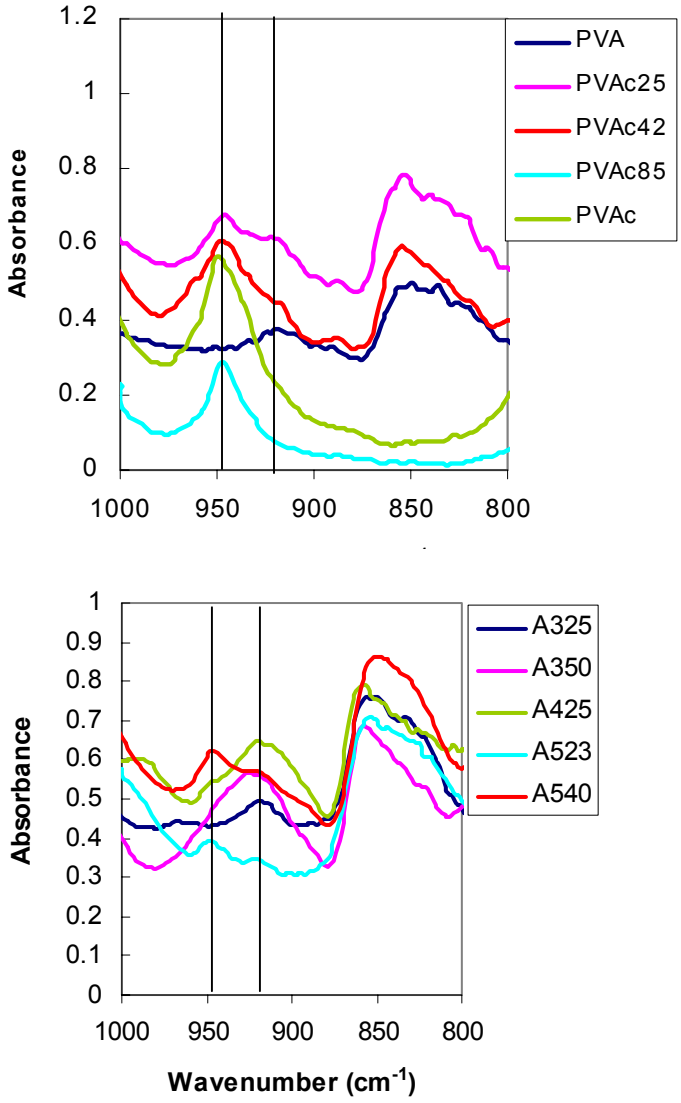

Figure 4.13 *Infrared spectra of polyvinyl alcohol. Stereoregularity of the polymer is changing with the acetyl content.*

The band at 1141 cm^{-1} is also believed to be related to the crystallinity of the polymer (19). There is expected to be a linear relationship between the intensity of this peak and the level of crystallinity. Figure 4.14 shows the difference in crystallinity of the polyvinyl alcohol samples. The peak at 1141cm^{-1} is sharper in the case of a more hydroxylated polymer (PVA, A325, A350, A425 in Figure 4.14). The same peak disappears in A540. This could

be affected by the acetyl content of polyvinyl alcohol. Again, it would appear that high acetyl content decreases the crystallinity of PVA.

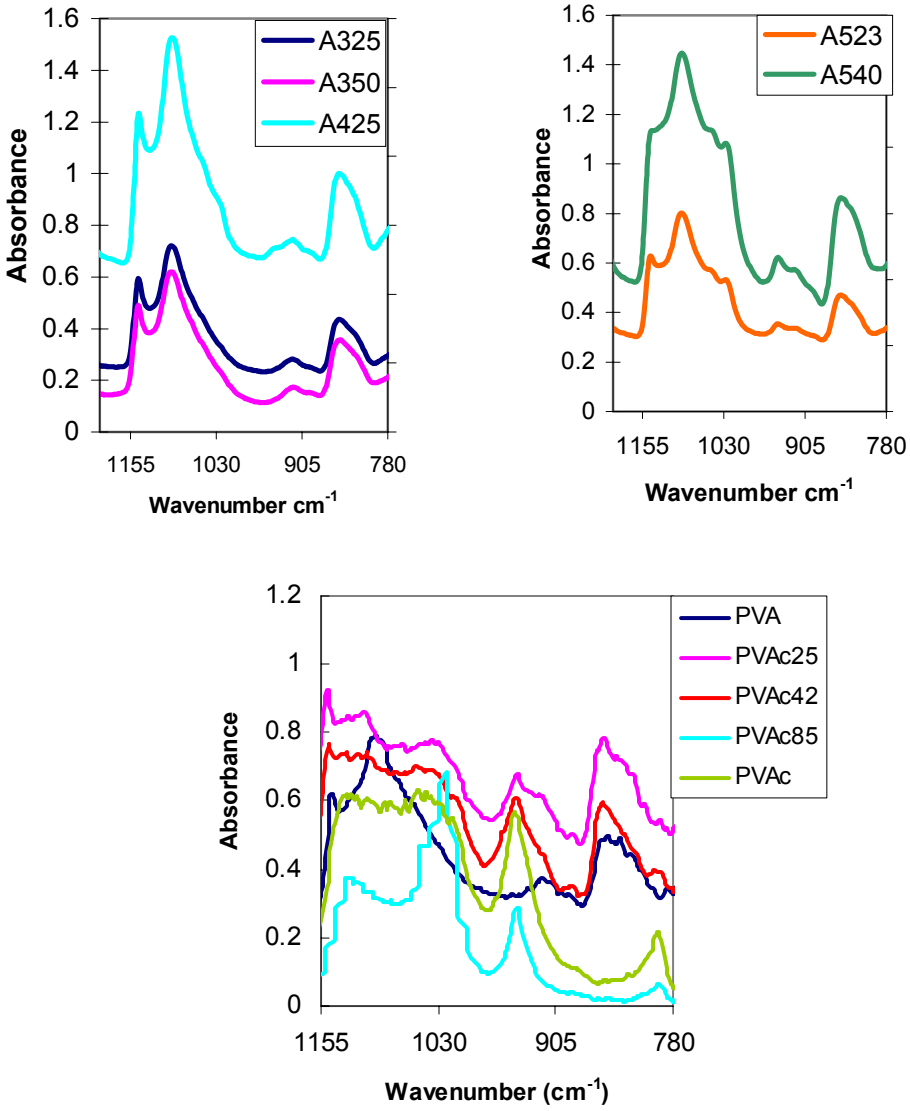

Figure 4.14 *Crystalline structure of polyvinyl alcohol.*

Figure 4.15 demonstrates the hydroxyl group stretching frequencies of polyvinyl alcohol. These correspond to the free hydroxyl group (3629 cm^{-1}) and intra and intermolecular hydrogen bonded hydroxyl groups (3400-3500 cm^{-1}) (20). The stretching frequencies for these groups are listed in Table 4.4.

It was found that the free hydroxyl group could be observed at a wavenumber of 3629 cm^{-1} for the PVAc85 polymer. However, the free hydroxyl wavenumbers for all of the other polymers were difficult to read based on the overlap of the intra- and intermolecular hydroxyl peaks with the free hydroxyl peaks. Therefore, this wavenumber was used to calculate the frequency shifts and determine the heats of interaction for all of the polymers.

FTIR is a measurement that senses bulk or volume properties. Thus, it may not be able to detect the thin film-metal interface interaction. However, if one were to interpret these data as indicating a frequency shift upon adsorption of the polymer layer on the oxide surface, then it is reasonable to propose a model involving a transformation from a free hydroxyl condition to an associated state of hydroxyl groups. Thus, we assume that figure 4.16 and figure 4.17 demonstrate at least a partial representation of the interaction between polyvinyl alcohol and the metal oxide surface. The interaction appears to cause a shift in the wavenumber of the hydroxyl group (O-H) vibration in the FTIR spectra. This figure suggests that a change in the hydrogen bonding of the PVA hydroxyl groups to the metal surface is occurring. The precise position of the hydroxyl group frequency indicates the strength of hydrogen bond (20). When the heat of interaction is calculated from a frequency shift, the biggest frequency shift should give the highest value of the heat of interaction.

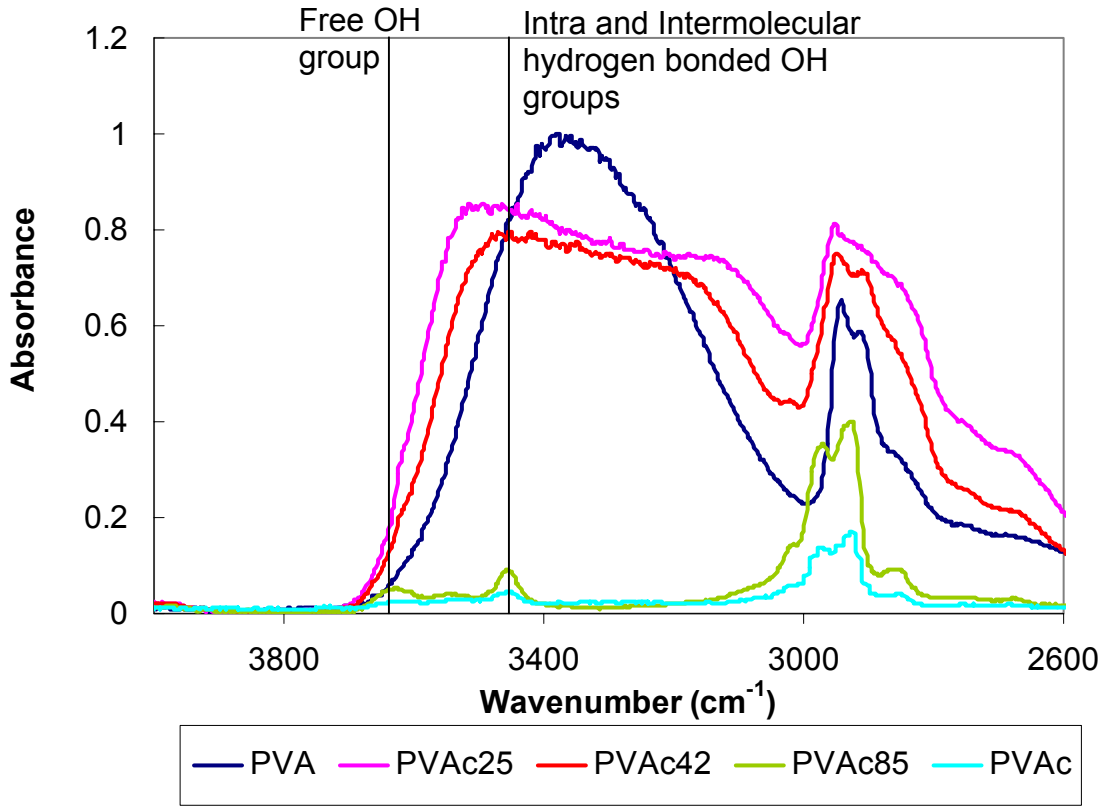

Figure 4.15 *Free and intra and intermolecular hydrogen bonded hydroxyl group on polyvinyl alcohol.*

Table 4.4 *Hydroxyl group band assignment on polyvinyl alcohol.*

Polymer Sample	**Intramolecular OH (cm^{-1})**	**Free OH (cm^{-1})**
PVOH99	3433	-
PVAc25	3496	-
PVAc42	3480	-
PVAc85	3520	3629
A325	3447	
A350	3461	
A425	3455	
A523	3440	
A540	3459	

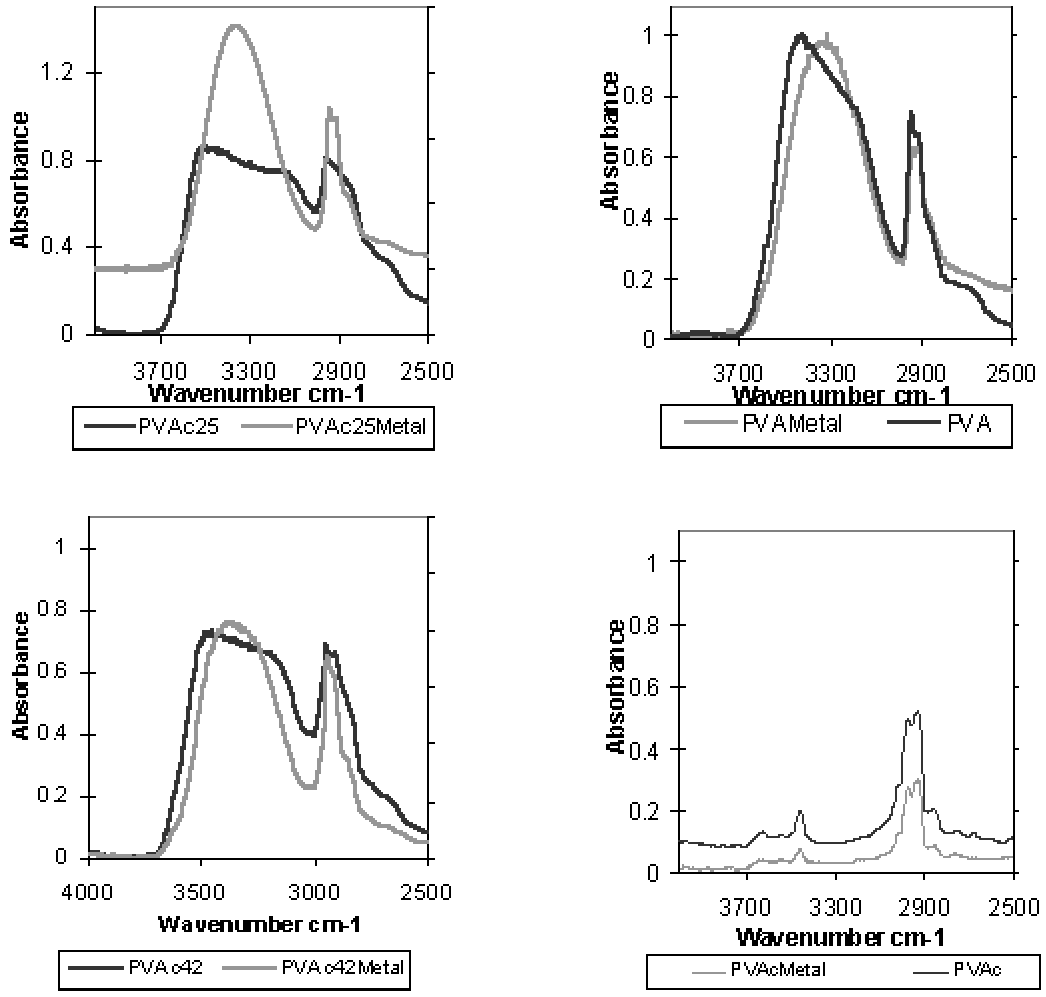

Figure 4.16 *Polyvinyl alcohol hydroxyl group frequency before and after interaction with cast iron surface.*

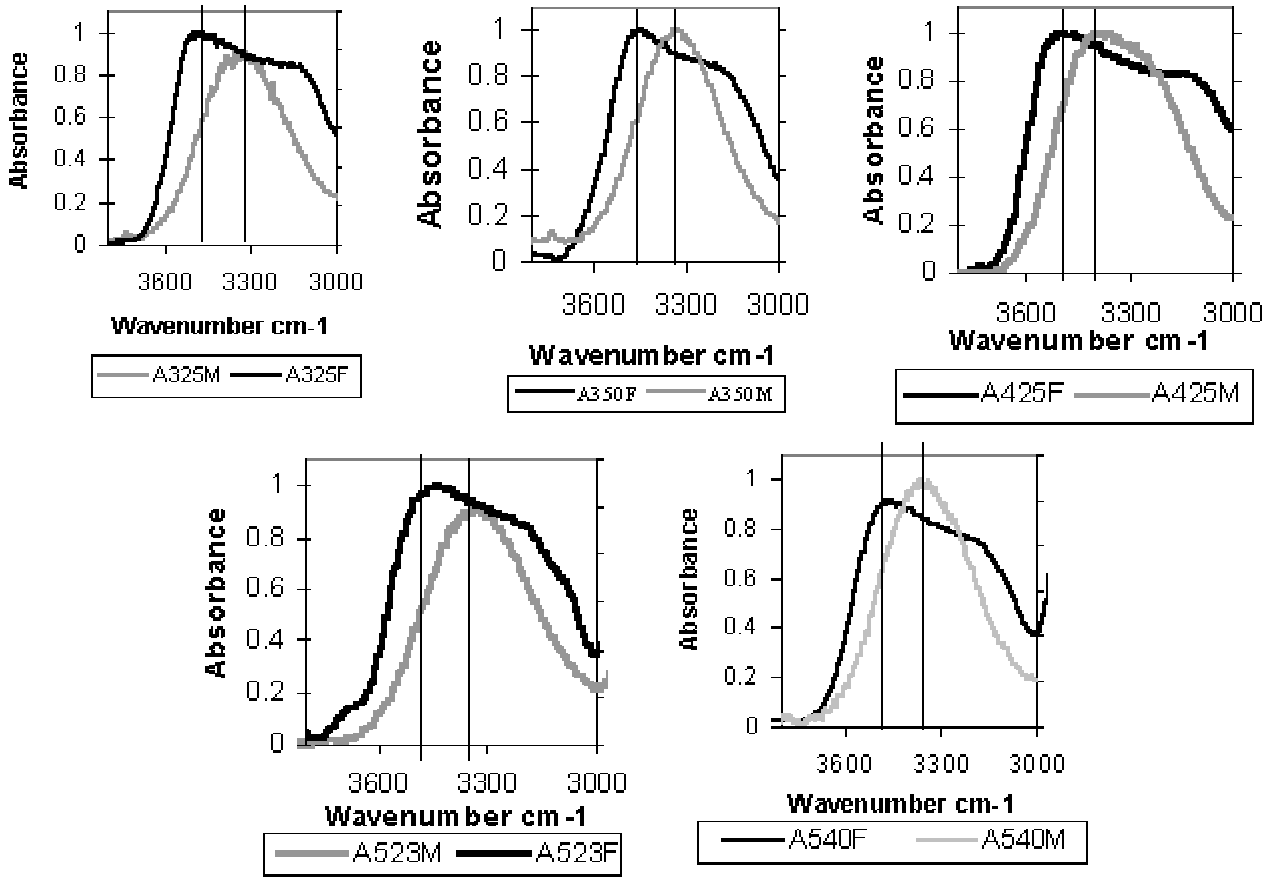

Figure 4.17 *Hydroxyl group stretching frequency in industrial grade polyvinyl alcohol. Polyvinyl alcohol hydroxyl group frequency is in between 3400 and 3500 cm^{-1}. After interaction with metal surface, it shifts to downfield around 3300 cm^{-1}.*

Drago *et al*. have studied hydrogen-bonding interactions between acidic and basic small molecules and established a linear enthalpy (ΔH)-frequency shift ($\Delta\upsilon$) correlation (21-26). This relationship was applied to a number of different acids such as phenol, t-butanol, trifluoroethanol, etc. Later, Kwei *et al*. reported that for the same series of bases applied to different acids, a plot of $1/(\Delta\upsilon_{OH})_1$ vs $1/(\Delta\upsilon_{OH})_2$ gave a linear relationship (27). They concluded that if frequency shifts for these acid-base pairs gives a linear correlation, then their enthalpy change should also give the same linear relationship. Therefore, our objective is to find a correlation between known acids and the polyvinyl alcohol copolymer hydroxyl group frequency shifts so that we can find a ΔH in order to determine the work of adhesion.

Using the method of Kwei *et al*. (27) for t-butanol, we studied the acid-base interactions between the PVA samples and various bases. The shift in the PVA hydroxyl frequency in the five different bases is shown in Figure 4.18. As the correlation between the polyvinyl alcohol and t-butanol (R^2 = 0.94) is within acceptable limits, the correlation between the frequency shift and heat of interaction developed for t-butanol can be used:

$$-\Delta H = 0.0106\Delta\nu_{OH} + 1.65 \qquad [4.6]$$

The values of the PVA sample OH stretching frequencies and the corresponding enthalpies are listed in Table 4.5.

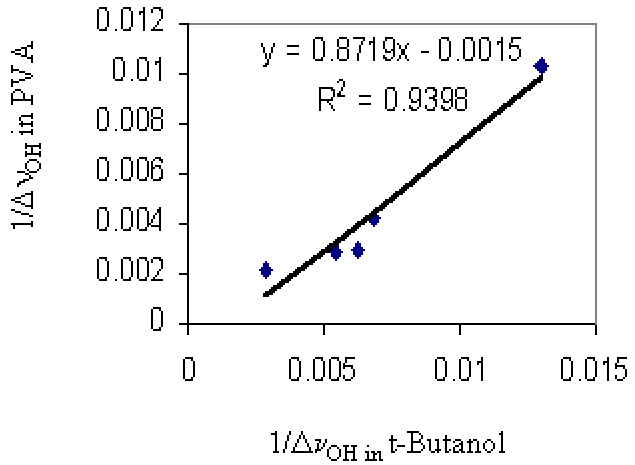

Figure 4.18 *Frequency shift correlation of t-butanol and polyvinyl alcohol in their mixtures with different bases.*

Table 4.5 *Polyvinyl alcohol OH group band assignment. The interaction of hydroxyl groups with a cast iron surface causes a shift of hydroxyl frequency to downfield. This change is related to the heat of interaction and obtained from the equation.*

Sample	OH group frequency in polyvinyl alcohol (cm^{-1})	$\Delta\upsilon$ (cm^{-1})	$-\Delta H$ (kcal/mol)
PVA	3433	89	2.6
PVAc25	3496	126	3
PVAc42	3475	108	2.8
PVAc85	3629*	69	2.4

*Free hydroxyl group frequency

From the values obtained from the shift in hydroxyl frequency and ΔH, the work of adhesion due to acid-base interactions was determined. The work of adhesion (W_a) is given by the following equation (28-33):

$$W^{ab}_{sl} = -f\, n_{ab}\, \Delta H^{ab} \qquad [4.7]$$

where W^{ab}_{sl} is the work of adhesion due to acid-base interaction between solid and liquid, f is a constant for converting heats of interfacial acid-base interaction into the free energies of interfacial acid-base interaction, n_{ab} is the interfacial concentration of acid-base bonds (mol/m^2) and ΔH^{ab} is the heat of interaction due to acid-base interaction (28-33). Since the value of n_{ab} is not available, the actual value of W_{ab} cannot be calculated. However, the trend of W_{ab} can be understood based on the relationship between $-\Delta H$ and W_{ab}. As can be seen from equation [4.7], n_{ab} and $-\Delta H$ are directly proportional to W_a. When $-\Delta H$ increases, the work of adhesion increases.

Based on the results in the previous two chapters, it is expected that the work of adhesion would decrease with increased acetyl substitution. Based on the overall decrease in $-\Delta H$ values with increased acetyl concentration (Table 4.5), W_{ab} appears to follow this trend. However, PVA does not follow this trend. As mentioned before, the OH peaks were difficult to identify and the peak may have been incorrectly located for PVA in this case. Also, FTIR may sense bulk phenomena and may not be able to detect the thin film-metal interface interaction. Since one data point was produced in this research, repeat of this data point in the future may be necessary to confirm the results.

Based on the proposal by Ramasubramanian *et al*. that the adhesive-dryer interface undergoes shear failure during the creping process, the ASTM 1002-99 lap shear strength test method was used to determine the apparent shear strength of the polymer adhesives (34) (Table 4.6). Polystyrene was used as a control for the adhesion strength test. Since polystyrene is a hydrocarbon, it interacts chemically with the surface only thorough van der Waals forces. Therefore, we may consider that the primary strength contribution of polystyrene is due mainly to mechanical interlocking.

Table 4.6 *Adhesion strength of polyvinyl alcohol and acetate derivatives.*

Polymer Sample	***Adhesion Strength (kN)***
Polystyrene	0.2±0.1
PVOH	14.7.±8.0
PVAc25	17.3±5.0
PVAc42	12.8±3.0
PVAc85	14.6±6.0
PVAc	5.8±3.0

The adhesive strength of polystyrene was found to be 0.2kN (Table 6). This value is much smaller than the values obtained for the other polymers. Thus, the mechanical interlocking contribution to the adhesive strength of any polymer may not be too high on a polished cast iron surface. For the most and least acetyl-substituted polymers, i.e. PVA and PVAc, the adhesive strength obtained from lap shear tests was proportional to the acetyl content, i.e. adhesive strength decreased with increasing acetyl content. These observations indicate two things. First, that the adhesive strength is due to more than mechanical interlocking based on the difference in strength between polystyrene and the other polymers. These results also support the hypothesis that acid-base interactions play a role in the interaction of the polymer and cast iron surface.

Work of adhesion and lap shear strength analyses were also conducted for the industrial grade polymers. Table 4.7 shows the results for the frequency shift and heat of interaction.

Table 4.7 *Polyvinyl alcohol(industrial grade) OH group band assignment. The interaction of hydroxyl group with cast iron surface causes to shift hydroxyl frequency to downfield. This change is related to the heat of interaction and obtained from equation [4.6].*

Sample	OH group frequeny in original polymer (cm^{-1})	$\Delta\upsilon$ (cm^{-1})	$-\Delta H$ (kcal/mol)
A325	3447	123	2.9
A350	3461	138	3.1
A425	3455	94	2.6
A523	3440	95	2.6
A540	3459	57	2.3

The heat of interaction and work of adhesion trends for the industrial grade polymers were similar to the synthesized polymers in Tables 4.5. The highest frequency shift was observed in A350, which is a high molecular weight polymer with low (2%) acetyl content. The lowest frequency shift and thus lower W_{ab} were obtained for the A540 polymer with the high (12%) acetyl content and high molecular weight. Therefore, we would expect to have higher adhesive strength from the more hydroxylated polymers.

As can be seen in Table 4.8, the highest lap shear strength was measured from A350. This result was consistent with the heat of interaction obtained from FTIR spectra measurement. Polyvinyl alcohol A540 gave the lowest creping force and lap shear strength. These results are again consistent with prior results in which increasing acetyl content decreased adhesion.

Table 4.8 *Adhesive strength of the polymers.*

Polymer Sample	Lap Shear Strength (kN)
A325	22.2±1.02
A350	25.5±1.1
A425	16.6±1.2
A523	14.4±1.7
A540	10.7±1.9

4.4 Conclusions

The interaction between the polyvinyl alcohol copolymer and the cast iron surface was investigated in this chapter. Cast iron is a porous material and in theory, adhesive could penetrate openings and crevices in the surface after application. However, many pore sizes appear to be smaller than polymer radius of gyration (e.g Polystyrene Rg=214nm), which would prevent the uniform penetration of the polymer into the surface. Therefore, the adhesion strength contribution due to mechanical interlocking may be too small to play a significant role in creping process.

The adsorption of polymers onto iron oxide appears to be controlled by hydrogen bonding. In general, as the polymer hydroxyl content increased, an increase in the adsorption of the polymer on the metal surface was observed. A microscopic FTIR spectroscopy study showed that with an increase in hydroxyl content, work of adhesion between the polymer and metal surface increased. Lap shear strength again showed that with an increase in hydroxyl content, shear strength increased. These results were supported by two different sets of polymers, one industrial grade and one synthesized, and support our hypothesis that the adhesive strength between the polymer and cast iron surface appears to be mainly controlled by acid-base interactions.

4.5 References

1. van Ooij, W.J.; “Interfacial Interactions between Polymers and Other Materials and Their Effects on Bond Durability” in Physicochemical Aspects of Polymer Surfaces, Edited By K.L Mittal, Plenum press, 1035, 1981.
2. Fourche, G.; “An Overview of the Basic Aspects of Polymer Adhesion. Part 1: Fundamentals” Polymer Engineering and Science, **35**(12), 957, 1985.
3. Moskvitin, N.I.; Physicochemical Principles of Gluing and Adhesion Processes, 3, 1969.
4. Comyn, J.; Adhesion Science, RSC Paperbacks, 3, 1997.
5. Fowkes, F.M.; “Attractive Forces at Interfaces”, Ind. Eng. Chem. **56**(12), 40, 1964.
6. Timmons, C.O, Zisman, W.A ; “Relation of Initial Spreading Pressure of Polar Compounds on Water to Interfacial Tension, Work of Adhesion and Solubility” J.Colloid Int. Sci., **28**(1), 106, 1968.
7. Fowkes, F.M.; “Calculation of Work of Adhesion by Pair Potential Summation” J.Colloid Int. Sci., **28**(3/4), 493, 1968.
8. Good, R.J.; “Theory of Cohesive Versus Adhesive Separation in an Adhering System” J. Adhesion, **4**, 133, 1972.
9. Fowkes, F.M.; “Donor-Acceptor Interactions at Interfaces” J. Adhesion, **4**, 155, 1972.
10. Zisman, W.A.; “Surface Energetics of Wetting, Spreading and Adhesion” J.Paint Technology, **44**(564), 42, Jan.1972.
11. Kinloch, A.J.; Adhesion and Adhesives Science and Technology, Chapman Hall, 18, 1987.
12. Good, R.J.; “Contact Angle Wetting and Adhesion – A Critical Review” J. Adhesion Sci. Tech., **6**(12) 1269, 1992.

13. Fowkes, F.M., Mostafa, M.A.; “Acid-Base Interaction in Polymer Adsorption” Ind. Eng. Chem. Prod., Res. Dev. **17**(1), 3, 1978.
14. Fowkes, F.M., Huang, Y.C., Shah, B.A., Kulp, M.J., Lloyd, T.B; ”Surface and Colloid Chemical Studies of Gamma Iron Oxides for Magnetic Memory Media” Colloids Surfaces, **29**, 243, 1988.
15. Vanderhoff, J.W., Bennetch, L.M., Cantow, M.J., Earhart, K.A., El-Aasser, M.S., Huang, T.C., Kang, M.H., Micale, F.J., Shaffer, O.L. and Timmons, D.W.; “Acid-Base Interaction of Polymeric Vehicles with the Corrosion Products of Iron”, Organic Coatings and Applied Polymer Science Proceedings, **46** (12), 1982.
16. Fowkes, F.M.; Molecular Forces at Interfaces, in Surfaces and Coatings Related to Paper and Wood, Edited by R.H. Marchessault, C. Skaar, Syracuse University Press, 99, 1967.
17. Platanov,B.E., Baran, A.A., and Polischuk, T.A.; “Adsorption of Poly(vinyl alcohol) and its effect on the electrosurface characteristic of some oxides”, Acta Physica et Chemica **25**(3-4), 201, 1979.
18. Fujii, K., Mochizuki, T., Imoto, S., Ukida, J., Matsumoto, M.;”Investigation of the Stereoregularity of Poly (vinyl alcohol)” J. Polymer Science Part A, **12**, 2327, 1964.
19. Pritchard, J.G; Polyvinyl Alcohol Basic Properties and Uses, Gordon and Breach Science,London, 34,1970.
20. Williams, D.H., Fleming, I.; Spectroscopic Methods in Organic Chemistry, 4th Edition McGraw Hill, London, 1989.
21. Drago, R. S., O’Bryan,N., Vogel, G.C.; ”Frequency Shift-Enthalpy Correlation for a Given Donor with Various Hydrogen-Bonding Acids”, J. Am. Chem. Soc., **92**(13), 3924, 1970.
22. Drago, R.S, Vogel, G.C.,Needham, T.E.;” 4-Parameter Equation for Predicting Enthalpies of Adduct Formation”, J. Am. Chem. Soc., **93**(23), 6014, 1971.

23. Epley, T.D., Drago, S. R.; “Calorimetric Studies on some Hydrogen Bonded Adducts” J.Am.Chem. Soc., **89**(23), 5770, 1967.
24. Drago, R.S., Epley, T.D.; “Enthalpies of Hydrogen Bonding and Changes in Delta NuOH for a Series of Adducts with Substituted Phenols” J.Am.Chem. Soc., **91**(11), 2883, 1969.
25. Drago, R.S., Parr, L.B., Chamberlain, C.S.; “Solvent Effects and Their Relationship to E and C Equation” J.Am.Chem.Soc. **99**(10), 3203,1977.
26. Drago, R., Vogel, G.C.; “Interpretation of Spectroscopic Changes upon Adduct Formation and Their Use to Determine E Parameter and C Parameter” J.Am.Chem. Soc., **114**, 9527, 1992.
27. Kwei, T.K., Pearce, E.M., Ren, F., Chen, J.P.; “Hydrogen Bonding in Polymer Mixtures” J. Polymer Sci. Part B, Polymer Physics, **24**, 1597, 1986.
28. Fowkes, F.M.; “Quantitative Characterization of the Acid-Base Properties of Solvents, Polymers and Inorganic Surfaces” J. Adhesion Sci. Tech., **4**(8) 669, 1990.
29. Fowkes, F.M., Tischler, D.O., Wolfe, J.A., Lannigan, L.A., Hallwell, M.J.; “Acid-Base Complexes of Polymers”, J.Polymer Sci. Polymer Chem., **22**, 547, 1984.
30. Allara, D.L., Fowkes, F.M., Noolandi, J., Rubloff, G.W., Tirrel, MV; “Bonding and Adhesion of Polymer Interfaces ” Materials Sci. Eng., **83**, 213, 1986.
31. Joslin, S.T., Fowkes, F.M.; “Surface Acidity of Ferric Oxide Studied by Flow Microcalorimetry” Ind. Eng. Chem. Prod., Res. Dev. **24**, 369, 1985.
32. Petrie, E.; Handbook of Adhesives and Sealants, McGraw Hill, NY, 202, 2000.
33. Fowkes, F.M.; “Role of Acid-Base Interfacial Bonding in Adhesion” J. Adhesion Sci. Tech., **1**(1), 7, 1987.

34. Ramasubramanian, M.K., Crews, W.R.; “Shear strength of an Adhesively Bonded Metal Paper Interface” J. Pulp Pap Science **24**(1), 31, 1998.

Chapter 5 - Conclusions

This dissertation presented a study of the adhesion mechanism between PVA and an iron oxide surface. Although the specific application of the present study was to understand the adhesion mechanism as it pertains to the creping process, the results obtained from this study can be applied to many other applications such as coating, corrosion, *etc*.

In order to determine the effect of adhesion between PVA and an iron oxide surface, the polymer physical properties were first characterized. The physical properties indicate that with higher hydroxyl content better contact could be made between the polymer and the cast iron surface. This would enhance the molecular interactions between the two materials.

Adsorption was conducted via a gravimetric method using iron particles and polymer solutions. The adsorption of polymers onto iron oxide appears to be controlled by hydrogen bonding. Increasing acetyl content on the polymer decreased adsorption.

Adhesion properties of different polymers were determined by using colloidal probe microscopy on a cast iron surface in aqueous solution. These results demonstrated that the chemical properties of the polymer affect the adhesive strength. Increased hydroxyl content in the polymer increased the adhesion forces in CPM.

These experimental results led us to study extensively the adhesion mechanism of the polymer on the metal surface. Model systems were developed for the adhesive and metal surface interactions to limit unknowns in our system. Chemical Force Microscopy was used. Functionalized probe tips were prepared from hydroxyl and methyl group terminated thiol compounds. A hydroxyl-terminated surface was also prepared. Adhesion force measurement was carried out in aqueous solution to eliminate capillary forces. Modification of the probe tip with different ratios of the functional groups allowed us to control adhesive strength. Results showed that

hydrogen bonding played a very important role in the model system. Manipulation of the probe tip and changing concentrations of functional groups led to study of the polymers with different concentrations of functional groups along the chain. This treatment let us control adhesion on the metal surface.

FT-infrared spectroscopy was applied for the investigation of the chemical bonding between polymers and metal surfaces. FT-infrared spectroscopy frequency shifts allow us to determine heat of interaction. Heat of interaction calculations allowed us to observe the trend for work of adhesion versus hydroxyl content. The trend showed that the work of adhesion could increase with increasing hydroxyl content. This trend was also observed in other empirical force measurements based on chemical force microscopy, lap shear test and creping process.

In order to determine the contribution of mechanical interlocking in adhesive interaction with the metal surface, contact mode AFM and optical microscopy were used. The tests demonstrated that the cast iron surface has pores and crevices. However, surface roughness obtained from contact mode AFM shows that polymer penetration into the cast iron surface is sparse and not uniform. Therefore, mechanical interlocking may play a less important role.

Finally, creping experiments were run using industrial grade polyvinyl alcohol. The results gave a pathway to understand how the adhesion properties of the coating chemistry will affect on the crepe paper properties. The mechanical properties of the creped paper, *e.g*. tensile strength, Young's modulus, creping wavelength, and creping force, were examined. Tensile strength and Young's modulus of the crepe paper were dramatically decreased compared to uncreped tissue paper. Increased adhesion to the drum surface caused a fine creping structure, and smaller wavelengths resulted from higher creping force.

Chapter 6 - Proposal for Future Work

Although polymer interfaces have been the focus of extensive study as well as application for many years, the level of understanding has been limited to measures of their physical and chemical properties. Recently, development of microscopic and spectroscopic technique has potential to study the phenomena in greater depth. The adhesion phenomenon studied in this dissertation is a general problem that exists broadly in every adhesive-metal interface. A single dissertation research could hardly cover all the topics related to adhesion phenomena. An important factor in creping process is the uniform and controlled adhesion on Yankee Dryer surface. This will increase speed and give consistent uniform tissue paper. The following are recommendations for future works in this area:

- It is known that Yankee dryer coatings affect the creping process. The effect of hemicellulose on adhesion can be studied by Atomic Force Microscopy.
- Friction forces can be studied on AFM by modifying the cantilever tip.
- Different pulp fiber and types require different adhesive strengths to improve creping. Fiber source and adhesive strength can also be studied on AFM.
- The quality of tissue paper is influenced by contaminants that may be present in the pulp or in the system water. The effects of these contaminants such as xylan, lignin, and resin acid can be studied on AFM. Adhesion properties of the polymer on tissue paper and tissue paper adhesion on metal surface in the presence of contaminants can be examined.
- Adhesive strength can be controlled by tailoring the polymer structure. Therefore, synthesizing block copolymers may help to improve adhesion properties to the Yankee dryer surface.

When polymer properties change, the adhesion mechanism may be affected. There are several theories to explain the adhesion mechanism. It is not possible to apply one theory on every adhesive system. Thus, study of ionic polymer may help to improve the understanding of the adhesion mechanism.

- Stereoregular and crystalline properties of the polymer may affect the adhesion properties.
- The creping process breaks some of the fiber-to-fiber bonds and reduces the strength properties of tissue paper. The interaction of adhesive with the paper can be studied to control strength loss.
- The effects of softening and debonding agents can be studied with AFM.

APPENDIX

Appendix A - Hydrogen Bonding

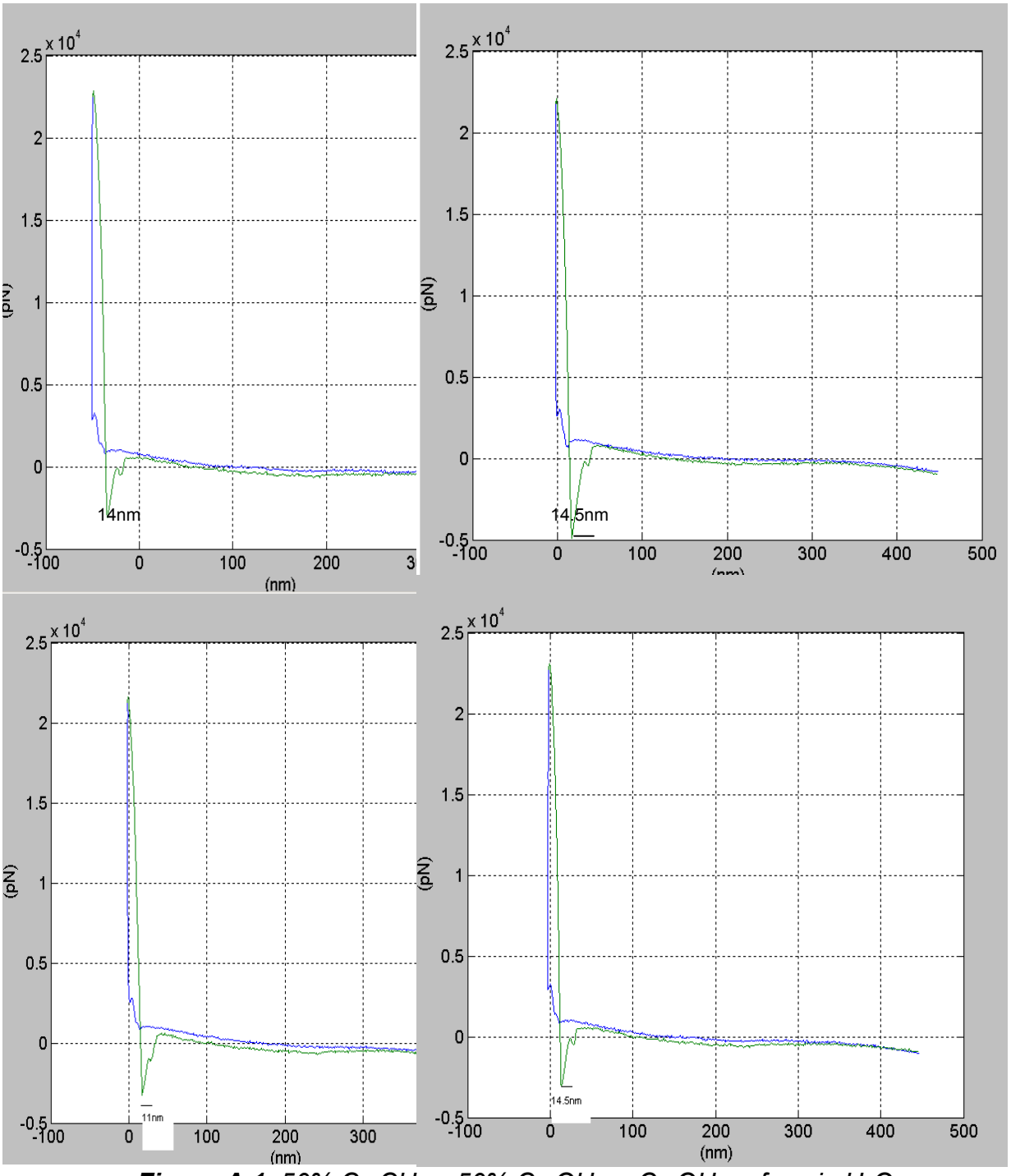

Figure A.1 *50% $C_{10}CH_3$ + 50% $C_{10}OH$ on $C_{10}OH$ surface in H_2O*

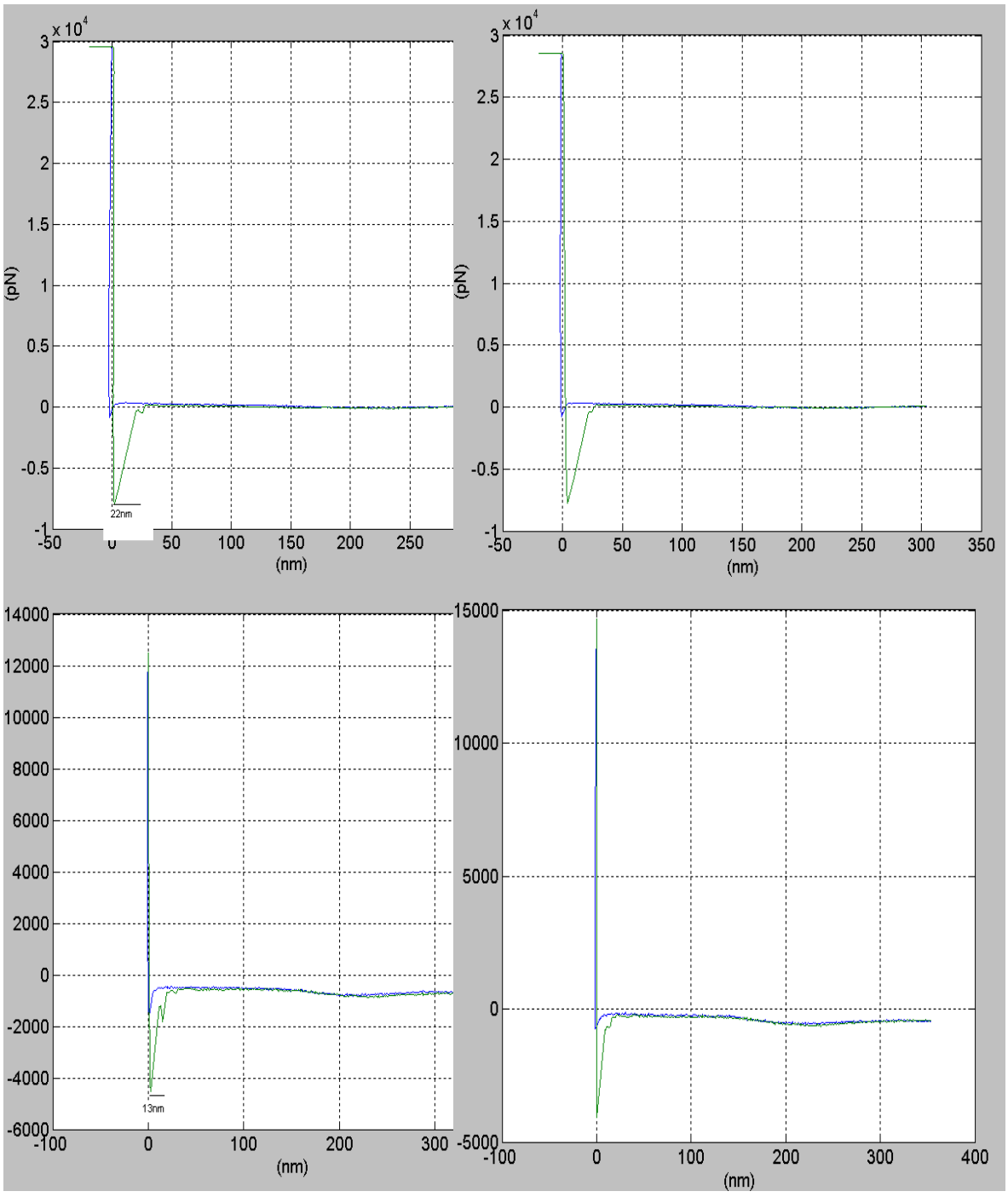

Figure A.2 *100% $C_{10}OH$ on $C_{10}OH$ surface in H_2O*

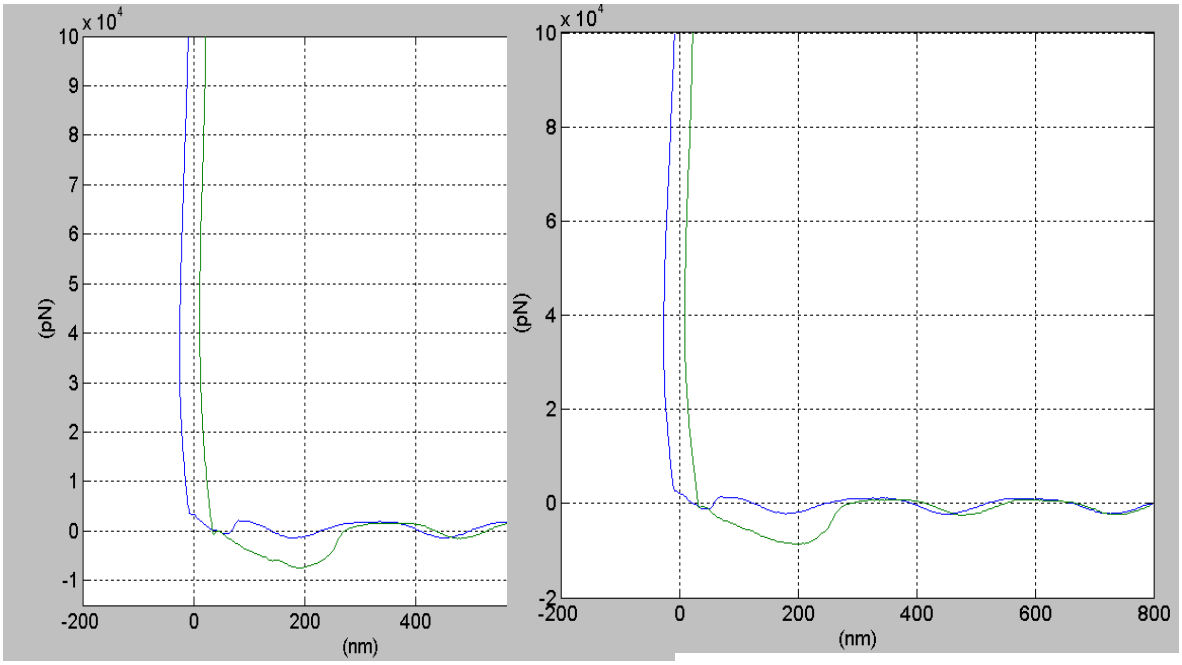

Figure A.3 *100% $C_{10}CH_3$ on $C_{10}OH$ surface in H_2O*

Appendix B – Probe Tip and Force Data

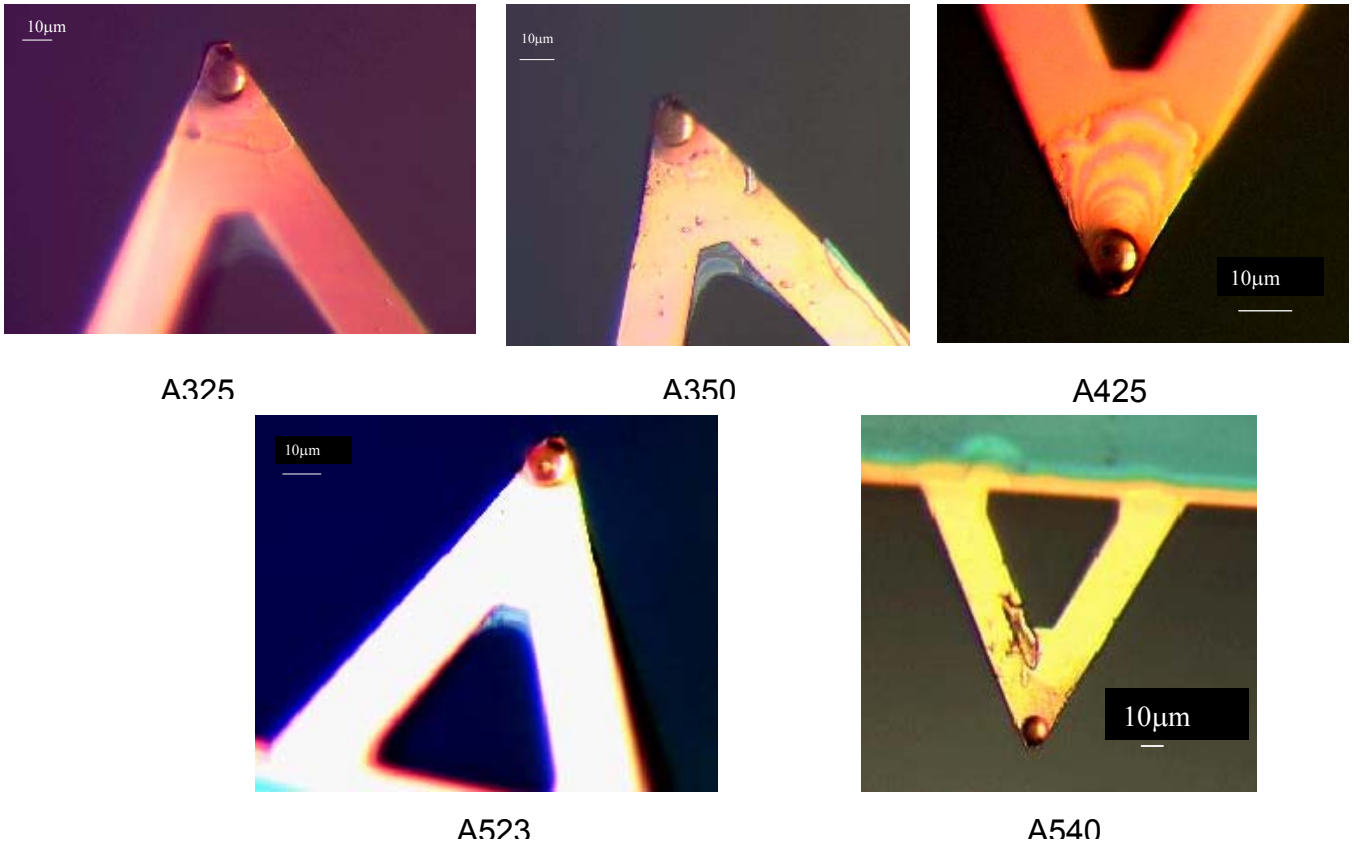

Figure B.1 *Polyvinyl alcohol probe tip to measure adhesion forces on CPM.*

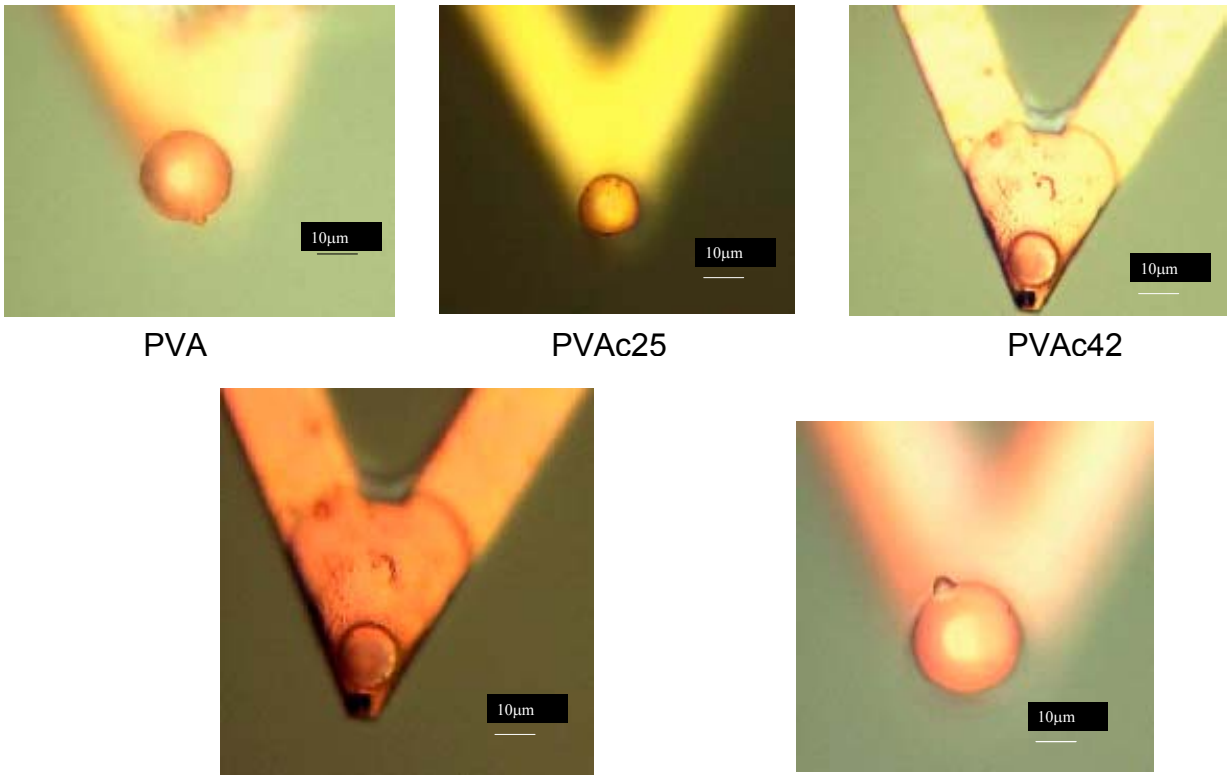

Figure B.2 *Polyvinyl alcohol acetate copolymer probe tip for adhesive force measurement in CPM.*

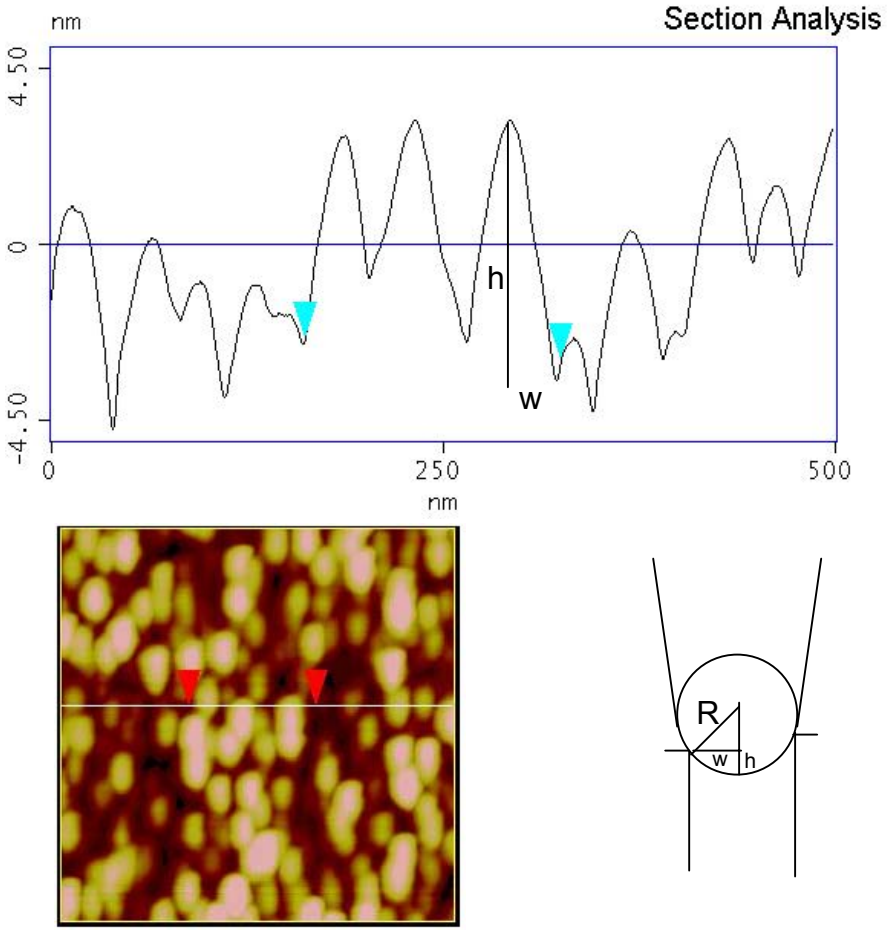

$$R = \frac{w}{2h} + \frac{h}{2}$$

Functional Tip	Radius (nm)
100% OH	117
75% OH	63.11
50% OH	105
25% OH	54.1

Figure B.3 *Determination of tip radius R using section analysis on gold-coated surface.*[1]

1 Voutsos, V, Van der Vegte, E.W., Grim, P.C.M. and Hadzioannou, G.; "Isolated Polymer Chains via Mixed Self-Assembled Monolayers: Morphology and Friction Studied by Scanning Force Microscopy, Macromoleculas, 31, 116-123, 1998.

Table B.1 *Force Data obtained from hydroxyl containing surface with functionalized tip.*

Force nN					force nN				
Funct. Group	100% OH	75% OH	50% OH	25% OH	Funct. Group	100% OH	75% OH	50% OH	25% OH
1	12.55956	1.266407	1.197	0.368601	20	12.57672	3.087341	2.842	0.253909
2	7.18848	1.485189	1.0584	0.683103	21	13.72176	2.280375	2.688	0.317387
3	6.78912	1.984178	1.8508	0.488343	22	12.753	3.450013	2.4808	0.977407
4	6.8796	1.984178	2.5396	1.030064	23	13.06344	2.35779	2.3128	0.379421
5	6.3336	1.178053	2.758	0.394569	24	13.13052	2.975426	3.2144	0.375093
6	6.02004	0.841467	2.6096	0.631167	25	13.11492	2.975426	2.8504	0.372208
7	14.02284	1.470884	2.66	0.04328	26	13.4784	3.026756	2.786	0.473916
8	12.22104	0.420733	3.1892	0.172399	27	14.51112	1.905081	2.8	0.164464
9	14.38476	0.934028	2.814	0.589329	28	14.38944	2.364521	2.6222	0.705464
10	15.71076	1.395152	5.285	0.154365	29	14.10708	2.718779	2.8938	0.293583
11	15.06024	0.812015	4.1384	0.072133	30	14.64216	1.316895	2.3226	1.123116
12	12.5736	1.38842	4.2084	0.741531	31	14.64216	1.635811	2.5494	0.209908
13	14.79192	2.5244	3.479	0.1623	32		2.100301	1.8942	0.12984
14	11.98548	0.387075	3.164	0.376536	33		1.777178	1.3468	0.072133
15	14.1804	2.140691	5.376	0.946389	34		0.955906	2.9092	0.555427
16	12.59544	2.507571	2.7944	0.214236	35		1.556713	2.7034	0.693923
17	12.91212	1.209188	3.0366	0.153644	36		1.701446	2.7664	0.440735
18	12.44412	1.770446	4.9728	0.785532	37		1.649275	2.408	
19	12.6906	2.418375	3.1556	0.165907	38		1.518847	2.1756	
					39			2.023	

Table B.2 *Force Data obtained from cast iron surface with functionalized tip.*

	Force nN					Force nN			
Func. Group	100%OhwFe	75%OhwFe	50%OhwFe	25%OhwFe	Func. Group	100%OhwFe	75%OhwFe	50%OhwFe	25%OhwFe
1	5.969	1.757	3.584	1.656	22	9.918	4.097	3.871	2.145
2	6.327	1.847	1.481	1.443	23	8.112	3.563	1.291	2.155
3	4.822	0.970	2.279	1.587	24	8.387	3.934	2.594	1.964
4	7.373	0.630	3.884	1.530	25	7.827	3.973	5.331	2.074
5	3.165	1.153	1.988	1.550	26	2.264	3.913	5.505	2.316
6	6.646	2.321	2.870	1.335	27	5.117	3.190	1.557	2.134
7	3.781	2.794	2.377	1.655	28	3.120	2.036	1.674	2.136
8	3.477	3.753	1.849	1.330	29	3.432	3.315	2.835	1.882
9	4.680	2.599	3.118	0.586	30	2.994	4.073	3.556	2.048
10	4.822	2.921	2.782	0.572	31	2.608	4.182	2.068	2.011
11	7.738	4.736	2.999	0.745	32	4.543	4.385	1.933	2.031
12	6.251	4.182	1.638	0.278	33	4.257	4.877	1.996	1.928
13	5.203	3.018	2.544	1.641	34	4.504	5.049	1.289	1.961
14	4.106	2.753	4.738	1.283	35	2.566		5.410	1.865
15	3.613	3.257	1.700	0.618	36	3.629		5.908	1.928
16	7.973	2.814	1.547	1.928	37	6.279		6.733	1.205
17	7.730	3.576	2.276	1.979	38	7.940		4.379	1.579
18	7.408	4.855	4.000	2.075	39	4.193		4.270	1.472
19	4.150	3.835	4.896	0.180	40	6.221		5.201	
20	9.777	4.515	1.919	0.426	41	5.491			
21	7.433	4.315	5.085	1.938	42	4.449			
					43	4.827			
					44	10.444			

Table B.3 *Pull-off forces measured with colloidal probe microscopy on a cast iron surface.*

Force nN											
Polymer	PVA	PVAc25	PVAc42	PVAc85	PVAc	Polymer	PVA	PVAc25	PVAc42	PVAc85	PVAc
1	13.48	2.41	3.95	0.85	2.03	22	10.78	1.96	3.20	3.81	5.58
2	12.33	1.23	5.72	3.35	0.96	23	13.90	1.73	3.48	1.71	1.78
3	9.61	1.03	6.83	4.78	2.02	24	8.30	1.79	3.53	4.88	2.76
4	8.26	1.87	1.82	5.72	1.96	25	8.45	1.44	3.52	1.25	3.26
5	13.43	1.36	2.78	3.28	2.20	26	12.76	1.69	4.21	2.03	2.93
6	9.68	1.34	2.40	5.72	2.09	27	8.48	9.23	4.92	3.58	0.92
7	44.50	2.06	3.43	5.79	1.69	28	9.65	3.97	2.76	0.81	0.73
8	3.38	4.51	2.73	5.53	3.10	29	8.11	4.39	3.42	3.14	0.93
9	7.98	3.36	2.01	5.94	1.34	30	10.07	4.35	4.07	4.25	0.46
10	2.86	6.09	2.00	6.18	1.96	31	9.69	2.31	3.82	3.73	0.91
11	17.37	6.37	2.07	5.23	1.57	32	13.40	5.02	6.07	2.88	0.55
12	21.13	8.55	3.05	3.97	3.83	33	10.70	3.97	4.83	3.90	0.96
13	15.16	6.82	2.51	3.12	2.20	34	11.86	3.58	3.88	2.24	
14	11.88	3.71	2.28	4.94	1.15	35		7.07	5.83	2.58	
15	13.78	3.69	2.68	4.71	2.27	36		6.55	4.04		
16	14.57	4.28	2.84	4.37	3.30	37		6.05	7.24		
17	15.18	2.39	2.26	3.88	5.54	38		5.89	6.35		
18	15.94	5.55	3.99	3.18	1.60	39		3.82	7.18		
19	12.65	5.10	3.82	3.74	5.58	40		2.41	4.03		
20	4.40	2.41	4.18	2.06	2.43	41		5.45	4.11		
21	11.33	2.12	3.09	4.56	5.52	42		4.52	5.14		
						43			4.89		
						44			4.27		
						45			4.77		
						46			4.40		

Table B.4 *Pull-off forces measured with colloidal probe microscopy on a cast iron surface.*

	Force nN						Force nN				
polymer	A325	A350	A425	A523	A540	polymer	A325	A350	A425	A523	A540
1	4.236	26.725	5.096	4.054	3.125	27	30.443	60.159	5.884	3.567	2.070
2	6.963	46.430	3.142	3.301	3.051	28	39.051	79.605	6.079	2.000	1.930
3	23.868	176.443	4.543	1.825	2.874	29	28.960	23.589	4.595	2.424	1.700
4	34.701	64.251	4.609	6.930	0.075	30	56.319	88.315	4.789	1.924	2.570
5	10.470	45.100	2.973	1.243	3.432	31	47.456	55.190	6.445	6.788	0.200
6	5.028	80.286	4.796	1.738	3.840	32	43.900	29.714	5.268	1.279	0.027
7	10.937	176.980	3.720	2.744	3.166	33	46.738	25.690	3.976	1.725	2.470
8	7.278	118.002	4.099	5.581	5.300	34	42.794	4.223	5.344	0.900	0.661
9	41.258	114.599	3.440	3.218	1.400	35	44.745	17.620	6.000	2.121	2.010
10	45.845	71.755	4.167	6.000	3.540	36		12.234	5.083	0.372	2.135
11	31.697	73.220	4.063	11.860	3.170	37		3.000	4.084	0.121	3.076
12	58.180	85.390	4.556	4.369	3.097	38		4.500	4.320	11.051	1.264
13	40.925	70.908	3.195	9.400	6.333	39		10.915	4.457	0.842	2.846
14	37.774	107.354	4.128	3.922	3.996	40			6.375	2.888	2.939
15	36.000	66.306	3.268	0.685	3.502	41			6.026	0.593	1.623
16	46.474	42.220	4.157	1.632	4.685	42			6.259	1.186	1.335
17	25.997	82.430	5.214	3.942	3.250	43			6.044	4.055	
18	41.313	83.878	4.461	1.569	3.094	44			5.487		
19	31.070	77.405	4.500	1.436	2.707	45			6.365		
20	38.932	44.464	5.478	2.635	3.062	46			6.860		
21			5.054			47			4.217		
22			4.523			48			2.973		
23			5.096			49			4.796		
24			3.142			50			3.730		
25			3.364			51			4.100		
26			2.447								

Appendix C – NMR Spectra

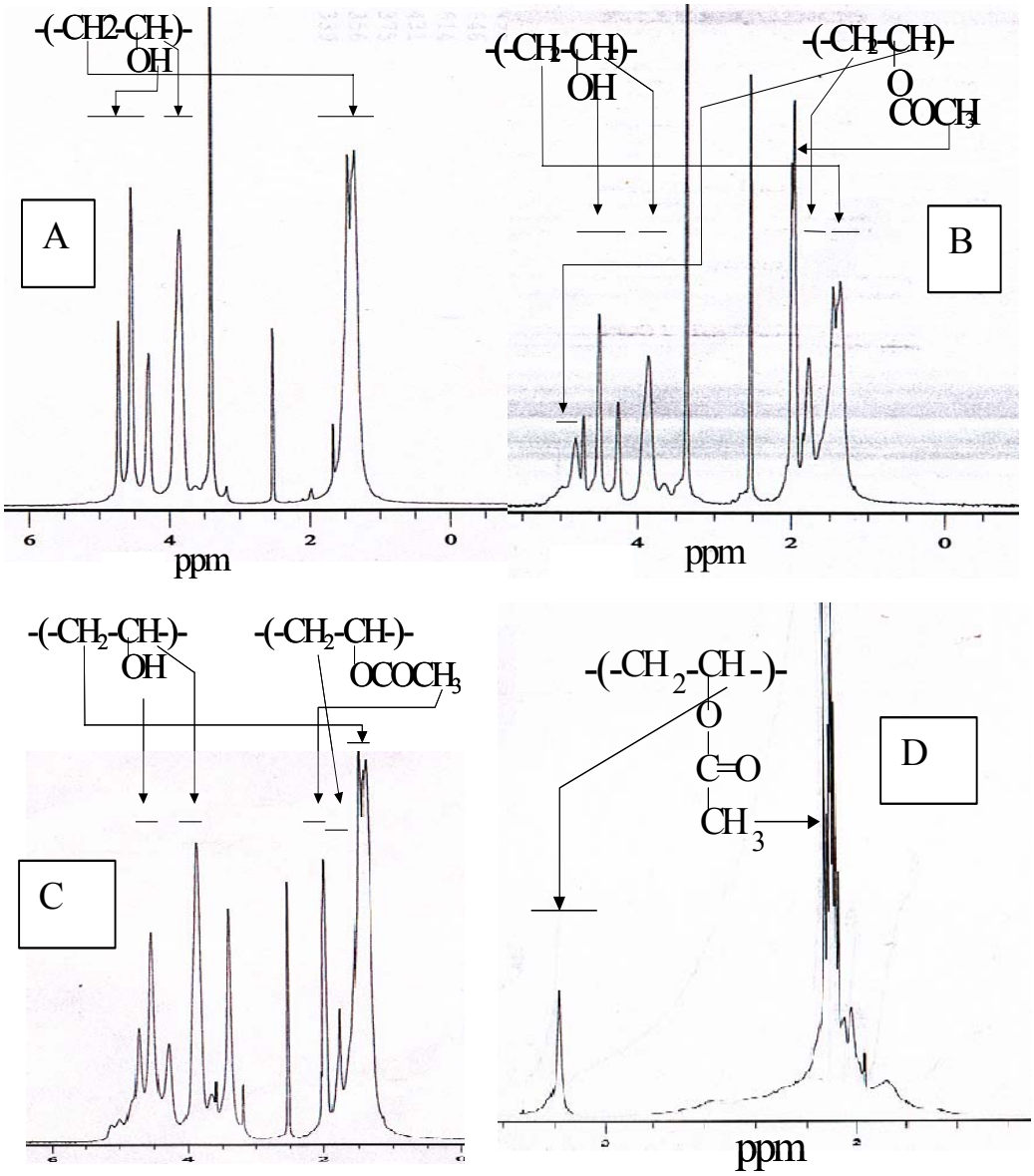

Figure C.1 *^{1}H-NMR spectra of polyvinyl alcohol (PVA) in DMSO. PVA 99-100 % hydrolyzed(A). PVA 42 % acetylated(B). PVA 25 % Acetylated (C). Polyvinyl acetate in Acetone (D).*

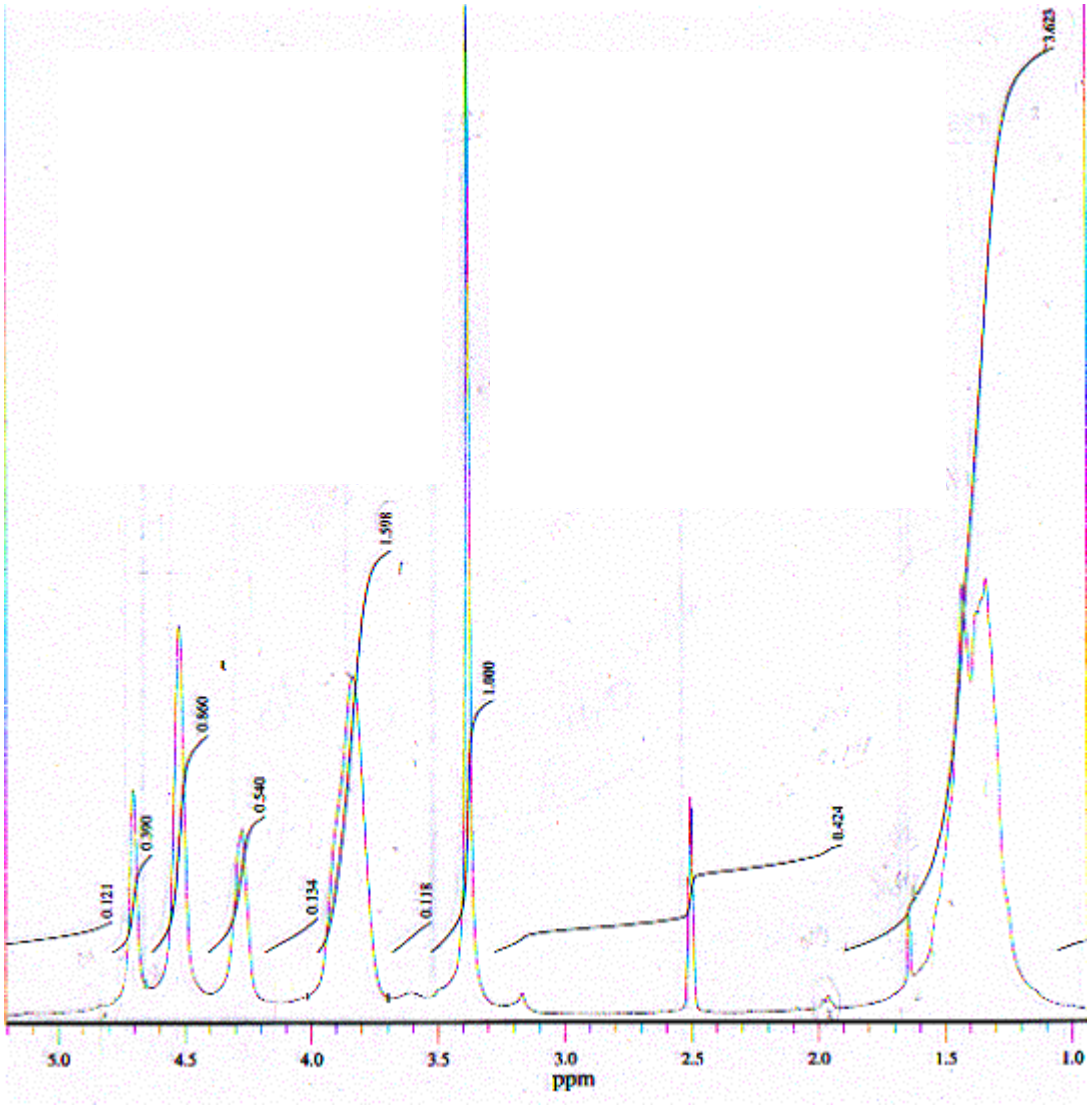

Figure C.2 *Polyvinyl alcohol (PVA)*

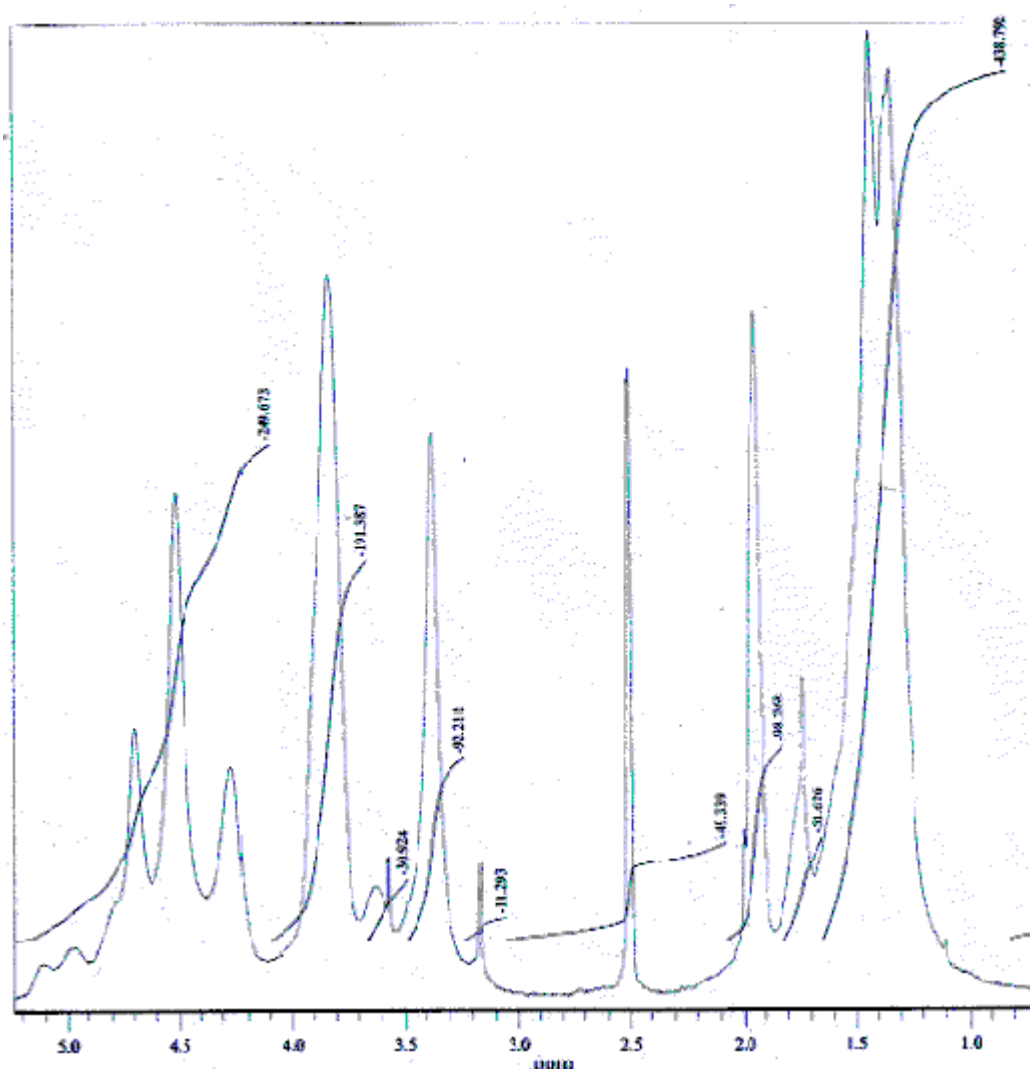

Figure C.3 *Polyvinyl alcohol acetate copolymer (PVAc25).*

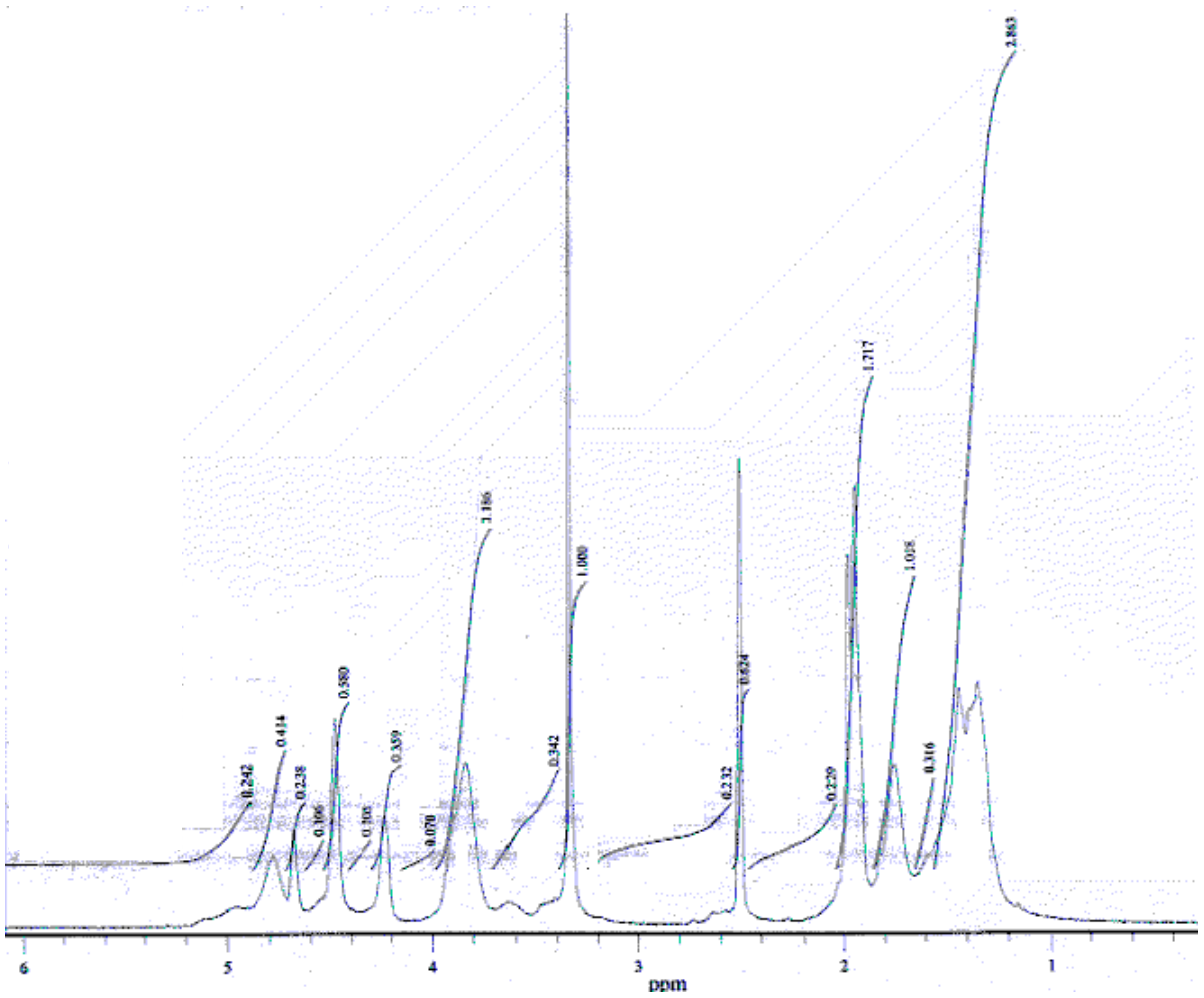

Figure C.4 *Polyvinyl alcohol acetate copolymer (PVAc42).*

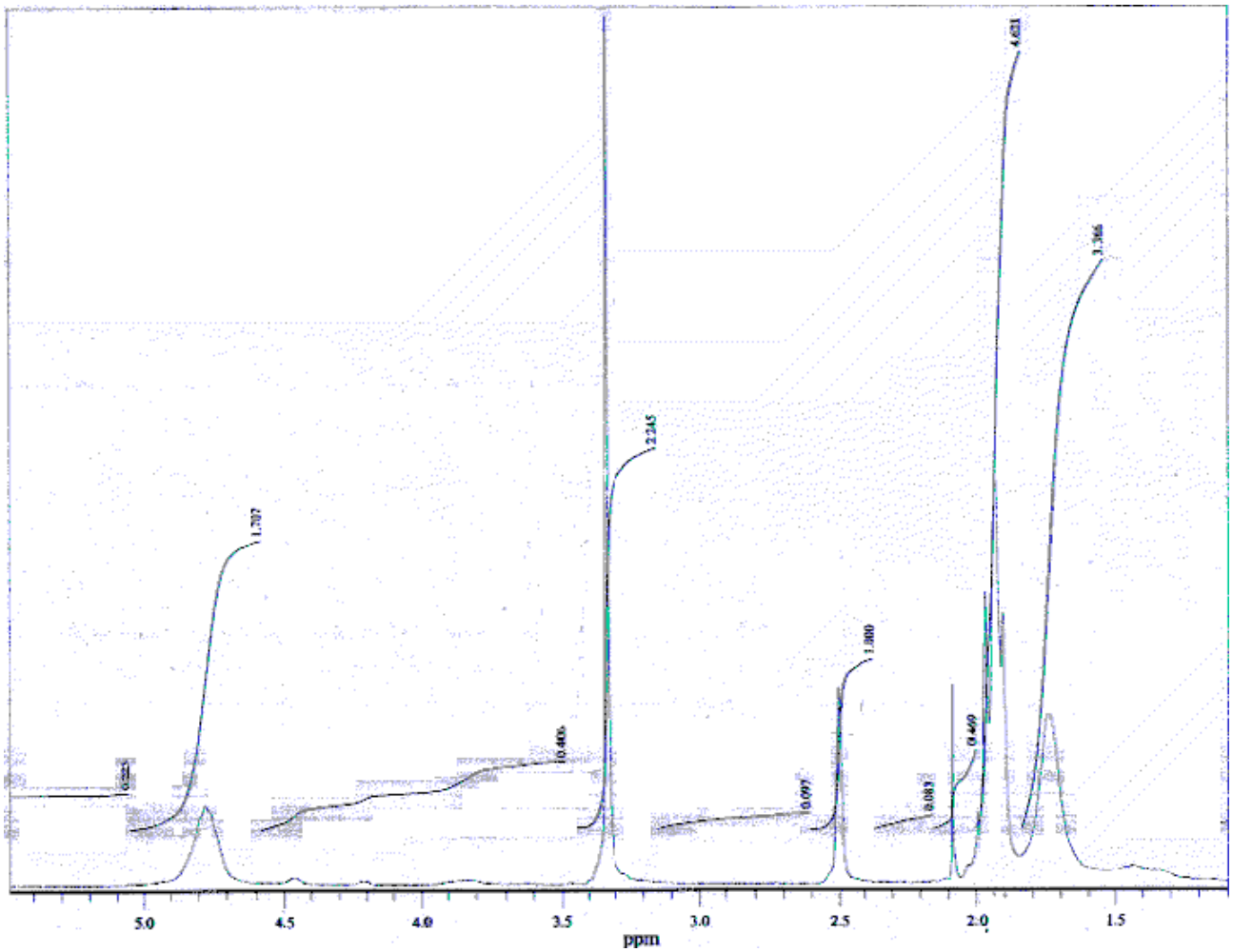

Figure C.5 *Polyvinyl alcohol acetate copolymer (PVAc85)*

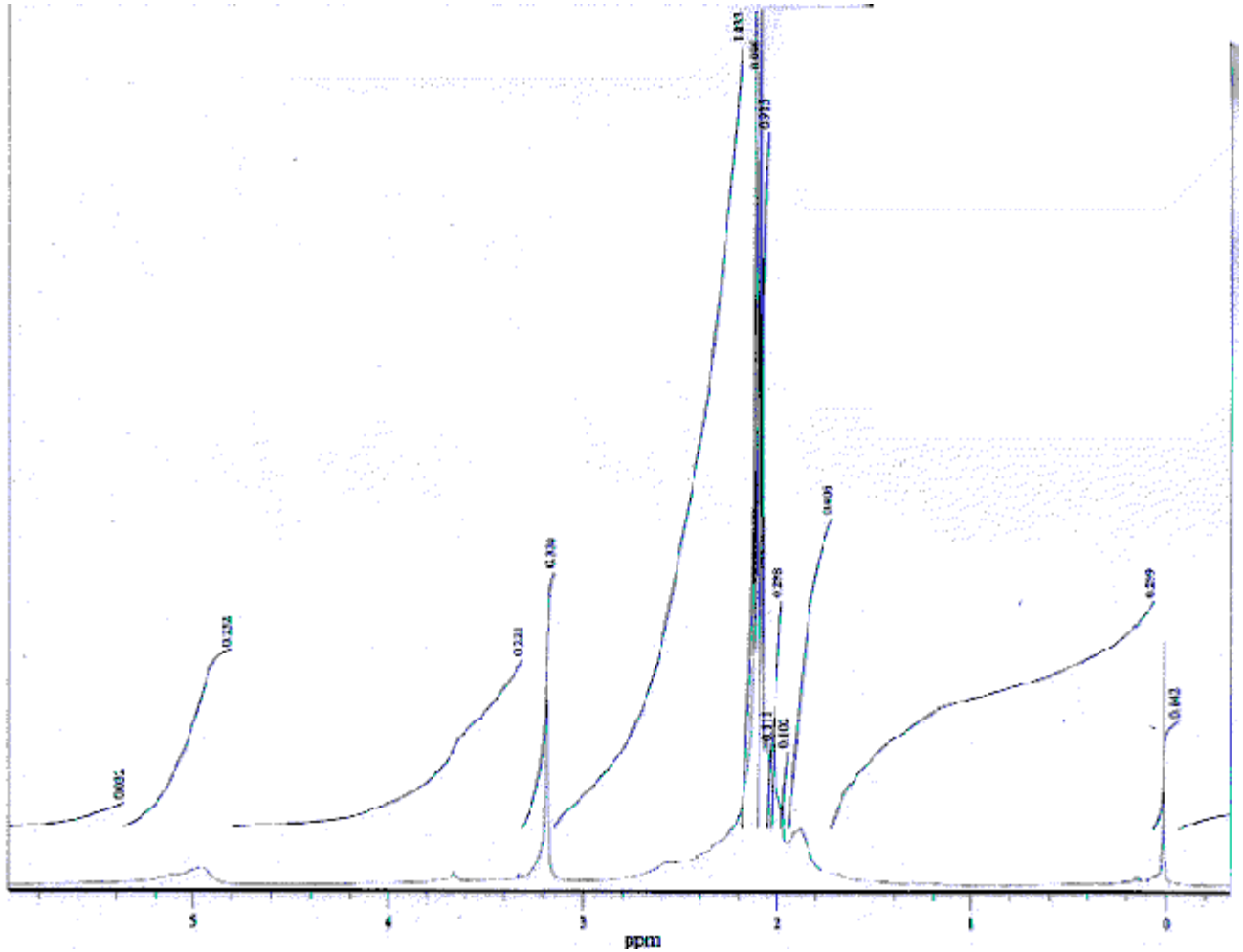

Figure C.6 *Polyvinyl acetate (PVAc).*